BNL-73263-2004

Proceedings of RIKEN BNL Research Center Workshop Volume 64

Theory Summer Program on RHIC Physics

Summer 2004

Organizers:

D. Kharzeev, S. Kretzer, D. Teaney, K. Tuchin, R. Venugopalan, and W. Vogelsang

RIKEN BNL Research Center

Building 510A, Brookhaven National Laboratory, Upton, NY 11973-5000, USA

DISCLAIMER

This report was prepared as an account of work sponsored by an agency of the United States Government. Neither the United States Government nor any agency thereof, nor any of their employees, nor any of their contractors, subcontractors or their employees, makes any warranty, express or implied, or assumes any legal liability or responsibility for the accuracy, completeness, or any third party's use or the results of such use of any information, apparatus, product, or process disclosed, or represents that its use would not infringe privately owned rights. Reference herein to any specific commercial product, process, or service by trade name, trademark, manufacturer, or otherwise, does not necessarily constitute or imply its endorsement, recommendation, or favoring by the United States Government or any agency thereof or its contractors or subcontractors. The views and opinions of authors expressed herein do not necessarily state or reflect those of the United States Government or any agency thereof.

FOR UNCLASSIFIED, UNLIMITED STI PRODUCTS

Available electronically at-

OSTI:

http://www.osti.gov/bridge

Available for a processing fee to U.S. Department of Energy and its contractors, in paper from-

U.S. Department of Energy
Office of Scientific and Technical Information
P.O. Box 62
Oak Ridge, TN 37831
(865) 576-8401
Facsimile: (865) 576-5728
E-mail: reports@adonis.osti.gov

National Technical Information Service (NTIS):

Available for sale to the public from-

U.S. Department of Commerce
National Technical Information Service
5285 Port Royal Road
Springfield, VA 22131
(800) 553-6847
Facsimile: (703) 605-6900
Online ordering: http://www.ntis.gov/ordering.htm

Printed on recycled paper

Preface to the Series

The RIKEN BNL Research Center (RBRC) was established in April 1997 at Brookhaven National Laboratory. It is funded by the "Rikagaku Kenkyusho" (RIKEN, The Institute of Physical and Chemical Research) of Japan. The Center is dedicated to the study of strong interactions, including spin physics, lattice QCD, and RHIC physics through the nurturing of a new generation of young physicists.

During the first year, the Center had only a Theory Group. In the second year, an Experimental Group was also established at the Center. At present, there are four Fellows and eight Research Associates in these two groups. During the third year, we started a new Tenure Track Strong Interaction Theory RHIC Physics Fellow Program, with six positions in the first academic year, 1999-2000. This program had increased to include ten theorists and one experimentalist in academic year, 2001-2002. With five fellows having already graduated, the program presently has eleven theorists and three experimentalists. Of these eleven RHIC Physics Fellows, five have been awarded/offered tenured positions, and this will be their final year in the program.

Beginning in 2001 a new RIKEN Spin Program (RSP) category was implemented at RBRC. These appointments are joint positions of RBRC and RIKEN and include the following positions in theory and experiment: RSP Researchers, RSP Research Associates, and Young Researchers, who are mentored by senior RBRC Scientists. A number of RIKEN Jr. Research Associates and Visiting Scientists also contribute to the physics program at the Center.

RBRC has an active workshop program on strong interaction physics with each workshop focused on a specific physics problem. Each workshop speaker is encouraged to select a few of the most important transparencies from his or her presentation, accompanied by a page of explanation. This material is collected at the end of the workshop by the organizer to form proceedings, which can therefore be available within a short time. To date there are 62 proceeding volumes available.

The construction of a 0.6 teraflops parallel processor, dedicated to lattice QCD, begun at the Center on February 19, 1998, was completed on August 28, 1998. A 10 teraflops QCDOC computer in under development and expected to be completed this year.

N. P. Samios, Director
April 1, 2004

*Work performed under the auspices of U.S.D.O.E. Contract No. DE-AC02-98CH10886.

CONTENTS

Preface to the Series

Introduction
D. Kharzeev, S. Kretzer, D. Teaney, K. Tuchin, R. Venugopalan, and W. Vogelsang i

Quantum Optics – and Heavy Ions?
R. Glauber 1

Drell-Yan, J/ψ and High-p_T Hadrons at Large X_F: Breakdown of QCD Factorization
B. Kopeliovich 13

Theory Underlying Coulomb – Nuclear Interference CNI Polarimeter
E. Leader 25

Color Glass Condensate at the LHC: Hadron Multiplicities in *pp*, *pA* and *AA* Collisions
E. Levin and M. Nardi 37

Testing Saturation with Forward Jets
C. Marquet 65

Heavy Quark Correlators aboveDeconfinement
A. Mocsy 77

New Insights in High Energy QCD from General Tools of Statistical Physics
S. Munier 85

Non-Ideal Fluid Dynamics for Relativistic Nuclear Collisions
A. Muronga 97

Partcipants 127

Additional RIKEN BNL Research Center Proceeding Volumes 129

Theory Summer Program on RHIC Physics

– Introduction and Overview –

We are presently in a very exciting and important phase of the RHIC era. A huge body of data has been gathered in heavy-ion collisions that provides very convincing evidence for the formation of a quark gluon plasma in central collisions. Recently, studies of nuclear modification factors in forward dAu collisions have shown tantalizing signatures that may be understood most naturally in terms of a universal form of matter controlling the high energy limit of strong interactions, the Color Glass Condensate. Finally, important advances have also been made in spin physics, where first measurements of single-transverse and double-longitudinal spin asymmetries have been presented, marking a qualitatively new era in this field.

The wealth of the new experimental data called for a workshop in which theorists took stock and reviewed in depth what has been achieved, in order to give guidance as to what avenues should be taken from here. This was the idea behind the workshop "Theory Summer Program on RHIC Physics". We decided to invite a fairly small number of participants – some world leaders in their field, others only at the beginning of their careers, but all actively involved in RHIC physics. Each one of them stayed over an extended period of time from two to six weeks. Such long-terms stays led to particularly fruitful interactions and collaborations with many members of the BNL theory groups, as well as with experimentalists at BNL. They also were most beneficial for achieving the main goal of this workshop, namely to perform detailed studies. The participants were (in alphabetical order): Hisato Eguchi (Niigata Univ.), Roy Glauber (Harvard Univ.), Boris Kopeliovich (MPI, Heidelberg), Elliot Leader (Imperial College), Eugene Levin (Tel Aviv Univ.), Cyrille Marquet (SPhT, Gif-sur-Yvette), Agnes Mocsy (Frankfurt Univ.), Stephane Munier (Ecole Polytechnique, Palaiseau), Azwinndini Muronga (Frankfurt University) and Marzia Nardi (Torino Univ.).

The workshop has been a great success. Significant advances have been made. We are grateful to all participants for coming to the Center, and for their dedicated efforts relating to the theory relevant to RHIC. The support provided for this workshop by Prof. T.D. Lee, Dr. N. Samios and the RIKEN-BNL Research Center has been magnificent, and we are very thankful for it. We thank Dr. L. McLerran for his encouragement. We are grateful to Brookhaven National Laboratory and the U.S. Department of Energy for providing the facilities to hold it. Finally, sincere thanks go to Pamela Esposito for her invaluable help in organizing and running the workshop.

BNL, September 2004

D. Kharzeev, S. Kretzer, D. Teaney, K. Tuchin, R. Venugopalan, W. Vogelsang.

Quantum Optics – and Heavy Ions?

R. J. Glauber
Harvard University

The field we call quantum optics these days is, of course, fundamentally just quantum electrodynamics. But it's fair to say that the need for a fully quantum mechanical treatment of the electromagnetic field was not felt strongly until the 1950's and '60's, when interest was directed toward a number of problems involving multi-photon states. Among these were the development of the laser, the study of Hanbury Brown-Twiss (HBT) photon corrections, and the various meanings of coherence. We shall begin by discussing the HBT experiments on intensity interferometry and photon correlations and show how these suggest the definition of a hierarchy of orders of coherence. The fully coherent states are shown to wipe out the HBT correlations. Those correlations are shown to be due to the random mixtures of coherent states present in ordinary light. The laser, on the other hand, is based on an essentially classical polarization current which oscillates with a stabilized amplitude. It radiates a mixture of coherent states random only in phase. The HBT correlation seen in heavy-ion events is due, by contrast, to the highly random nature of the source. We conclude by discussing a novel HBT experiment due to Shimizu, which detects the correlation in a beam of extremely slow ^{20}He atoms falling under gravity.

R. Hanbury Brown + R.Q. Twiss

Intensity interferometry

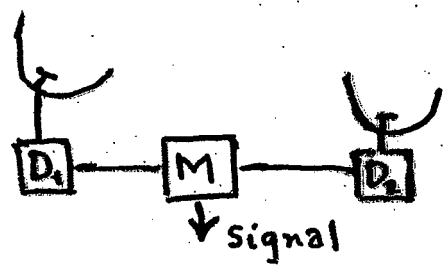

$$E(rt) = E^{(+)}(rt) + E^{(-)}(rt)$$

$$E^{(+)}(rt) \sim e^{-i\omega_k t}$$

$$E^{(-)}(rt) \sim \{E^{(+)}(rt)\}^*$$

Ordinary (Amplitude) interferometry measures $G^{(1)}(rt\,r't') \equiv \langle E^{(-)}(rt)\,E^{(+)}(r't')\rangle_{av.}$

Intensity interferometry measures

$$G^{(2)}(rt\,r't'\,r't'\,rt) = \langle E^{(-)}(rt)\,E^{(-)}(r't')\,E^{(+)}(r't')\,E^{(+)}(rt)\rangle$$

Two-photon dilemma

Hanbury Brown + Twiss '56

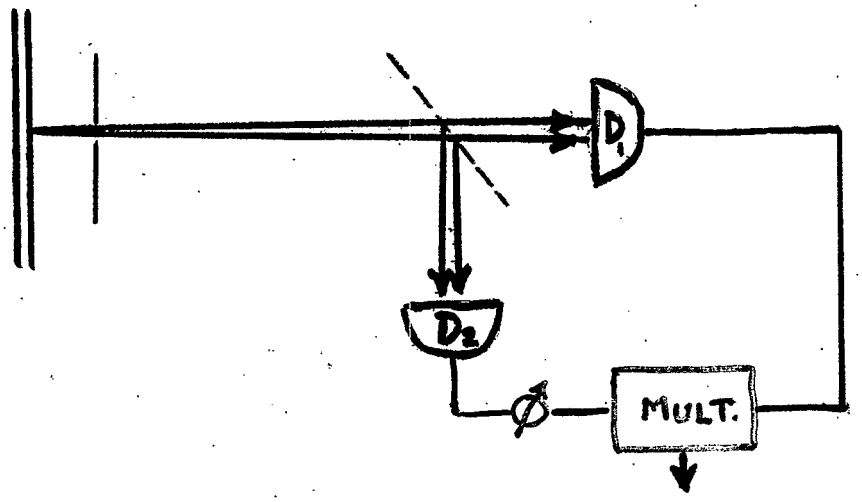

Pound + Rebka '57

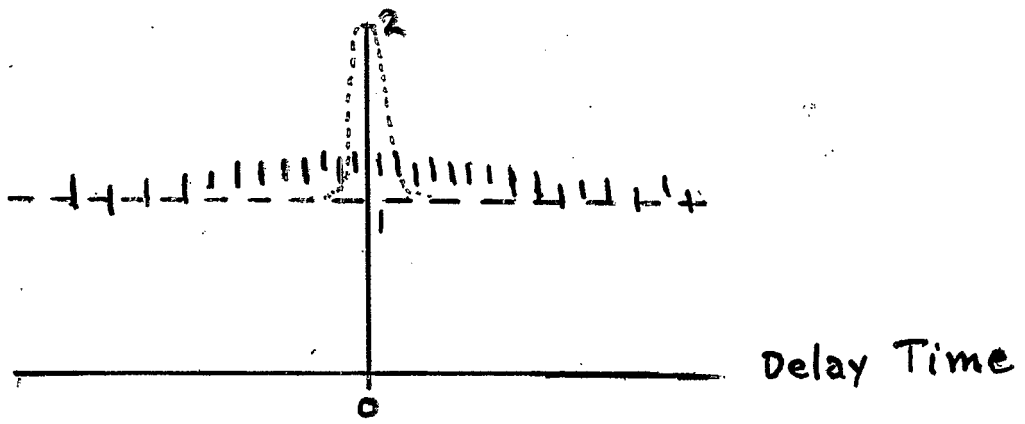

.C.A.B.

Quantized field operator: $E(rt) = E^{(+)}(rt) + E^{(-)}(rt)$

$$E^{(+)}(rt) = \sum_k \sqrt{\frac{\hbar\omega_k}{2}}\, \hat{e}(k)\, a_k\, e^{i(k\cdot r - \omega_k t)}$$

For ideal photon counter

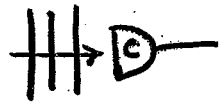

$$\text{Count rate} = w^{(1)}(rt) = s\langle E^{(-)}(rt)\, E^{(+)}(rt)\rangle$$
$$= s\, \mathrm{Tr}\{\rho E^{(-)}(rt)\, E^{(+)}(rt)\}$$
$$= s\, G^{(1)}(rt, rt)$$

where the First Order Correlation Function is:

$$G^{(1)}(rt\, r't') = \mathrm{Tr}\{\rho E^{(-)}(rt)\, E^{(+)}(r't')\}$$

For two counters –

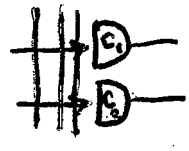

Joint counting rate

$$w^{(2)}(rt, r't') = s^2\, \mathrm{Tr}\{\rho E^{(-)}(rt) E^{(-)}(r't') E^{(+)}(r't') E^{(+)}(rt)\}$$
$$= s^2\, G^{(2)}(rt\; r't', r't'\; rt)$$

with Second Order Correlation Fn:

$$G^{(2)}(x_1 x_2\, x_3\, x_4) = \mathrm{Tr}\{\rho\, E^{(-)}(x_1)\, E^{(-)}(x_2)\, E^{(+)}(x_3)\, E^{(+)}(x_4)\}$$
$$x = (\vec{r}, t)$$

NOTE: Normal ordering of field operators.

Define correlation fn. $G^{(1)}(r_1 t_1, r_2 t_2) = \langle E^{(-)}(r_1 t_1) E^{(+)}(r_2 t_2) \rangle$

Young's 2-pinhole exp't:

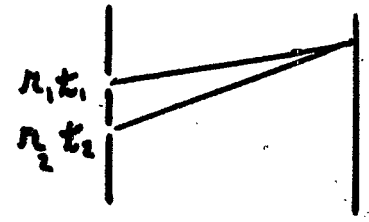

~ measures $G^{(1)}(r_1 t_1, r_1 t_1) + G^{(1)}(r_2 t_2, r_2 t_2) + 2\,\mathrm{Re}\, G^{(1)}(r_1 t_1, r_2 t_2)$

coherence maximizes fringe contrast

Schwarz inequality: $|G^{(1)}(x_1 x_2)|^2 \leq G^{(1)}(x_1 x_1) G^{(1)}(x_2 x_2)$

Optical coherence: $|G^{(1)}(x_1 x_2)|^2 = G^{(1)}(x_1 x_1) G^{(1)}(x_2 x_2)$

Sufficient condition: $G^{(1)}$ factorizes

i.e. $G^{(1)}(x_1 x_2) = \mathcal{E}^*(x_1)\, \mathcal{E}(x_2)$

~ also necessary

Titulaer + G. Phys Rev 140 (1965)
145 (1966)

Define higher order coherence: e.g. Second order

$$G^{(2)}(x_1 x_2 x_3 x_4) = \langle E^{(-)}(x_1) E^{(-)}(x_2) E^{(+)}(x_3) E^{(+)}(x_4) \rangle$$
$$= \mathcal{E}^*(x_1) \mathcal{E}^*(x_2) \mathcal{E}(x_3) \mathcal{E}(x_4)$$

$\Rightarrow$ Joint count rate factorizes

$$G^{(2)}(x_1 x_2 x_2 x_1) = |\mathcal{E}(x_1)|^2 |\mathcal{E}(x_2)|^2$$

$\Rightarrow$ Wipes out HB-T correlation

n-th order coherence $n \to \infty$

What field states factorize all $G^{(n)}$?

Recall normal ordering

Sufficient to have $E^{(+)}(r t) | \rangle = \mathcal{E}(r t) | \rangle$

~ defines coherent states

Convenient basis for averaging normally ordered products

Many-mode fields: $\{a_k\} \rightarrow \{\alpha_k\}$ in coh. states

$$E^{(+)}(r\,t) = i \sum_k \sqrt{\frac{\hbar\omega_k}{2}}\, a_k\, u_k(r)\, e^{-i\omega_k t}$$

$$\mathcal{E}(r\,t) = i \sum_k \sqrt{\frac{\hbar\omega_k}{2}}\, \alpha_k\, u_k(r)\, e^{-i\omega_k t}$$

In a Coh. state of field: $E^{(+)}(r\,t)|\{\alpha_k\}\rangle = \mathcal{E}(r\,t)|\{\alpha_k\}\rangle$

$$G^{(1)}(r\,t\;r'\,t') \equiv \langle E^{(-)}(r\,t)\, E^{(+)}(r'\,t')\rangle$$
$$= \mathcal{E}^*(r\,t)\, \mathcal{E}(r'\,t')$$

~ First order coherence

Coherence $\longleftrightarrow$ Factorization

Let $x_i = (r_i\, t_i)$

Full coherence , $n = 1, 2, 3, \ldots$

$$G^{(n)}(x_1 \cdots x_{2n}) = \mathcal{E}^*(x_1) \cdots\cdots \mathcal{E}(x_{2n})$$

L.D.L.

Full coherence $\longrightarrow$ $P(n)$ = Poisson distrib.

n-detector joint counting rates

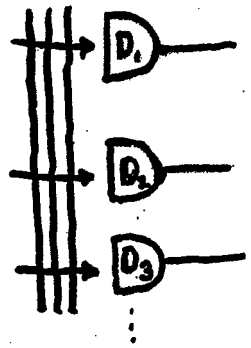

$$G^{(n)}(x_1 \cdots x_n x_n \cdots x_1) = \prod_{j=1}^{n} G^{(1)}(x_i x_i)$$

~ Uncorrelated <u>No</u> HB-T effect

Ordinary - non coherent - light sources have randomly distributed amplitudes α_k.

I.D.L.

e.g. Gaussian distrib. of amplitudes $\{\alpha_k\}$

Single-mode density operator

$$\rho_{chaotic} = \frac{1}{\pi\langle n\rangle}\int e^{-\frac{|\alpha|^2}{\langle n\rangle}} |\alpha\rangle\langle\alpha|\, d^2\alpha$$

$$= \frac{1}{1+\langle n\rangle}\sum_{j=0}^{\infty}\left(\frac{\langle n\rangle}{1+\langle n\rangle}\right)^j |j\rangle\langle j|$$

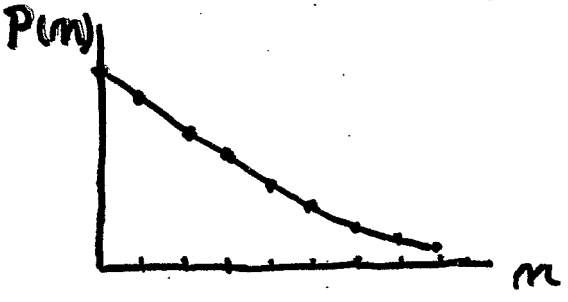

Two-Fold joint count rate:

$$G^{(2)}(x_1 x_2 x_2 x_1) = G^{(1)}(x_1 x_1)\, G^{(1)}(x_2 x_2) + \underbrace{G^{(1)}(x_1 x_2)\, G^{(1)}(x_2 x_1)}_{\text{HB-T Effect}}$$

Note for $x_2 \to x_1$

$$G^{(2)}(x_1 x_1 x_1 x_1) = 2\left[G^{(1)}(x_1 x_1)\right]^2$$

:O.L.

One mode excitation

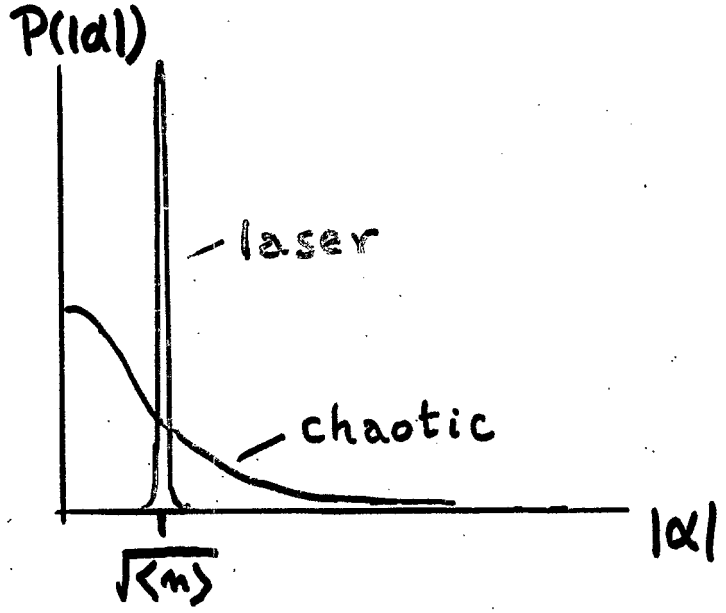

Photocount distrib's (w = average count rate)

Coherent state:

$$p(n) = \frac{(wt)^n}{n!} e^{-wt}$$

Chaotic state: $$p(n) = \frac{(wt)^n}{(1+wt)^{n+1}}$$

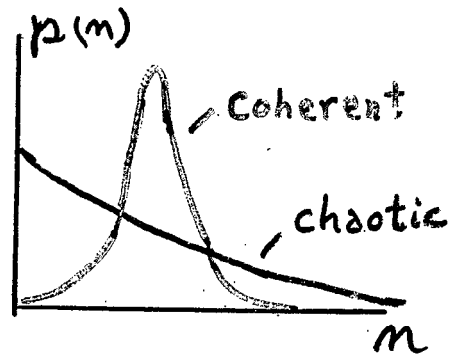

Distrib. of time intervals till first count

coherent: $$P(t) = w e^{-wt}$$

chaotic: $$P(t) = \frac{w}{(1+wt)^2}$$

Given count at t=0, distrib. of intervals till next count

Coherent: $$P(0|t) = w e^{-wt}$$

chaotic: $$P(0|t) = \frac{2w}{(1+wt)^3}$$

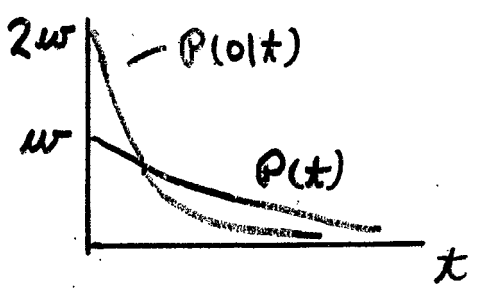

F. Shimizu Experiment

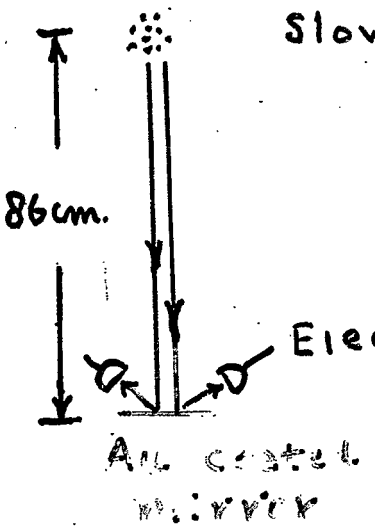

Slowed $^{20}Ne^*$ atoms, $J=0$ bosons

$\langle v \rangle_{Th} \sim 20$ cm/sec.

~ 100 atoms / sec.

Free fall velocity $= \sqrt{2gh}$

$= \sqrt{2 \times 980 \times 86}$

$= 410$ cm/sec $\gg \langle v \rangle_{Th}$

Hanbury Brown - Twiss Experiment for $^{20}Ne^*$ atoms

~ measures distrib. of intervals between successive electron counts

M. Yasuda + F. Shimizu, Phys Rev. Lett. 77 3090 (1996)

Note: $^{21}Ne^*$ is a $J=\frac{3}{2}$ fermion

Drell-Yan, J/ψ and high-p_T hadrons at large x_F: Breakdown of QCD factorization

B. Kopeliovich
MPI Heidelberg

Unexpected results from d-Au

versus X compared to lower

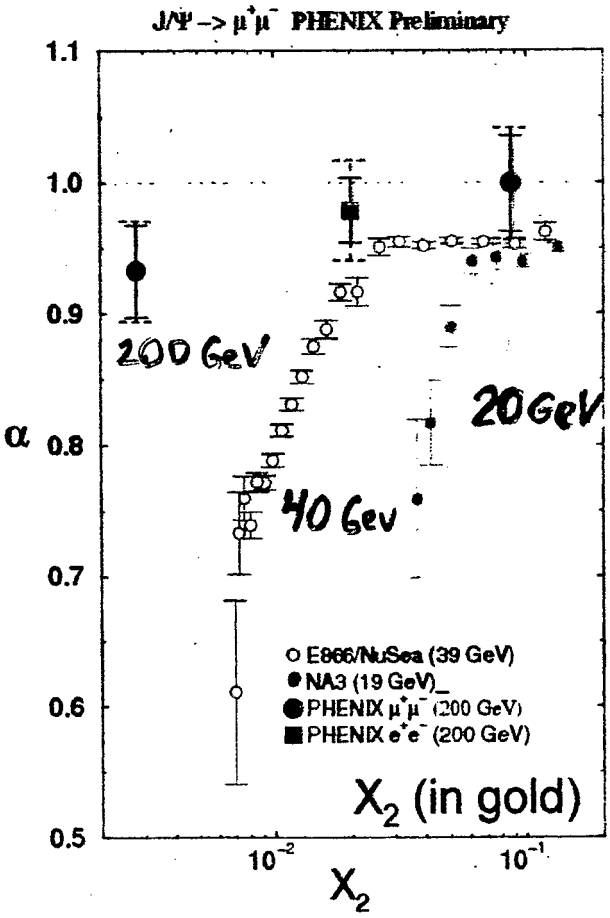

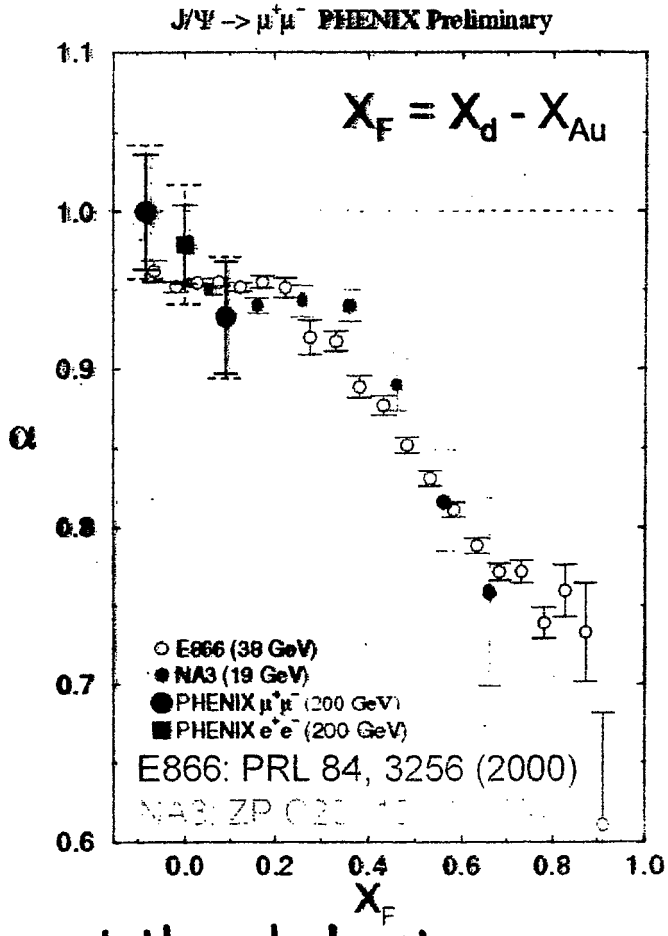

universal versus X_2 : shadowing is not the whole story.

ıe versus X_F for diff √s. Incident parton energy loss ? (high X_d :

ˈgy loss expected to be weak at RHIC energy.

anuary 2004 QM04 – Raphaël Granier de Cassagnac

x_1 - , rather than x_2 - scaling

expected by everybody

Drell-Yan reaction

E-772

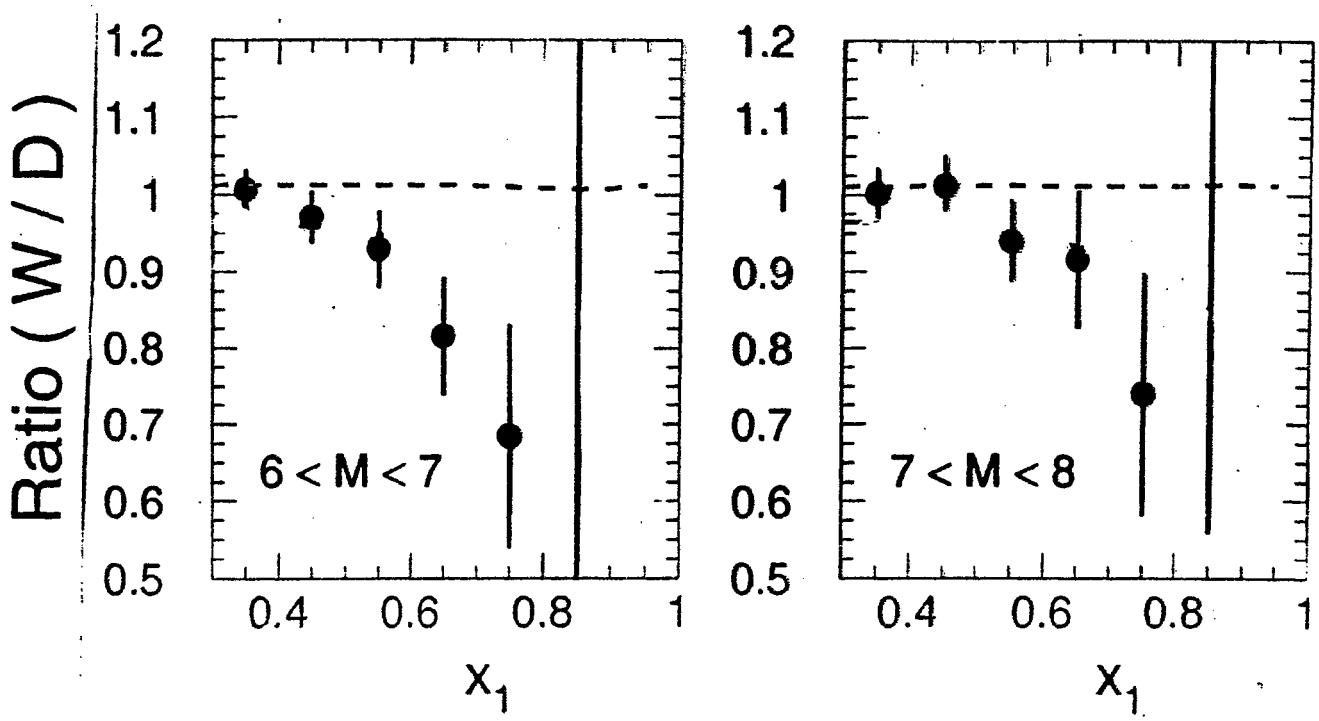

W. Geist, QM 1991

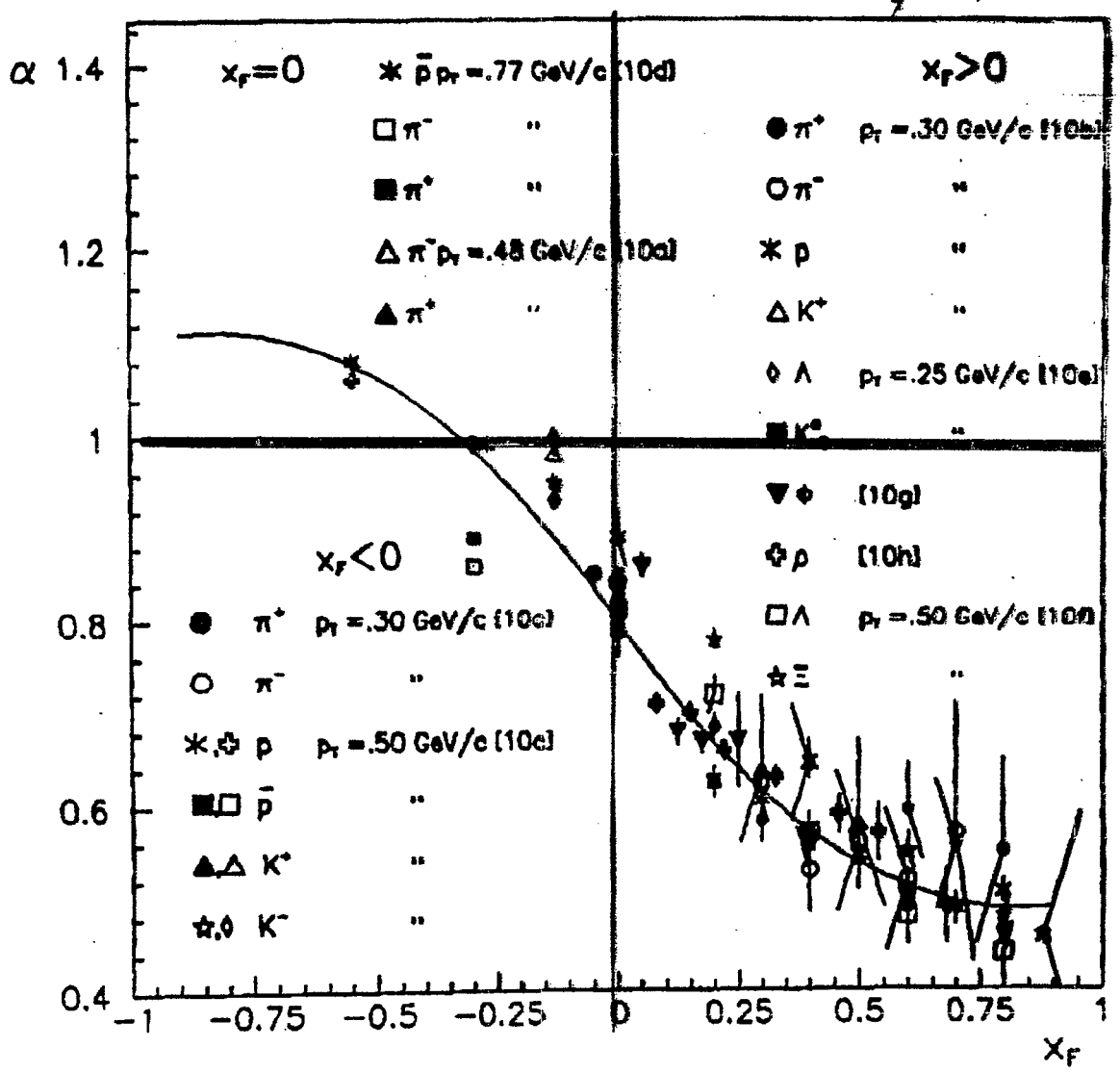

Fig. 5 : α as function of x_F for various hadron species produced in pA collisions.

Conclusion: soft valence quarks are suppressed in pA at large rapidities.

M. Johnson et al

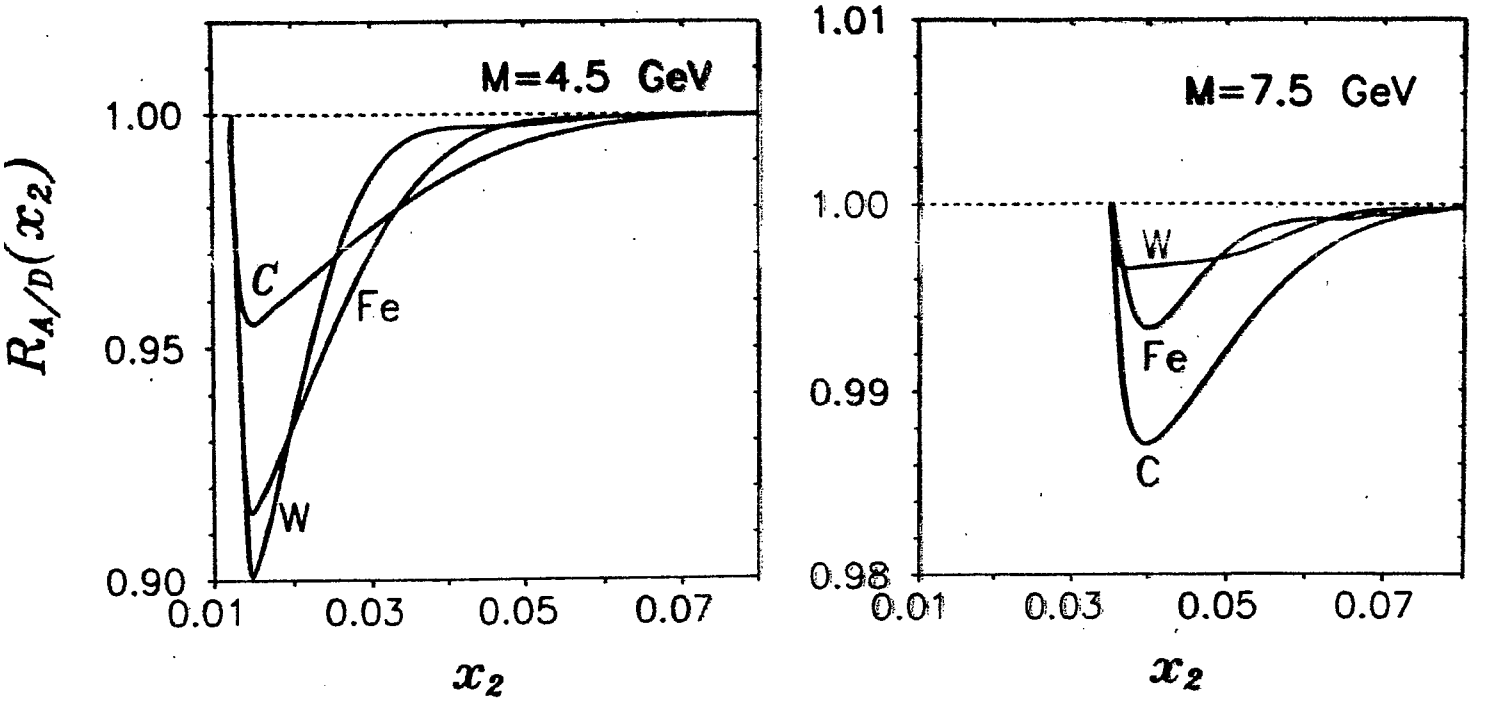

Figure 14: *Shadowing in DY reaction on carbon, iron and tungsten as function of x_2 at $M = 4.5\,GeV$. Nuclear shadowing disappears at large and small x_2 because the coherence length, Eqs. (7) and (8), vanishes in these limits.*

Figure 15: *The same as in Fig. 14, but at $M = 7.5\,GeV$.*

Breakdown of factorization at $x_1 \to 1$

Coherence length for 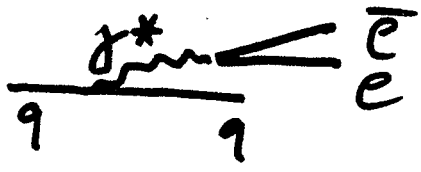

$$\ell_c = \frac{2 E_q\, x(1-x)}{M^2(1-x) + x^2 m_q^2 + k_T^2}$$

$x > x_1$ therefore $\ell_c \to 0$ at $x_1 \to 1$

although x_2 reaches minimum

Coherence length in DIS

$$l_c = \frac{P}{m_N x_2}$$

P varies for longitudinal, transverse photons and gluon shadowing

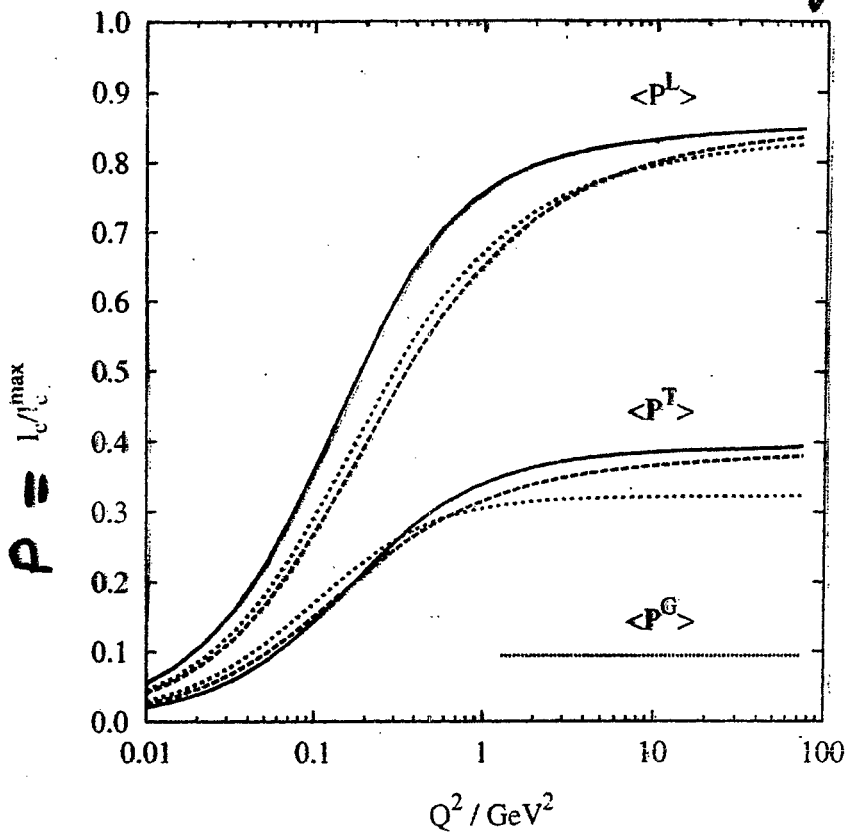

J. Raufeis
A. Tarasov
B.K.
2001

Figure 1: Q^2 dependence of the factor $\langle P \rangle = l_c/l_c^{max}$ defined in (1) at $x_{Bj} = 0.01$. for $\bar{q}q$ fluctuations of transverse and longitudinal photons, and for $\bar{q}qG$ fluctuation, from the top to bottom, respectively. Dotted curves correspond to calculations with perturbative wave functions and an approximate dipole cross section $\propto r_T^2$. Dashed curves are the same, except the realistic parameterization (14). The solid curves show the most realistic case based on the nonperturvative wave function (25). The coherence length for gluons calculated in sec. (2.4) is also shown.

In Drell-Yan reaction and heavy flavor production one should replace $\boxed{x_2 \to \tilde{x}_2 \approx \frac{x_2}{1-x_1}}$

There is no room for gluon shadowing either in DY, or J/ψ production at 800 GeV

$$\ell_c = \frac{P_G}{m_N} \frac{s}{M^2} x_1 (1-x_1)$$

Even for J/ψ

- $\ell_c^{max} = 0.8 \text{ fm}$ at $x_1 = 0.5$

What suppresses DY pairs and J/ψ at large x_2 ?

¡The projectile parton distribution at $x_1 \to 1$ depends on the target!

(anoter source of factorization breakdown)

The number of projectile partons and Fock state decomposition depends on resolution of the interaction.

The resolution of a nuclear target is controlled by the <u>saturation scale</u> Q_s which rises with A.

The more partons is resolved by the target, the steeper is behavior of the single-parton distribution at $x_1 \to 1$. $f_a(x_1) \propto (1-x_1)^{n(A)}$

Further description of data is model dependent

- QGSM / dual parton model

A. Kaidalov
A. Capella

Ingridients:

- The hadronic spectrum is a convolution of the initial parton distribution with the fragmentation functions.
  Both are controlled by the Regge behavior.
- The weights of multi-Pomeron cuts are given by AGK cutting rules and Glauber numbers of collision.
- Energy conservation brakes down the AGK cancellation at $x_1 \Rightarrow 1$
- Every extra cut Pomeron adds a factor $(1-x_1)$ to the parton distribution

¡The AGK cutting rules can be applied to multiple interactions in a nucleus only if the coherence length for the relevant Fock states exceeds the nuclea size.!

This condition is easily satisfied for soft hadronic fluctuations, even at low energies, but not for hard processes (no gluon shadowing for DY and J/ψ at 800 GeV).

However, at $x_1 \to 1$ a <u>short-living</u> hard fluctuation emerges inside a <u>long-living</u> valence quark. Therefore it must follow the quark distribution i.e. it gets <u>suppressed</u> at $x_1 \to 1$

M. Johnson
J. Newchil
I. Potashnikova
B.K.

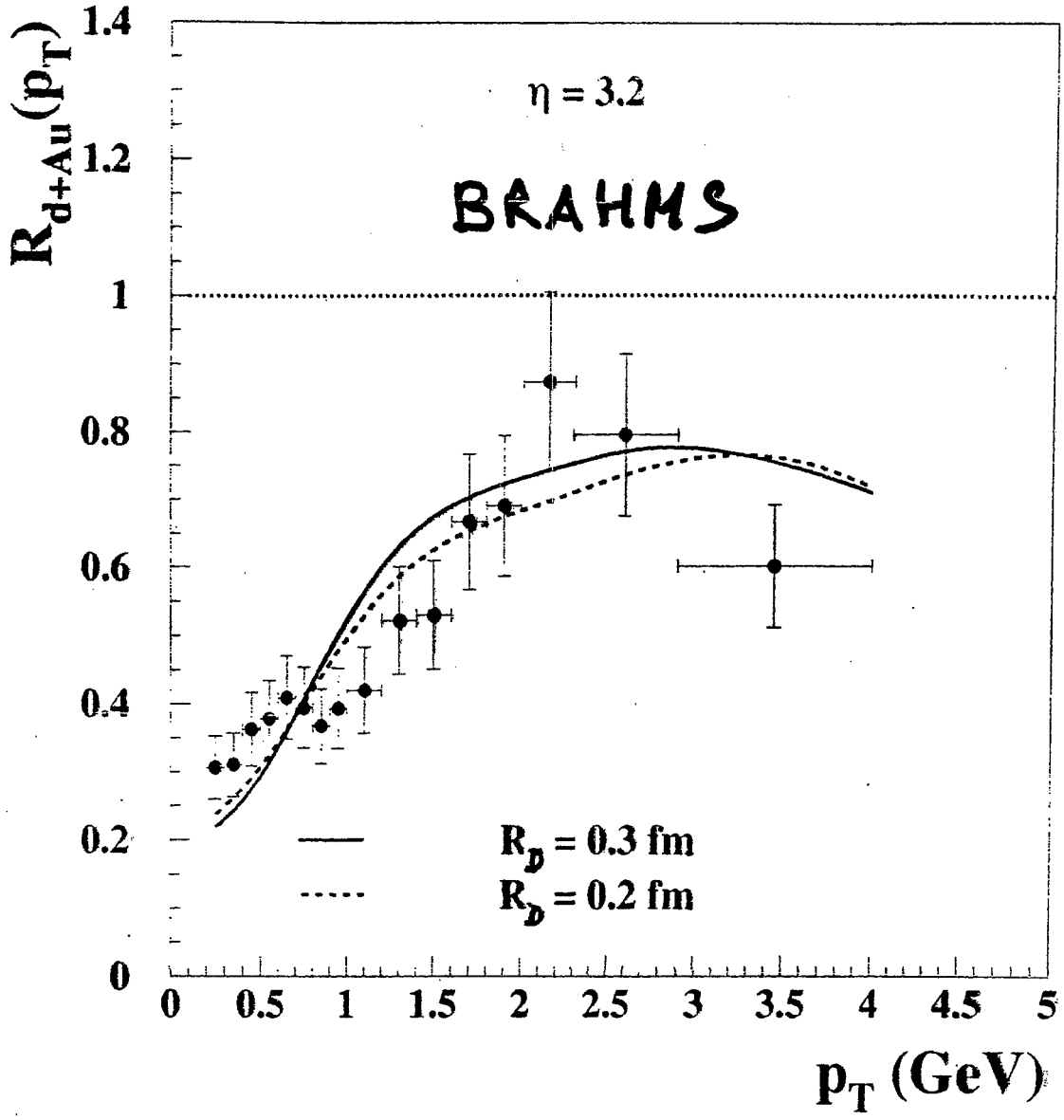

Fragmentation functions $u \to \pi^-$ and $d \to \pi^-$ were used

Conclusions

- Nuclei suppress cross sections. of inclusive production approaching the kinematic limit ($x_F \to 1$, $x_T \to 1$...
- In this limit coherence effects (interferences/shadowing) vanish
- QCD factorization fails in this limit.
- Parton distributions become process dependent.
- x_2 scaling fails for DY and J/ψ production. It is replaced by x_1 scaling
- The Cronin effect turns into a suppression at large η at RHIC

Theory Underlying Coulomb – Nuclear Interference CNI Polarimeter

Elliot Leader
Imperial College, UK

The Analyzing Power A

$$p\,(\text{Poln } \underline{P}) + B\,(\text{unpol}) \rightarrow C + D$$

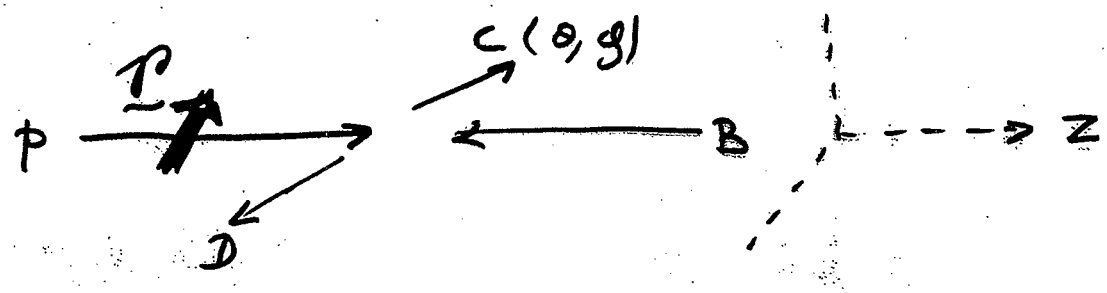

$$\frac{d^2\sigma}{dt\,d\phi} = \frac{1}{2\pi}\frac{d\sigma}{dt}\left\{1 + A(s,t)\left[P_y \cos\phi - P_x \sin\phi\right]\right\}$$

A = analyzing power of reaction.

= function of energy + mom. transfer

Usually elastic scattering:

$$p(\underline{P}) + p \rightarrow p + p$$

$$p(\underline{P}) + N \rightarrow p + N$$ ← nucleus

Usually: Know $\mathcal{P}$, MEASURE A,

Test models of strong interactions.

Usually: In NON-PERTURBATIVE regime.

RHIC: Try to know A, use to

measure $\mathcal{P}$ (to $\pm$ 5%)

NO HOPE OF CALCULATING A FROM

NON-PERTURBATIVE STRONG INTERACTIONS

RESCUED BY ELECTROMAGNETIC —

HADRONIC INTERFERENCE.

ELECTROMAGNETIC – HADRONIC INTERFERENCE

PROTON – PROTON SCATTERING

VERY QUALITATIVE DISCUSSION.

DETAILS IN PAPERS LISTED.

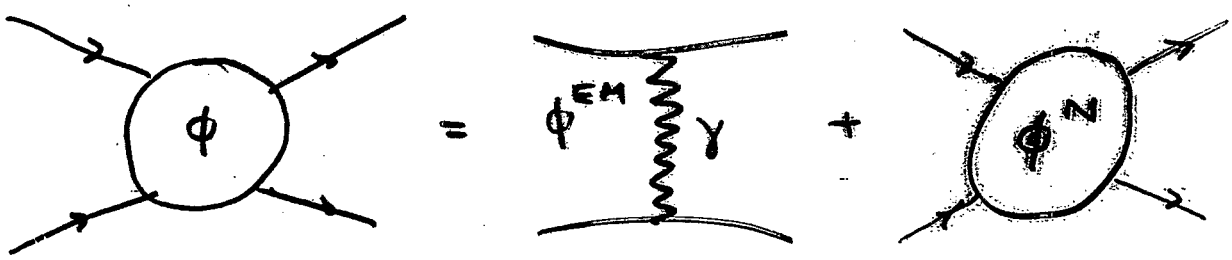

FIVE AMPLITUDES: $\phi_i \quad i = 1 \cdots 5$

APPROX: $\phi_i = \phi_i^{EM} + \phi_i^{N}$

	ϕ_1 ++ ; ++	ϕ_3 +− ; +−	ϕ_2 ++ ; −−	ϕ_4 +− ; −+	ϕ_5 ++ ; −+
N	CONST	CONST	CONST	t	$\sqrt{-t}$
EM	$1/t$	$1/t$	CONST	CONST	$1/\sqrt{-t}$
	NO HELICITY FLIP		DOUBLE HELICITY FLIP		SINGLE HEL. FLIP

BEHAVIOUR AS $t \to 0$

SMALL t — (REAL)

$$\phi_1^{EM} = \sqrt{4\pi}\,\frac{\alpha}{t} \qquad \phi_3^{EM} = \sqrt{4\pi}\,\frac{\alpha}{t} \qquad \phi_5^{EM} = -\sqrt{4\pi}\,\frac{\alpha\kappa}{2m\sqrt{-t}}$$

ANOM. MAG. MOM

HIGH ENERGY AND SMALL t :

1) HADRONIC NON-FLIP AMPLITUDES

$\approx$ IMAGINARY

2) ϕ_2^N BELIEVED NEGLIGIBLE

$$\phi_1^N(t) + \phi_3^N(t) \approx i\,\mathrm{Im}\left[\phi_1^N(0) + \phi_3^N(0)\right]$$

the "big" amplitud

$$= \frac{i}{\sqrt{4\pi}}\,\sigma_{TOT} \quad \text{(OPTICAL THEOREM)}$$

$$\therefore \frac{d\sigma}{dt} \approx \frac{1}{2}\left[|\phi_1|^2 + |\phi_3|^2\right]$$

$$\approx 4\pi\left[\frac{\alpha^2}{t^2} + \left(\frac{\sigma_{TOT}}{8\pi}\right)^2\right]$$

$\therefore$ EM and HADRONIC COMPARABLE AT

$$|t_c| = \frac{8\pi\alpha}{\sigma_{TOT}}$$

$\therefore$ EM DOMINATES FOR $|t| \lesssim 2\times10^{-3}\left(\frac{\mathrm{GeV}}{c}\right)^2$

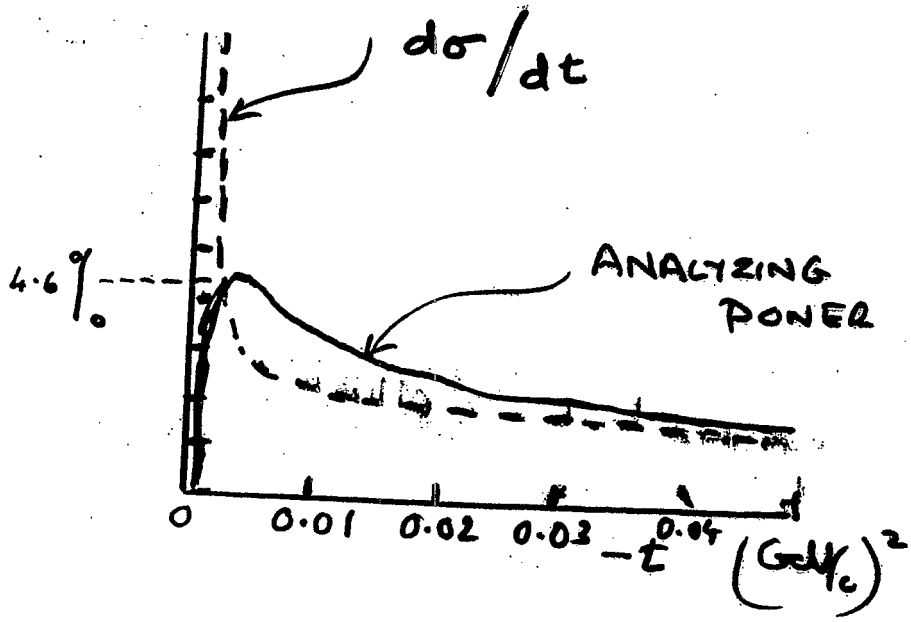

ANALYZING POWER:

USE EM ampl: REAL

USE N ampl: IMAGINARY

$$A \approx -\frac{2\,\mathrm{Im}\left[\phi_5^*\left(\phi_1+\phi_3\right)\right]}{|\phi_1|^2+|\phi_3|^2}$$

$$A(s,t) \approx A_{MAX}\left\{\frac{4\left(t/t_{MAX}\right)^{3/2}}{3\left(t/t_{MAX}\right)^2+1}\right\}$$

$$t_{MAX} = -\frac{8\sqrt{3}\,\pi\alpha}{\sigma_{TOT}} = -\sqrt{3}\,|t_c|$$

A has a MAX at t_{MAX}:

$$A_{MAX} = \frac{\pi \sqrt{-3\, t_{MAX}}}{4\, m}$$

$p_L = 200$ GeV/c $\quad \sigma_{TOT} \sim 100$ (GeV/c)^2

$$\Rightarrow \quad t_{MAX} \approx -3 \times 10^{-3} \ (\text{GeV/c})^2$$

$$\Rightarrow \quad A_{MAX} \approx 4 \cdot 6 \ \%$$

USE OF ANALYZING POWER:

BEAM OF POLARIZED PROTONS ALONG OZ:

Spin-polarization vector $\underline{P}$

$$\frac{d^2\sigma}{dt\, d\phi} = \frac{1}{2\pi} \frac{d\sigma}{dt} \left[1 + A(s,t) \left(P_y \cos\phi - P_x \sin\phi \right) \right]$$

$\therefore$ KNOWING $A(s,t)$ ALLOWS MEASUREMENT OF P_x, P_y.

$\Rightarrow$ " Coulomb interference polarimeter"

PROBLEM: $A(s,t)$ GIVEN ABOVE IS

APPROXIMATE : NEGLECTS ϕ_5^N

HOW BAD IS THIS APPROX ??

CAN WE MEASURE $\underset{\sim}{\mathcal{P}}$ to 5% ACCURACY?

THE COMPLETE EXPRESSION at small t is:

$$\frac{m\sqrt{-t}}{\sigma_{TOT}} A \frac{d\sigma}{dt} = \alpha\left(\frac{\varkappa}{2} - I_5 + \frac{\varkappa}{2} I_2\right)$$

$$+ \frac{\sigma_{TOT}}{8\pi}\left[R_5(1+I_2) - I_5(\rho + R_2)\right] t$$

$$\left[|t| = O\left(\frac{8\pi\alpha}{\sigma_{TOT}}\right)\right]$$

$$R_2 + i I_2 \equiv \frac{\phi_2^N}{\mathrm{Im}\left(\phi_1^N + \phi_3^N\right)}$$

$$R_5 + i I_5 \equiv \left(\frac{m}{\sqrt{-t}}\right) \frac{\phi_5^N}{\frac{1}{2}\,\mathrm{Im}\left(\phi_1^N + \phi_3^N\right)}$$

$$\rho \equiv \left.\frac{\mathrm{Re}\left(\phi_1^N + \phi_3^N\right)}{\mathrm{Im}\left(\phi_1^N + \phi_3^N\right)}\right|_{t=0}$$

We <u>think</u> these terms are very small at high energies, but we don't really

Regge Pole theory of elastic scattering

ϕ^N :

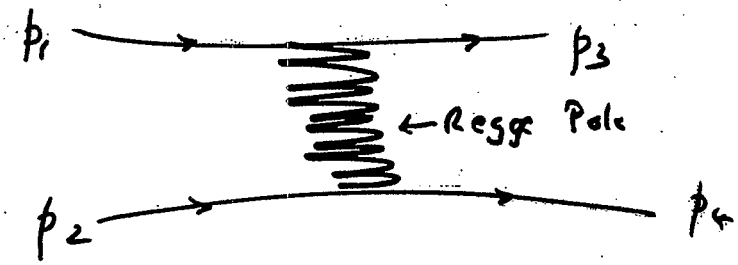

$$s = (p_1 + p_2)^2 \qquad t = (p_1 - p_3)^2$$

Poles labelled by: Signature $\tau = \pm$, I-spin ...

$$A_+(s,t) = -\beta(t)\, s^{\alpha(t)-1}\left[i - \cot\frac{\pi\alpha(t)}{2}\right]$$

$$A_-(s,t) = +\beta(t)\, s^{\alpha(t)-1}\left[i + \tan\frac{\pi\alpha(t)}{2}\right]$$

Pole	τ	I	$\alpha(t) = \alpha(0) + \alpha' t$	Flip Helicity?
$\mathbb{P}$ = Pomeron	+	0	$\approx 1 + 0.3t$	??
ρ	−	1	$\approx \frac{1}{2} + t$	strong
a_2	+	1		strong
ω	−	0		weak
f	+	0		weak

[t in (GeV/c)^2]

For very small t in Int. region:

$$A_{\mathbb{P}} \simeq i\beta_{\mathbb{P}} \qquad f, a_2 : A \simeq \beta s^{-1/2}(-i+1)$$

$$\rho, \omega : A \simeq \beta s^{-1/2}(i+1) \qquad [\beta = \beta(0)]$$

Eventually, as $s \to \infty$, only $A_{\mathbb{P}}$ survives.

KEY QUESTIONS

1) Does $\mathbb{P}$ flip helicity? If it does I_2 will never be negligible. Suspect flip is very small or zero

2) At RHIC can we neglect ρ, ω, f, a_2? Depends on relative size of residues. Depends on which amplitude: ρ, a_2 have large flip.

The proton-carbon CNI polarimeter.

Carbon is better as target for 2 reasons: Practical + Theoretical.

THEORETICAL ADVANTAGES.

1) $I = 0$ $\therefore$ only R-poles with $I = 0$ can contribute: $\mathbb{P}$, ω, f — small helicity flip.

2) Spin 0: simpler amplitude structure Φ^c_{NF} and Φ^c_F

3) The pC amplitudes can be related to the pp amplitudes with moderate confidence.

Result: A^{pC} depends on 3 real parameters from $pp \to pp$: $\beta_{\mathbb{P}}$, β_ω, β_f

With best estimate of these:

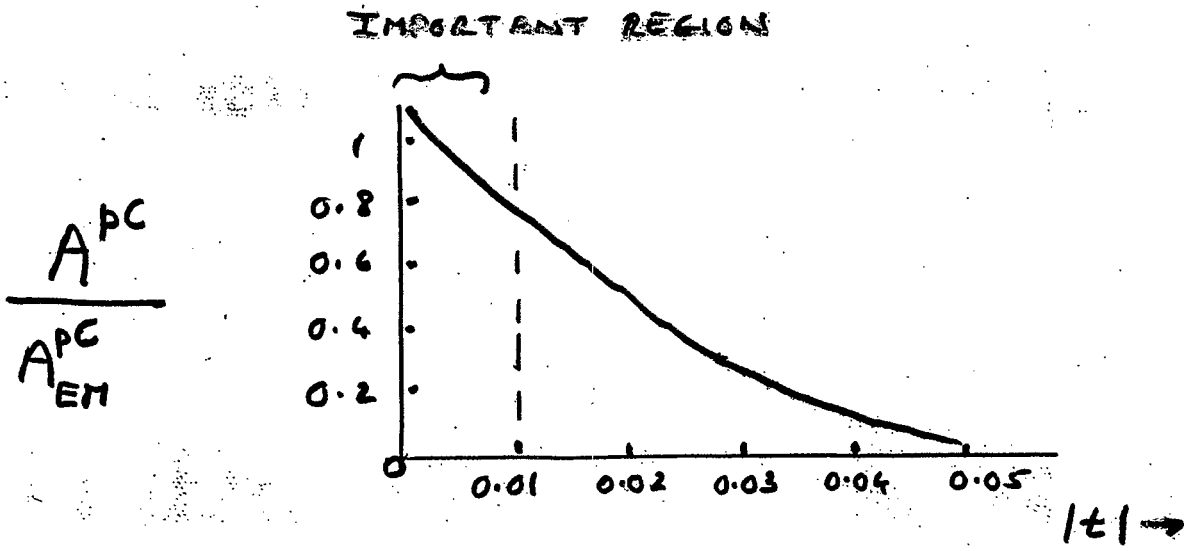

(Trueman: hep-ph/0305085)

∴ significant 20% effect due to hadronic amplitudes. Are they accurate to 5% ????

SAFEST : Use as RELATIVE polarimeter until can measure A

POLARIZED JET PROTON TARGET

Jet Beam polarization accurately known. ($P > 90\%$)

Scatter unpolarized protons. Measure asymmetry.

$\Longrightarrow$ value of A.

(IDENTICAL PARTICLES) : $\vec{p} + p \rightarrow p + p \;=\; p + \vec{p} \rightarrow p + p$)

BNL-NT-04/26
August 3, 2004

arXiv:hep-ph/0408050 v1 3 Aug 2004

Color Glass Condensate at the LHC: hadron multiplicities in pp, pA and AA collisions

Dmitri Kharzeev[a], Eugene Levin[a,b] and Marzia Nardi[a,c]

a) Department of Physics,
Brookhaven National Laboratory,
Upton, New York 11973-5000, USA

b) HEP Department, School of Physics,
Raymond and Beverly Sackler Faculty of Exact Science,
Tel Aviv University, Tel Aviv 69978, Israel

c) Dipartimento di Fisica Teorica dell'Università di Torino,
via P.Giuria 1, 10125 Torino, Italy

We make quantitative predictions for the rapidity and centrality dependencies of hadron multiplicities in AA, pA and pp collisions at the LHC energies basing on the ideas of parton saturation in the Color Glass Condensate.

INTRODUCTION

At high energies QCD is expected to enter the new phase : the Color Glass Condensate (CGC) which is characterized by strong coherent gluon fields leading to parton saturation [1, 2, 3, 4, 5]. Previously, we have applied this approach [11, 12, 13, 14, 15] to describe the wealth of experimental data [6, 7, 9, 10] from RHIC. The LHC will allow to extend further the investigations of QCD in the regime of high parton density. This is because the new scale of the problem, the saturation momentum Q_s, will become so large ($Q_s^2 \approx 5-10$ GeV^2) that a separation of CGC physics from non-perturbative effects should become easier. The main objective of this paper is to give predictions for the global characteristics of the inelastic events in nucleus-nucleus, proton-nucleus and proton-proton collisions at LHC energies basing on the ideas of parton saturation in the Color Glass Condensate (CGC).

To understand better the differences implied by a higher energy of the LHC, let us start with the main assumptions of the approach we used to describe the data from RHIC:

1. At Bjorken $x \leq 10^{-2}$ the inclusive production of partons (gluons and quarks) is driven by parton saturation in strong gluon fields as given by McLerran-Venugopalan model [3].

2. The region of $x \approx 10^{-3}$ (accessible at forward rapidities at RHIC) is considered as the low x region in which $\alpha_S \ln(1/x) \approx 1$ so the quantum evolution becomes important; we assume that $\alpha_S \ll 1$ to keep the calculation simple and transparent;

3. We assume that the interaction in the final state does not change significantly the multiplicities of partons resulting from the early stages of the process; this may be a consequence of local parton hadron duality, or of the entropy conservation. Therefore multiplicity measurements are extremely important for uncovering the reaction dynamics. However, we would like to state clearly that we do not claim that the interactions in the final state are unimportant. Rather, we consider the CGC as the initial condition for the subsequent evolution of the system, which can be described for example by means of hydrodynamics (such an approach has been followed in Refs. [16, 17]).

Even a superficial glance at these three assumptions reveals that the conditions for the applicability of our approach at the LHC improve. Indeed, at LHC energies the value of x will be two orders of magnitude lower than at RHIC. This makes the use of the well–developed methods of low x physics [4, 5, 12, 18, 19, 20, 22] better justified. At LHC energies we have a theoretical tool to deal with the high parton density QCD in the mean field approach (so called Balitsky-Kovchegov non-linear equation [4]), or on a general basis of the JIMWLK equation [5]; even more general approaches may be possible (see for example the Iancu-Mueller factorization [20, 21]). However, despite a number of well developed approaches which could be applied at low x we would like to warn that even the LHC energy is not high enough to apply any of the methods mentioned above without discussing possible "pre-asymptotic" corrections to them.

Consider for example the determination of the value of the saturation momentum – the key scale in the CGC phase of QCD. As was noticed first in Ref. [24] the value of the

saturation scale is affected by the next-to-leading order corrections to the BFKL kernel which were neglected in all of the discussed above approaches. Their numerical significance is so large that they cannot be neglected: if the next-to-leading order BFKL kernel is used, because of a large energy extrapolation interval to the LHC the value of Q_s^2 turns out to be 5 - 10 times smaller than if one uses the leading order kernel (see detailed discussion in Ref. [25]). However the good news is that the NLO corrections appear under theoretical control and we can take them into account.

The paper is organized as follows. In the second section we discuss the geometry of nucleus-nucleus and hadron-nucleus collisions and introduce the Glauber formalism we use. In the third section, we review the general formalism which we use to evaluate the multiplicities; we also discuss the influence of higher order corrections and the effects of the running coupling constant on the results. In the fourth section we list the parameters of our approach and justify the values we use; we then give a complete set of predictions for hadron multiplicities at the LHC energies in $Pb - Pb$, $p - Pb$, and pp collisions, including the dependences on rapidity and centrality. We then summarize our results.

THE GEOMETRY OF NUCLEUS-NUCLEUS AND HADRON-NUCLEUS COLLISIONS AND THE GLAUBER APPROACH

At high energies the paths of the colliding nucleons can be approximated by straight lines, since in a typical interaction $t/s \ll 1$ and the typical scattering angle is small. This is the most important approximation underlying the Glauber approach to nuclear interactions. Other approximations which simplify calculations but are in principle unnecessary are the smallness of the nucleon–nucleon interaction radius compared to the typical nuclear size, and the neglect of the real part of the NN scattering amplitude. Many quantities characterizing the geometry of the collision can be readily computed in this approach; a complete set of the relevant formulae can be found e.g. in [27] and we will not reproduce all of them here.

It is customary and convenient to parameterize the centrality of the collision in terms of the "number of participants" N_{part} – the number of nucleons which underwent at least one inelastic collision. This number can be directly measured experimentally (at least in principle) by detecting in the forward rapidity region the number of "spectator" nucleons N_{spect} which did not take part in any inelastic collisions; obviously, for a nucleus with mass

number A, $N_{part} = A - N_{spect}$.

The number of participating nucleons in a nucleus-A–nucleus-B interaction depends on the impact parameter b. In the eikonal approximation it can be evaluated as (see [26]):

$$N_{part}^{AB}(b) = \int d^2s\, n_{part}^{AB}(\mathbf{b},\mathbf{s}) \;=\; A \int d^2s\, T_A(\mathbf{s}) \left\{1 - [1 - \sigma_{in}\, T_B(\mathbf{b}-\mathbf{s})]^B\right\} + B \int d^2s\, T_B(\mathbf{b}-\mathbf{s}) \left\{1 - [1 - \sigma_{in}\, T_A(\mathbf{s})]^A\right\}, \qquad (1)$$

with the usual definition for the nuclear thickness function $T_A(\mathbf{s}) = \int_{-\infty}^{\infty} dz \rho_A(z,\mathbf{s})$, normalized as $\int d^2s\, T_A(\mathbf{s}) = 1$; σ_{in} is the proton-proton inelastic cross-section without diffractive component. For the LHC energies we assumed $\sigma_{in} = 70$ mb ([28]).

From Eq. (1) the definition of the local density of participants $n_{part}^{AB}(\mathbf{b},\mathbf{s})$ is evident; we will define its average over the transverse plane as

$$\langle n_{part}^{AB}\rangle(b) = \frac{\int d^2s\, [n_{part}^{AB}(\mathbf{b},\mathbf{s})]^2}{\int d^2s\, n_{part}^{AB}(\mathbf{b},\mathbf{s})}\,. \qquad (2)$$

In the following we will need to use the average number of participants computed separately for nucleus-A and nucleus-B; it is given by

$$\langle n_{part,A}^{AB}\rangle(b) = \frac{\int d^2s\, n_{part,A}^{AB}(\mathbf{b},\mathbf{s})\, n_{part}^{AB}(\mathbf{b},\mathbf{s})}{\int d^2s\, n_{part}^{AB}(\mathbf{b},\mathbf{s})}\,. \qquad (3)$$

Obviously, one has for their sum

$$\langle n_{part,A}^{AB}\rangle(b) + \langle n_{part,B}^{AB}\rangle(b) = \langle n_{part}^{AB}\rangle(b)$$

where $\langle n_{part,A}^{AB}\rangle(b)$ and $\langle n_{part,B}^{AB}\rangle(b)$ are the integrands of the first term and second term in the r.h.s of Eq. (1) respectively.

In table I we give the number of participants and their density (respectively Eqs. (1) and (2)) for Pb-Pb collisions at LHC.

The corresponding formulae for the proton–nucleus pA interaction can be deduced by setting $B = 1$ and using a delta-function for the proton thickness function (in the point-like approximation for the size of the proton). We get from Eq. (1):

$$N_{part}^{pA}(b) = A\,\sigma_{in}\, T_A(b) + \left\{1 - [1 - \sigma_{in}\, T_A(b)]^A\right\} = A\,\sigma_{in}\, T_A(b) + \left\{1 - P_0^{pA}(b)\right\}. \qquad (4)$$

b (fm)	N_{part}^{AB}	n_{part}^{AB} (fm^{-2})	b (fm)	N_{part}^{AB}	n_{part}^{AB} (fm^{-2})
0.00	406.9	2.98	8.00	166.8	2.21
1.00	402.4	2.97	9.00	127.5	1.97
2.00	387.8	2.93	10.00	91.9	1.69
3.00	363.2	2.88	11.00	61.1	1.35
4.00	330.3	2.80	12.00	36.2	0.98
5.00	291.9	2.70	13.00	18.3	0.59
6.00	250.6	2.57	14.00	7.5	0.27
7.00	208.3	2.41	15.00	2.5	0.09

TABLE I: Mean number of participants and their average density in Pb-Pb collisions at LHC as a function of b

In the previous formula the function $P_0^{pA}(b)$ is the probability of no interaction in a p-A collision at impact parameter b; the integration of $[1 - P_0^{pA}(b)]$ over b gives the inelastic proton-nucleus cross section σ_{pA}.

The average number of participants in a p-A collision can be obtained as:

$$\langle N_{part}^{pA} \rangle = \frac{\int \mathrm{d}^2 b \, N_{part}^{pA}(b)}{\int \mathrm{d}^2 b \, [1 - P_0(b)]} = A \frac{\sigma_{in}}{\sigma_{pA}} + 1; \tag{5}$$

the first term in the r.h.s. gives the mean number of participants $\langle N_{part,A}^{pA} \rangle$ in the nucleus. As in the case of nucleus-nucleus collision, we will need to compute the density of participants in nucleus A, defined as:

$$\langle n_{part,A}^{pA} \rangle = \frac{\langle N_{part,A}^{pA} \rangle}{\sigma_{in}} = \frac{A}{\sigma_{pA}}. \tag{6}$$

In practice, the information about the impact parameter dependence is extracted by analyzing the data in various centrality bins. The physical observable most frequently used to estimate the centrality of the collision is the multiplicity of charged particles N_{ch}. We will assume that the average value of N_{ch} produced in a collision at impact parameter b is determined by the number of participating nucleons $N_{part}(b)$. The actual multiplicity will fluctuate around its mean value according to:

$$\mathcal{P}(N_{ch}, \langle N_{ch}(b) \rangle) = \frac{1}{\sqrt{2\pi a \langle N_{ch}(b) \rangle}} C(\langle N_{ch}(b) \rangle) \exp\left\{ -\frac{[N_{ch} - \langle N_{ch}(b) \rangle]^2}{2a \langle N_{ch}(b) \rangle} \right\}, \tag{7}$$

where the factor $C(N) \equiv 2/[1 + erf(\sqrt{N/2a})]$ is introduced to ensure that the fluctuation function $\mathcal{P}(N_{ch}, N)$ satisfies $\int_0^\infty dN_{ch}\mathcal{P}(N_{ch}, N) = 1$. The numerical value of $C(N)$ is 1 with very good accuracy for almost all cases of practical interest (it can exceed 1 for very peripheral collisions, where the number of participants and consequently N_{ch} is small: in such a case it is important to include the factor $C(N)$ to have a correct normalization).

The parameter a gives the width of the fluctuations: its value is dependent on the experimental apparatus, therefore it is not possible for us to predict its value for the LHC experiments. For the experiments at SPS and RHIC the value of a varies from 0.5 to 1.5-2. We will assume $a = 0.5$ in the following; uncertainty in this parameter can affect the centrality dependence of our results. In the case of $PbPb$ collisions, we estimate the resulting uncertainty in the density of participants (and thus in the saturation scale, see below) to be about 5%; in the case of pPb collisions, this uncertainty can reach $10 \div 15\%$ for peripheral collisions.

We will also assume the proportionality between N_{ch} and N_{part} when computing the differential inelastic cross section; this proportionality is not exact, but the shape of minimum bias distribution of events which is normally used to fix the parameter a (and the proportionality constant between N_{ch} and N_{part}) has been found insensitive to this assumption (see [11]).

The minimum bias differential cross section can be obtained as ($N(b) \equiv qN_{part}(b)$, where q is a constant):

$$\frac{d\sigma_{mb}}{dN_{ch}} = \int d^2b\, \mathcal{P}(N_{ch}, N(b))\, [1 - P_0(b)]\,; \tag{8}$$

here $P_0(b)$ is the probability of no interaction at the impact parameter b: for a nucleus-nucleus collision $P_0(b) = [1 - \sigma_{in}T_{AB}(b)]^{AB}$ where T_{AB} is the overlap function : $T_{AB}(b) = \int d^2s\, T_A(s)T_B(\mathrm{b} - \mathrm{s})$; in the case of B=1, $P_0(b)$ reduces to $P_0^{pA}(b)$ defined above. In the following, all of the formulae will refer to A-B collisions; with obvious modifications they are valid also in the p-A case.

The total nucleus-nucleus cross section is then obtained by integrating Eq. (8) over dN_{ch}:

$$\sigma_{AB} = \int dN_{ch}\, \frac{d\sigma_{mb}}{dN_{ch}} = \int d^2b\, [1 - P_0(b)]\,. \tag{9}$$

The mean value of any physical observable $\mathcal{O}$ (given in terms of the impact parameter b)

centr. cut	$\langle N_{part}^{AB} \rangle$	$\langle n_{part,A}^{pA} \rangle$ (fm^{-2})
0-100 %	103.2	1.33
0-6 %	369.0	2.89
0-10 %	346.6	2.83
0-25 %	274.2	2.62
25-50 %	103.7	1.75
50-75 %	27.0	0.76
75-100 %	3.9	0.14
0-50 %	186.7	2.17
50-100 %	15.7	0.45

TABLE II: Mean number of participants and their density in Pb-Pb collisions at LHC for different centrality bins

can be computed as:

$$\langle \mathcal{O} \rangle = \frac{1}{\sigma_{AB}} \int dN_{ch} \frac{d\sigma_{mb}}{dN_{ch}} \mathcal{O}(b) \tag{10}$$

To obtain the corresponding average for a given centrality cut we have to limit the integrations in the previous formula in the appropriate way, for instance the expression:

$$\langle \mathcal{O} \rangle \Big|_{N_{ch}>N_0} = \frac{\int_{N_0} dN_{ch} \frac{d\sigma_{mb}}{dN_{ch}} \mathcal{O}(b)}{\int_{N_0} dN_{ch} \frac{d\sigma_{mb}}{dN_{ch}}}, \tag{11}$$

gives the average value of the observable $\mathcal{O}$ in the fraction of the total cross section defined by the limit N_0. In this work the previous formula has been used to compute the mean density of participating nucleons (Eq. (2)) in different centrality bins, as shown in table II.

Table III gives the results of Eq. (5) for the case of p-Pb collisions at LHC energy. The corresponding densities are obtained according to Eq. (6).

centr. cut	$\langle N_{part}^{AB} \rangle$
0-100 %	7.41
0-20 %	13.07
0-50 %	11.31
20-50 %	10.29
50-100 %	3.58

TABLE III: Mean number of participants in p-Pb collisions at LHC for different centrality bins

THE GENERAL FORMULAE

Let us discuss the main features of the approach we use to describe the production dynamics. As in our previous papers [12, 13, 13, 14] we use the following formula for the inclusive production [1, 23]:

$$E\frac{d\sigma}{d^3p} = \frac{4\pi N_c}{N_c^2-1}\,\frac{1}{p_t^2}\,\times\int^{p_t} dk_t^2\,\alpha_s\,\varphi_{A_1}(x_1,k_t^2)\,\varphi_{A_2}(x_2,(p-k)_t^2), \tag{12}$$

where $x_{1,2} = (p_t/\sqrt{s})\exp(\mp y)$ and $\varphi_{A_1,A_2}(x,k_t^2)$ is the unintegrated gluon distribution of a nucleus (for the case of the proton one of φ_A should be replace by φ_p.) This distribution is related to the gluon density by

$$xG(x,Q^2) \;=\; \int^{Q^2} d\,k_t^2\,\varphi(x,k_t^2). \tag{13}$$

We can compute the multiplicity distribution by integrating Eq. (12) over p_t, namely,

$$\frac{dN}{dy} \;=\; \frac{1}{S}\int d^2p_t E\frac{d\sigma}{d^3p}; \tag{14}$$

S is either the inelastic cross section for the minimum bias multiplicity, or a fraction of it corresponding to a specific centrality cut.

Saturation scale

Let us define two saturation scales: one for the nucleus A_1 and another for the nucleus A_2. We will see below that even in the case of $A_1 = A_2$ the introduction of two saturation scales will be useful. It is convenient to introduce two auxiliary variables, namely

$$
\begin{aligned}
Q_{s,min}(y,W) &= min\left(Q_s(A_1;x_1=\frac{p_t}{W}e^{-y}),Q_s(A_2;x_2=\frac{p_t}{W}e^{y})\right) \ ; \\
Q_{s,max}(y,W) &= max\left(Q_s(A_1;x_1=\frac{p_t}{W}e^{-y}),Q_s(A_2;x_2=\frac{p_t}{W}e^{y})\right) \ . \qquad (15)
\end{aligned}
$$

To understand the physical meaning of these two scales we start with the explicit formula for Q_s which was suggested in Ref. [29] for the description of HERA data on deep inelastic scattering and was successfully used to describe the data from RHIC [11, 12, 13, 14]:

$$
Q_s^2(x) \ = \ Q_0^2\left(\frac{x_0}{x}\right)^{\lambda} \qquad (16)
$$

with the central value of $\lambda \ = \ 0.288$ [29]; the value of λ has an uncertainty of $5-10\%$. Substituting $x_1 \ = \ (Q_s/W)\,e^{-y}$ and $x_2 \ = \ (Q_s/W)\,e^{y}$, where W is the energy of interaction, one can see that the energy and rapidity dependence of the saturation scale can be reduced to a simple formula

$$
Q_s^2(A,y,W) \ = \ Q_0^2(A;W_0)\left(\frac{W}{W_0}e^{y}\right)^{\frac{\lambda}{1+\frac{1}{2}\lambda}} \equiv Q_0^2(A;W_0)\left(\frac{W}{W_0}\right)^{\tilde{\lambda}} e^{\tilde{\lambda}y} \ . \qquad (17)
$$

In what it follows we will use the notation λ for $\tilde{\lambda} \ = \ \lambda/(1+\frac{1}{2}\lambda) \ = \ 0.252$ hoping that it will not lead to misunderstanding.

Using Eq. (17) one can see that for a production of the gluon mini-jet at rapidities $y \neq 0$ there are two different saturation momenta: $Q_s^2(A;y,W)$ and $Q_s^2(A;-y,W)$, even for the collision of identical nuclei (see Fig. 1). Fig. 1 shows that the density is quite different in two nuclei since at $y \neq 0$ (say $y > 0$) one of the nuclei probed at relatively large $x = x_1 > x_2$ is a rather dilute parton system while the second nucleus has much higher parton density than at $y = 0$. Therefore, for an $A+A$ collision at $y > 0$ $Q_{s,min} = Q_s(A;-y,W)$ while $Q_{s,max} = Q_s(A;y,W)$. In the case of a collision of two different nuclei we need to take into account the $A-$dependent values of $Q_0(A;W)$ in Eq. (17).

The saturation scale is the main parameter of our approach and we need to understand clearly the energy dependence of Q_s if we want to make predictions for the LHC energies. The first basic result on the behavior of this scale is the power-like energy dependence which follows directly from QCD for fixed QCD coupling. As was shown in a number of papers [1, 25, 30, 31, 32, 33, 34] the energy dependence of the saturation scale does not depend on the details of the behavior of the parton system in the saturation domain but can be determined

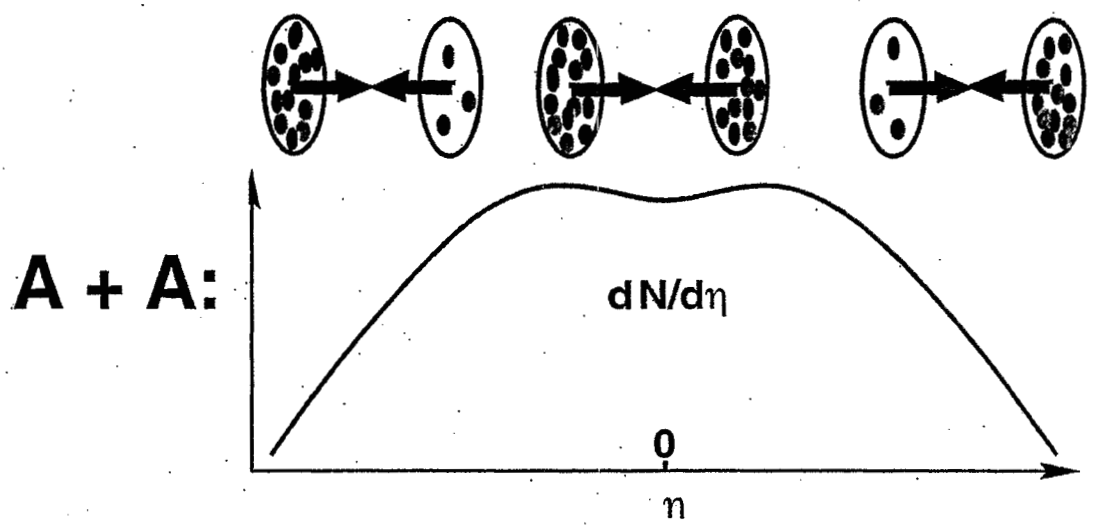

FIG. 1: The CGC approach for nucleus - nucleus collision with the saturation of parton density.

just by using the perturbative QCD approach in the BFKL region [35]. Indeed, consider the dipole-target scattering amplitude in the double Mellin transform representation, namely,

$$N(y, r^2) \;=\; \int \frac{d\omega\, d\gamma}{(2\pi i)^2}\, e^{\omega \ln(1/x) \,+\, (\gamma - 1)\, \ln(r^2 \Lambda^2_{QCD})}\; N(\omega, \gamma)\;. \tag{18}$$

The BFKL equation determines the value of ω at which $N(\omega, \gamma)$ has a pole:

$$\omega \;=\; \bar{\alpha}_S\, \chi(\gamma) \tag{19}$$

with a specific function χ which can be found e.g. in Ref. [25]; we denote $\bar{\alpha}_S \equiv N_c \alpha_S / \pi$. To find the energy dependence of the saturation scale we first need to find a critical value of $\gamma = \gamma_{cr}$ defined by the equation [1, 33, 34]

$$\frac{\chi(\gamma_{cr})}{1 - \gamma_{cr}} \;=\; -\frac{d\chi(\gamma_{cr})}{d\gamma}\;. \tag{20}$$

The meaning of this equation is the following: in the semi-classical approximation (see Ref. [32] and references therein) the scattering amplitude $N(y, \ln(r^2 \Lambda^2_{QCD}))$ has the following form:

$$N(y, \xi \equiv \ln(r^2 \Lambda^2_{QCD})) = \text{const} \times\; \exp\left[\omega(y, \xi) y - (1 - \gamma(y, \xi))\xi\right]. \tag{21}$$

The boundary of the saturation region is determined by the unique (critical) trajectory for the non-linear evolution equation in the (y, ξ) plane for which the phase $v_{phase} = \omega(y, \xi)/(1-$

$\gamma(y,\xi)$) and the group $v_{group} = -d\omega(y,\xi)/d\gamma(y,\xi)$ velocities are equal. The physical meaning of this trajectory can be illustrated by an analogy in geometrical optics: the boundary which it defines is similar to the focal reflecting surface (therefore, one can see that the surface of the Color Glass shines!). The equality of phase and group velocities thus gives the equation for the saturation scale:

$$\frac{d\ln(Q_s^2(x)/\Lambda_{QCD}^2)}{d\,\ln(1/x)} = \bar{\alpha}_S \frac{\chi(\gamma_{cr})}{1-\gamma_{cr}} \equiv \lambda \tag{22}$$

For fixed α_S Eq. (22) leads to

$$Q_s^2(x) = Q_0^2 \left(\frac{x_0}{x}\right)^{\lambda} \tag{23}$$

with λ given by Eq. (22). The numerical analysis of the value of λ can be found in Ref. [25]. The main conclusion from this analysis is the fact that the value of λ is sensitive to higher order correction in α_S. Therefore in this paper we choose to fix the value of λ from the phenomenological approach, see Eq. (17); we consider Eq. (23) as a justification for the use of such a parameterization.

Another observation on the equation for the saturation scale Eq. (22) is that the value of γ_{cr} is stable with respect to higher order corrections and almost does not depend on the value of the QCD coupling (see Ref. [25]). This fact helps us to solve Eq. (22) in the case of running α_S. The running of the coupling constant α_S leads to an additional dependence on Q_s in the r.h.s. of Eq. (22); from Eq. (22) using the explicit form of the running coupling constant we find

$$\frac{d\ln(Q_s^2(W)/\Lambda_{QCD}^2)}{d\,\ln(W/W_0)} = \frac{4\pi}{\beta_2}\frac{\chi(\gamma_{cr})}{1-\gamma_{cr}}\frac{1}{\ln(Q_s^2(W)/\Lambda_{QCD}^2)} \equiv \frac{\delta}{\ln(Q_s^2(W)/\Lambda_{QCD}^2)}; \tag{24}$$

as a result, the dependence on $Q_s(W)$ has become explicit. Integrating Eq. (24) we obtain

$$Q_s^2(W) = \Lambda_{QCD}^2 \exp\left(\sqrt{2\,\delta\,\ln(W/W_0) + \ln^2(Q_s^2(W_0)/\Lambda_{QCD}^2)}\right), \tag{25}$$

where $Q_s^2(W_0)$ is the saturation scale at the energy W_0 which we used as an initial condition in integrating Eq. (24). Here as well as in the rest of the paper Λ_{QCD}^2 is defined by $\alpha_S = 4\pi/\beta_2\,\ln(Q^2/\Lambda_{QCD}^2)$ and in numerical applications we took $\Lambda_{QCD}^2 = 0.04$ GeV^2 with $\beta_2 = 11 - 2/3\,N_f$ where $N_f = 3$ is the number of fermions (number of colors $N_c = 3$). We fix the value of δ through the empirical value of λ as given by Eq. (23) and the value of saturation

scale for the Au nucleus at fixed energy of $W = 130$ GeV, $y = 0$, corresponding to the cut of $0 - 6\%$ of most central collisions, $Q_{s0}^2 = 2$ GeV^2, so that $\delta = \lambda \ln(Q_{s0}^2/\Lambda_{QCD}^2)$.

The formula Eq. (25) reproduces all general features expected for the case of running QCD coupling; in particular, one can see that the saturation scale (25) does not depend on the mass number of the nucleus in the limit of high energies [36, 37] – the parton wave functions of different nuclei in this limit become universal. It is easy to generalize Eq. (25) to $y \neq 0$ by replacing $\ln(W/W_0)$ by $\ln(W/W_0) + y$; thus we have the following final formula for the case of running α_S:

$$Q_s^2(y, W) = \Lambda_{QCD}^2 \exp\left(\sqrt{2\lambda \ln(Q_{s0}^2/\Lambda_{QCD}^2)[\ln(W/W_0) + y] + \ln^2(Q_s^2(W_0)/\Lambda_{QCD}^2)}\right). \quad (26)$$

Formulae for the multiplicities

To derive the final expressions for the multiplicity it is convenient to re-write Eq. (14) using the fact that the main contribution to Eq. (14) is given by two regions of integration over k_t: $k_t \ll p_t$ and $|\vec{p}_t - \vec{k}_t| \ll p_t$; this leads to

$$\begin{aligned}\frac{dN}{dy} &= \frac{1}{S} \int dp_t^2 \left(E\frac{d\sigma}{d^3p}\right) = \frac{1}{S} \frac{4\pi N_c \alpha_S}{N_c^2 - 1} \times \\ &\times \int \frac{dp_t^2}{p_t^2} \left(\varphi_{A_1}(x_1, p_t^2) \int^{p_t} dk_t^2\, \varphi_{A_2}(x_2, k_t^2) + \varphi_{A_2}(x_2, p_t^2) \int^{p_t} dk_t^2\, \varphi_{A_1}(x_1, k_t^2)\right) = \\ &= \frac{1}{S} \frac{4\pi N_c \alpha_S}{N_c^2 - 1} \int_0^\infty \frac{d\,p_t^2}{p_t^4}\, x_2 G_{A_2}(x_2, p_t^2)\, x_1 G_{A_1}(x_1, p_t^2)\,, \end{aligned} \quad (27)$$

where we integrated by parts and used Eq. (13). In the KLMN treatment [11, 12, 13, 14] we assumed a simplified form of xG, namely,

$$xG(x; p_t^2) = \begin{cases} \dfrac{\kappa}{\alpha_S(Q_s^2)} S\, p_t^2\, (1 - x)^4, & p_t < Q_s(x)\,; \\[2ex] \dfrac{\kappa}{\alpha_S(Q_s^2)} S\, Q_s^2(x)\, (1 - x)^4, & p_t > Q_s(x)\,; \end{cases} \quad (28)$$

where the normalization coefficient κ has been determined from the RHIC data on gold-gold collisions. We introduce the factor $(1 - x)^4$ to describe the fact that the gluon density is small at $x \to 1$ as described by the quark counting rules [38, 39].

We have checked that the simplified form of Eq. (28) is adequate for the calculations of multiplicity since it is dominated by the low momenta region. At high p_t and small x, it

was shown [14] that the quantum effects of the anomalous dimension could be extremely important. However, at moderate values of x the simple form of Eq. (28) was used to calculate the p_t spectra in proton-proton and electron-proton collisions in Ref. [40] and the results appear very encouraging.

Having in mind Eq. (28), let us divide the p_t integration in Eq. (14) in three different regions:

1. $p_t < Q_{s,min}$

   In this region both parton densities for A_1 and A_2 are in the saturation region. This region of integration gives

$$\frac{dN}{dy} \propto \frac{1}{\alpha_S} S\, Q^2_{s,min} \propto \frac{1}{\alpha_S} N_{part}(A_1) \tag{29}$$

   where we have used the fact that the number of participants is proportional to SQ_s^2, where S is the area corresponding to a specific centrality cut.

2. $Q_{s,max} > p_t > Q_{s,min}$

   For these values of p_t we have saturation regime for the nucleus A_2 for all positive rapidities while the nucleus A_1 is in the normal DGLAP evolution region. Neglecting anomalous dimension of the gluon density below $Q_{s,max}$, we have $\varphi_{A_1}(x_1, k_t^2) \propto \frac{1}{\alpha_S} S\, Q_{s,min}/\tilde{k}_t^2$ which for $y > y_c$ leads to

$$\frac{dN}{dy} \propto \frac{1}{\alpha_S} S\, Q^2_{s,min} \ln \frac{Q^2_{s,max}}{Q^2_{s,min}} \propto \frac{1}{\alpha_S} N_{part}(A_1) \ln \frac{Q^2_{s,max}}{Q^2_{s,min}} \tag{30}$$

   This region of integration will give the largest contribution.

3. $p_t > Q_{s,max}$

   In this region the parton densities in both nuclei are in the DGLAP evolution region.

Substituting Eq. (28) into Eq. (27) we obtain the following formula [12]:

$$\frac{dN}{dy} = Const \times S\, Q^2_{s,min}(W,y) \frac{1}{\alpha_S(Q^2_{min}(W,y))} \times \tag{31}$$

$$\left[\left(1 - \frac{Q_{s,min}(W,y)}{W} e^y\right)^4 + \{\ln(Q^2_{max}(W,y)/Q^2_{s,min}(W,y)) + 1\} \left(1 - \frac{Q_{s,max}(W,y)}{W} e^y\right)^4\right].$$

One can see two qualitative properties of Eq. (31). For $y > 0$ and close to the fragmentation region of the nucleus A_1 , $Q_{s,min} = Q(A_1)$ and the multiplicity is proportional to $N_{part}(A_1)$, while in the fragmentation region of the nucleus $A_2(y < 0)$ $Q_{s,min} = Q(A_2)$ and $dN/dy \propto N_{part}(A_2)$. We thus recover some of the features of the phenomenological 'wounded nucleon' model [26].

PREDICTIONS

Choice of the phenomenological parameters

As discussed above our main phenomenological parameter is the saturation momentum. An estimate of the value of the saturation momentum can be found from the following condition: the probability of interaction in the target (or "the packing factor" of the partonic system) is equal to unity. The packing factor can be written in the following form:

$$P.F. = \frac{8\,\pi^2\,N_c\,\alpha_S(Q^2)}{(N_c^2-1)\,Q^2}\,\frac{xG(x,Q^2)}{\pi\,R^2} = \sigma\,\rho \tag{32}$$

where σ is the cross section for dipole - target interaction (the size of the dipole is about 1/Q) and ρ is the (two-dimensional) transverse density of partons inside the target of size R (see e.g. Refs. [11, 12] for details).

In the case of the nucleon we do not know the value of R or, in other words, we do not know the area which is occupied by the gluons ($S_N = \pi R^2$). However, we have enough information to claim that this area is less than the area of the nucleon (R is less than the electromagnetic radius of the proton). To substantiate this claim, let us recall for example the constituent quark model in which the gluons are distributed in the area determined by the small (relative to the size of the nucleon) size of the constituent quark. Having all these uncertainties in mind we use the phenomenological Golec-Biernat and Wuesthoff model [29] to fix the value of the saturation moment in the case of the nucleon target. Namely, the value of the saturation moment for proton is equal $Q_s(P; y = 0, W = 200\,\mathrm{GeV}) = 0.37\,\mathrm{GeV}^2$. In Ref. [41] this value of the proton saturation momentum was used to describe the deuteron-gold collisions at RHIC energies.

In the case of the nuclear target the saturation momentum can be found from the ex-

pression for the packing factor

$$P.F. = \sigma\,\rho_A = \sigma\,\rho_N\,\frac{\rho_{part}}{2}\,\frac{S_N}{S_A} = Q_S^2(N)\,\frac{\rho_{part}}{2}\,\frac{S_N}{S_A} \tag{33}$$

As we have discussed we do not know the last factor (S_N/S_A) and therefore, Eq. (33) cannot help us to determine the value of the saturation momentum for a nucleus. We fixed the value of the saturation momentum from the description of the RHIC data on the multiplicity in gold-gold collisions, namely, $Q_s^2(\text{Gold}, y = 0, W = 130\,GeV) = 2.02\,\text{GeV}^2$ for the centrality cut $0 - 6\%$ (see Refs. [11, 12] for details).

As far as energy dependence of the saturation scale is concerned, we used Eq. (16) and Eq. (26) with λ given by the Golec-Biernat and Wuesthoff model ($\lambda = 0.252$). However, we have to admit that the perturbative QCD estimates described above would lead to a larger value of λ : $\lambda \approx 0.37$. Such an uncertainty in the value of λ leads to an error of about $12 - 15\%$ in our prediction for the proton-nucleus and nucleus-nucleus collisions at the LHC energies. For the proton-proton interaction it could generate an error as big as about 50%.

In our main formula given by Eq. (31) we have to fix the normalization factor. As discussed in Ref. [12] theoretical estimates lead to a value of $Const$ in Eq. (31) which appears quite close to the value extracted by comparison with the RHIC data. In this paper we use the same normalization factor $Const$ as in [12], namely $Const\,S\,Q^2_{s,min}(W = 200\,GeV, y = 0) = 0.615\,N_{part}$. We also need to note that the experimental measurement are done at fixed pseudo-rapidity η, not rapidity y; therefore, as discussed in Ref. [12] we have to use the relation between η and y, and to multiply Eq. (31) by the Jacobian of this transformation $h(\eta, Q_s)$; see [12] for details and explicit expressions.

Proton-proton collisions present an additional problem caused by the deficiency of the geometrical interpretation of pp cross section. As mentioned above (see Eq. (14)) we calculated the ratio of the total inclusive cross section to the geometrical area of the interaction. This ratio is the measured multiplicity in the case of hadron-nucleus and nucleus-nucleus collisions. In the case of hadron-hadron interaction the multiplicity is the ratio of the inclusive cross section divided by the inelastic cross section. As discussed above, for pp interactions we do not know the relation between the interaction area and the value of the inelastic cross section. To evaluate multiplicities in proton-proton interactions we do the following: (i) fix the ratio S_N/σ_{in} at $W = 200\,GeV$ using the data for $dN/dy(y = 0)$; and (II) assume $S_N/\sigma_{in} \propto 1/\sigma_{in}$ as far as the energy dependence is concerned. In other words we assume

that the area S_N does not depend on energy. The energy dependence of the inelastic cross section, including energies outside of the region accessible experimentally at present, was taken from Ref. [28].

Proton - proton collisions

Rapidity distribution

Fig. 2 shows the calculated pseudorapidity distributions for the proton - proton (antiproton) collisions. The agreement with the experimental data is quite good despite the fact that pp collisions present special difficulties for our approach since the value of the saturation momentum is rather small and non-perturbative corrections could be essential. We would like to point out however that the value of the saturation momentum for the proton reaches $\approx 1\,GeV$ at the LHC energy. Our experience with RHIC data suggests that at such value of the saturation momentum our approach could apply with a reasonable accuracy. We thus expect that the very first pp data from the LHC can provide an important test of the CGC ideas. In Fig. 3 we plot the value of $dN/d\eta$ at $\eta = 0$ as a function of energy (in this plot we included also the available data at lower energies). The agreement with the experiment is seen to be quite good.

Total multiplicity

Integrating Eq. (31) over η in the entire region of $\eta = -\ln W \div +\ln W$ we can calculate the total multiplicity in proton-proton (antiproton) collisions. In Fig. 4 we present our calculation together with the experimental data taken from Refs. [44]; a good agreement with the data is seen in a wide range of energies. We would like to remind however that our predictions for the LHC energies could be as much as 1.5 times larger due to uncertainties in the energy behavior of the saturation scale discussed above.

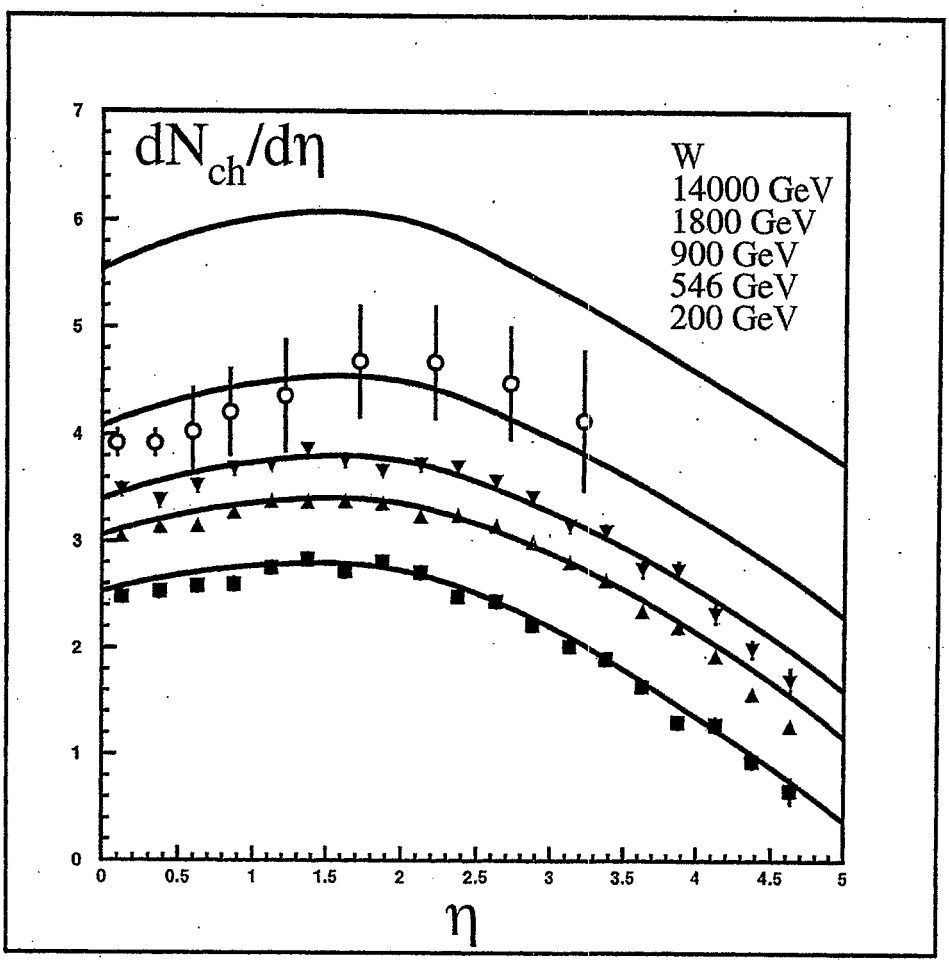

FIG. 2: Rapidity dependence $dN/d\eta$ of charged hadron multiplicities in proton - proton (antiproton) collisions as a function of the pseudorapidity at different energies. The data are taken from Ref. [42].

Nucleus-nucleus collisions.

Rapidity distribution dN/dy

Our prediction for lead-lead collision at the LHC energy is plotted in Fig. 5. The two sets of curves (solid and dotted) describe the cases of fixed and running QCD coupling respectively. We consider the two predictions as the natural bounds for our predictions, and expect the data to be in between of these two curves. However, we would like to mention again that our predictions have systematic errors of about $12 \div 15\%$ due to uncertainties in

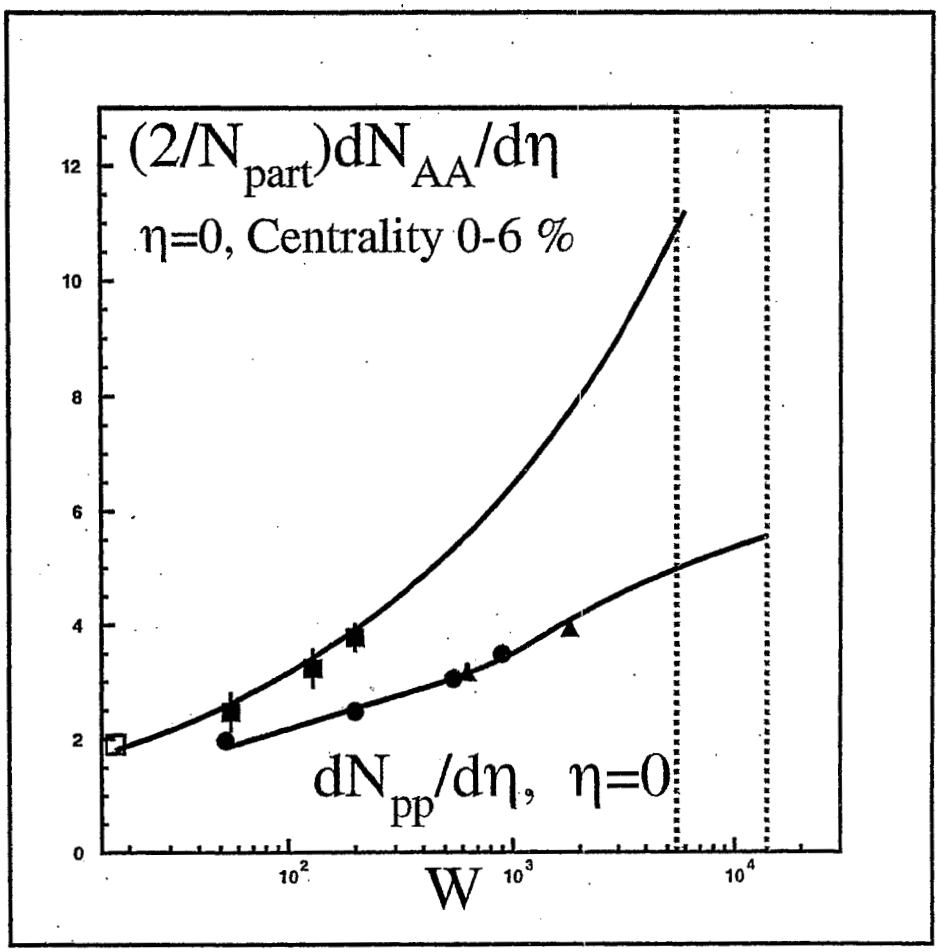

FIG. 3: Energy dependence of charged hadron multiplicity $dN/d\eta$ at $\eta = 0$ in proton - proton (antiproton) collisions and of charged hadron multiplicities per participant pair $(2/N_{part})\, dN/d\eta$ at $\eta = 0$ for central nucleus-nucleus collisions. The vertical dotted lines mark the LHC energies for nucleus-nucleus collisions ($W = 5500\, GeV$) and for proton-proton collisions ($W = 14000\, GeV$). collisions. The experimental data are from Ref. [42, 43].

the energy dependence of the saturation scale.

Centrality dependence: $(2/N_{part})\,(dN_{ch}/d\eta)$

Fig. 6 shows our predictions for the N_{part} dependence of the $(2/N_{part})\,(dN_{ch}/d\eta)$. This observable provides the most sensitive test of the value of the saturation scale and its de-

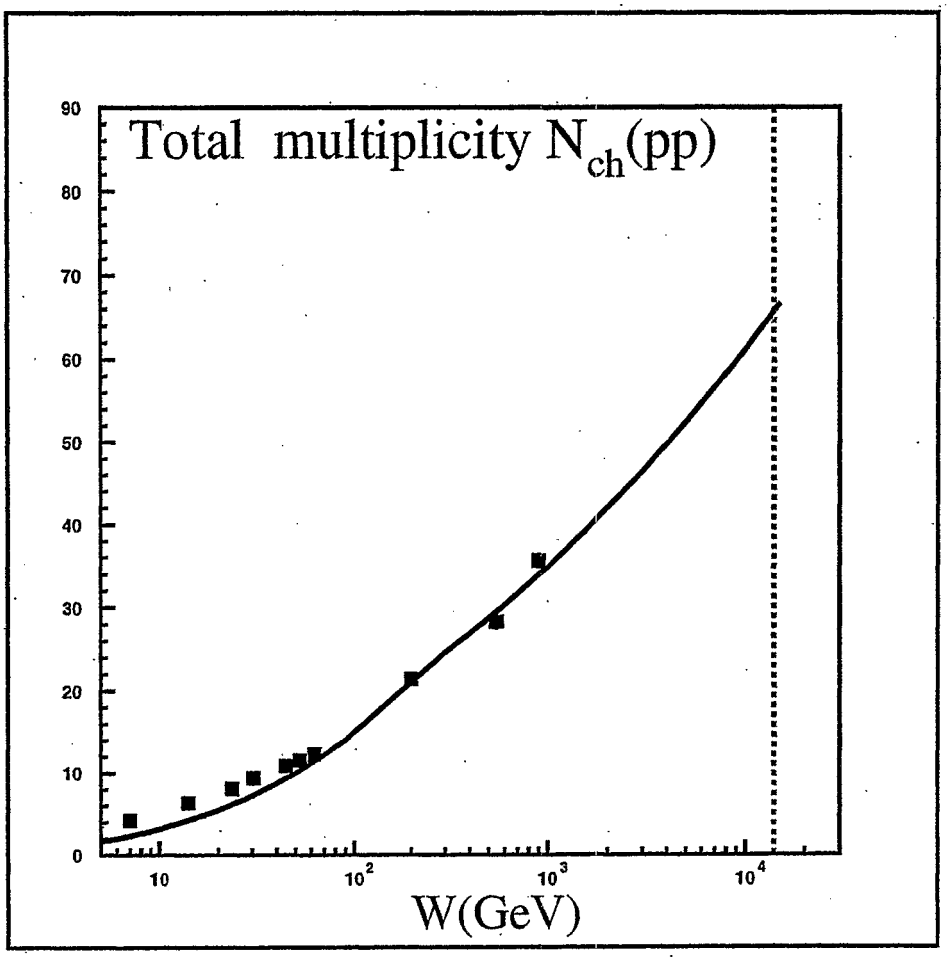

FIG. 4: Energy dependence of total multiplicity in proton - proton (antiproton) collisions. The vertical dotted line marks the LHC energies for proton-proton collisions ($W = 14000\,GeV$). collisions. The experimental data are taken from Ref. [44].

pendence on the density of the participants.

Fig. 3 shows the energy dependence of $(2/N_{ch})\,(dN/d\eta)$ at $\eta = 0$. One can see that we are able to describe the current experimental data. Note that if we neglect the difference between rapidity and pseudorapidity, $(2/N_{ch})\,(dN/d\eta)$ at $\eta = 0$ is given by a very simple formula [13]:

$$\frac{2}{N_{part}}\frac{dN_{ch}}{dy}|_{y=0} = 0.87\left(\frac{W}{W_0}\right)^{\lambda}\ln(Q_s^2(A,W,y=0)/\Lambda_{QCD}^2) =$$
$$= 0.87\left(\frac{W}{130}\right)^{0.252}(3.93 + 0.252\ \ln(W/130)) \qquad (34)$$

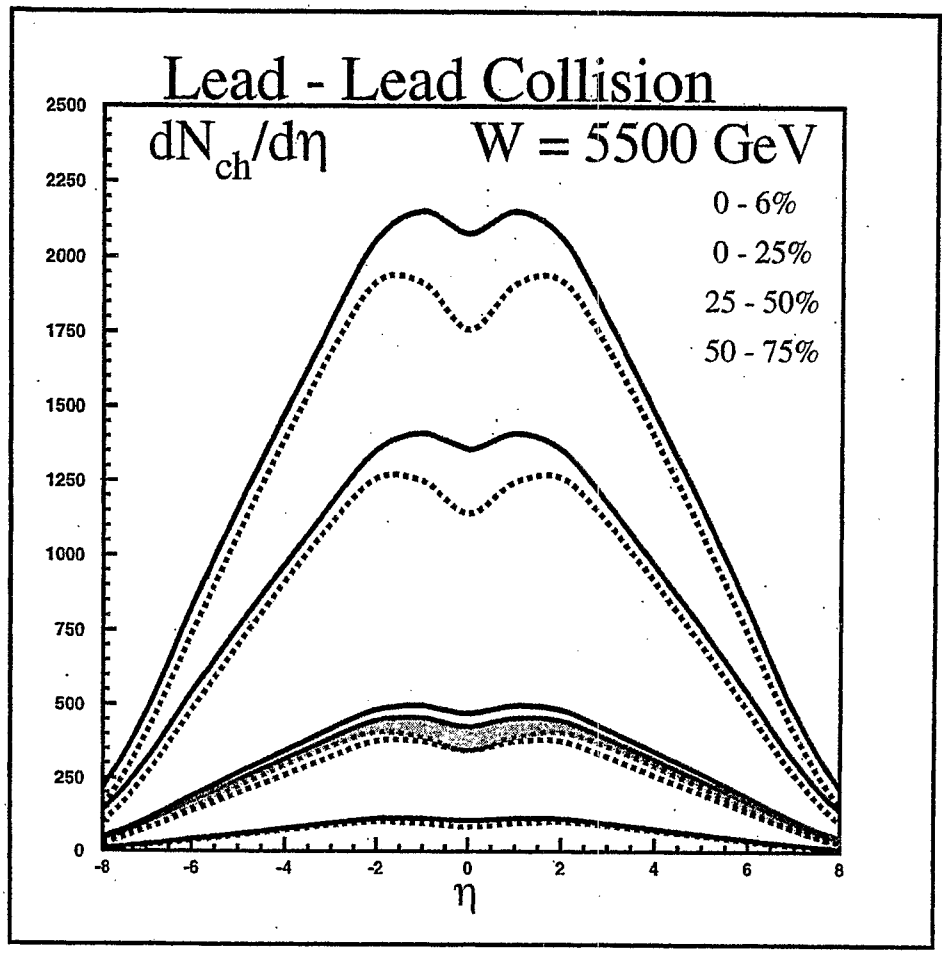

FIG. 5: Rapidity dependence of $dN/d\eta$ lead-lead collisions at the LHC energy at different centrality cuts. The solid lines corresponds to the prediction using Eq. (16) for the energy dependence of the saturation scale while the dotted lines show the predictions for Eq. (26) for running QCD coupling. The shadowed area shows the prediction for the minimal bias event.

This formula is in good agreement with the existing experimental data.

Proton - nucleus collisions

Fig. 7 shows our prediction for the proton-nucleus collisions at W=5500 GeV. In section 2 we described the procedure of computing the number and density of participants in this case; to evaluate the relevant value of the saturation momentum, we take account of the energy dependence to extrapolate from RHIC to the LHC energy. For example, the density of par-

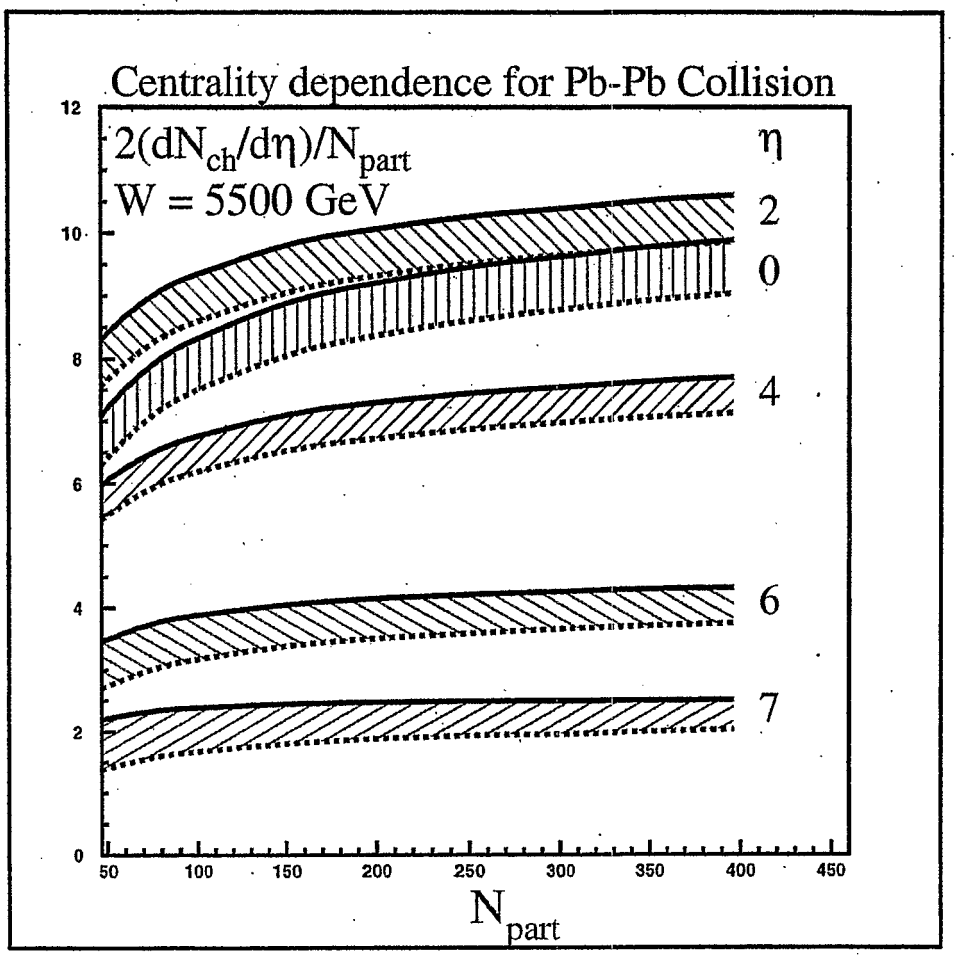

FIG. 6: N_{part} dependence of $(2/N_{ch})\, dN/d\eta$ for lead-lead collisions at the LHC energy at different rapidity cuts. The solid lines correspond to the prediction using Eq. (16) for the energy dependence of the saturation scale while the dotted lines show the predictions for Eq. (26) for running QCD coupling. The shadowed areas show the spread of our predictions.

ticipants $\rho_{part} \approx 1.84\ \mathrm{fm}^{-2}$ corresponds to the saturation scale of $Q_s^2 \approx 2\,\mathrm{GeV}^2(5500/200)^{0.252}$ $\approx 4.6\,\mathrm{GeV}^2$.

CONCLUSIONS

In this paper we have provided a complete set of predictions for the multiplicity distributions at the LHC basing on the CGC approach. In our approach, parton saturation results in a relatively weak, compared to most other approaches, dependence of the multiplicity on

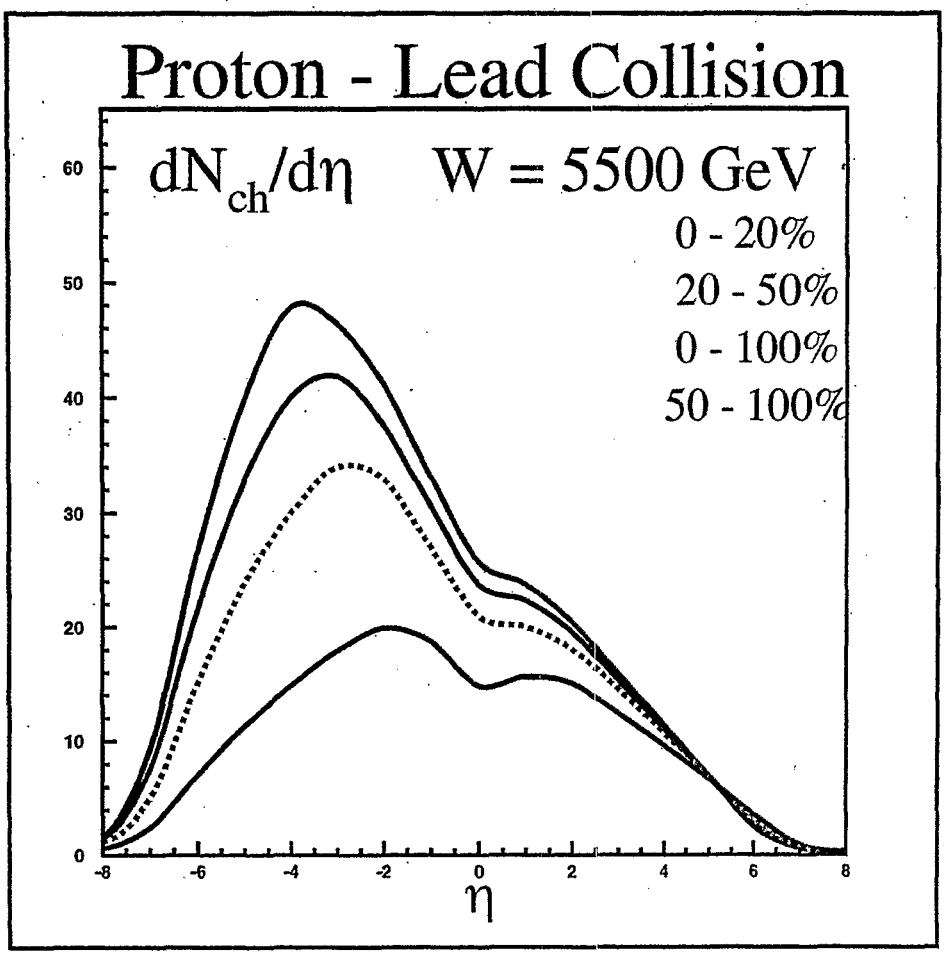

FIG. 7: Rapidity dependence of $dN/d\eta$ proton-lead collisions at the LHC energy at different centrality cuts. The dotted line corresponds to the minimal bias event.

energy. As one can see from Fig. 8 we expect rather small number of produced hadrons in comparison with the alternative approaches. What is the uncertainty in our predictions? We would like to recall the estimates for the uncertainty in our calculations at the LHC energies given above: $12 \div 15\%$ for nucleus-nucleus and hadron-nucleus collisions, and a large value of $40 \div 50\%$ for the proton-proton collisions. These uncertainties arise from the poor theoretical knowledge of the energy dependence of the saturation scale, and in the case of pp collisions also from the uncertainties in the application of the geometrical picture.

We hope that our estimates will be useful for the interpretation of the first results from LHC experiments. As illustrated in Fig. 8, a measurement of multiplicity at the LHC will

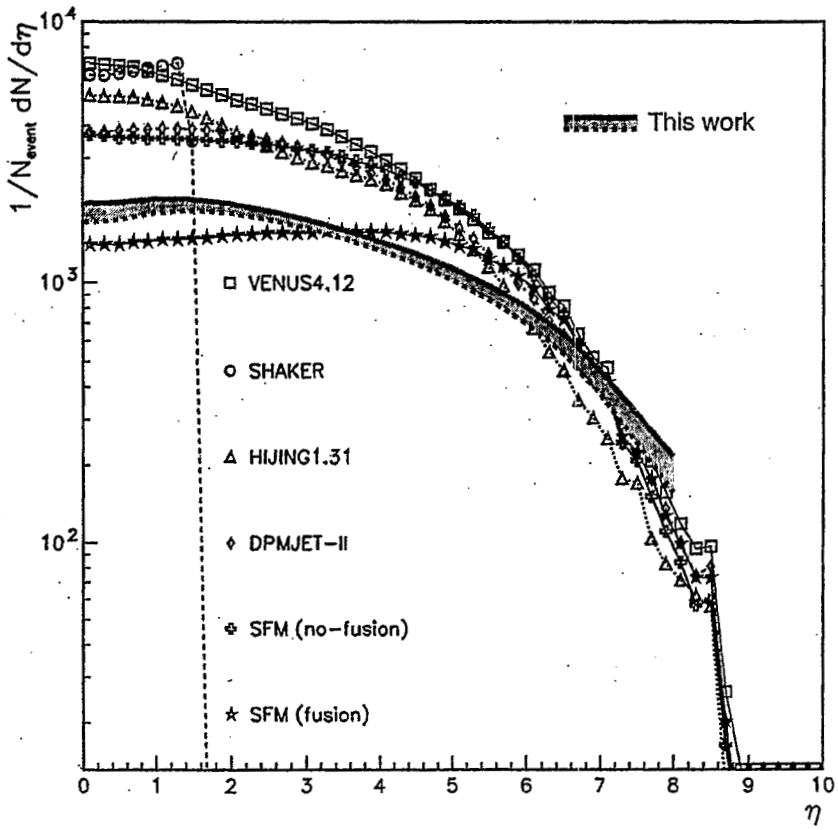

FIG. 8: Comparison of our predictions for charged hadron multiplicities in central ($b \leq 3$ fm) $Pb - Pb$ collisions with the results from other approaches, as given in Ref.[45]

provide a very important test of the CGC approach.

ACKNOWLEDGEMENTS

The work of D.K. was supported by the U.S. Department of Energy under Contract No. DE-AC02-98CH10886. E.L. and M.N. are grateful to the RIKEN-BNL Research Center and the Nuclear Theory Group at BNL for hospitality and support during the period when this work was done. The work opf E.L. was supported in part by the grant of Israeli Science Foundation ,founded by Israeli Academy of Science and Humanity.

[1] L. V. Gribov, E. M. Levin and M. G. Ryskin, Phys. Rep. **100** (1983) 1.

[2] A.H. Mueller and J. Qiu, Nucl.Phys. **B 268** (1986) 427;
J.-P. Blaizot and A.H. Mueller, Nucl. Phys. **B 289** (1987) 847.

[3] L. McLerran and R. Venugopalan, Phys. Rev. **D 49** (1994) 2233; 3352; **D 50** (1994) 2225.

[4] Ia. Balitsky, *Nucl.Phys.* **B463** (1996) 99;
Yu. Kovchegov, *Phys. Rev.* **D60** (2000) 034008.

[5] J. Jalilian-Marian, A. Kovner, A. Leonidov and H. Weigert, *Phys. Rev.* **D59** (1999) 014014 [arXiv:hep-ph/9706377]; *Nucl. Phys.* **B504** (1997) 415 [arXiv:hep-ph/9701284];
E. Iancu, A. Leonidov and L. D. McLerran, *Phys. Lett.* **B510** (2001) 133 [arXiv:hep-ph/0102009]; *Nucl. Phys.* **A692** (2001) 583 [arXiv:hep-ph/0011241];
H. Weigert, *Nucl. Phys.* **A703** (2002) 823 [arXiv:hep-ph/0004044].

[6] I. G. Bearden [BRAHMS Collaboration], Phys. Rev. Lett. **87** (2001) 112305; arXiv:nucl-ex/0403050; Phys. Rev. Lett. **88**, 202301 (2002) [arXiv:nucl-ex/0112001]; Phys. Lett. B **523**, 227 (2001) [arXiv:nucl-ex/0108016];
R. Debbe [BRAHMS Collaboration], arXiv:nucl-ex/0405018; I. Arsene *et al.* [BRAHMS Collaboration], arXiv:nucl-ex/0403005.

[7] A. Bazilevsky [PHENIX Collaboration], arXiv:nucl-ex/0304015; Nucl. Phys. A **715**, 486 (2003);

[8] A. Milov [the PHENIX Collaboration], Nucl. Phys. A **698**, 171 (2002) [arXiv:nucl-ex/0107006];
K. Adcox *et al.* [PHENIX Collaboration], Phys. Rev. Lett. **87**, 052301 (2001); Phys. Rev. Lett. **86**, 3500 (2001).

[9] B. B. Back *et al.* [PHOBOS Collaboration], Phys. Rev. Lett. **85**, 3100 (2000); Phys. Rev. C **65**, 061901 (2002); Phys. Rev. Lett. **87**, 102303 (2001); Phys. Rev. Lett. **85**, 3100 (2000); arXiv:nucl-ex/0406017; arXiv:nucl-ex/0405027;
R. Nouicer *et al.* [PHOBOS Collaboration], arXiv:nucl-ex/0403033;
M. D. Baker [PHOBOS Collaboration], arXiv:nucl-ex/0212009.

[10] Z. b. Xu [STAR Collaboration], arXiv:nucl-ex/0207019; C. Adler *et al.* [STAR Collaboration], Phys. Rev. Lett. **87**, 112303 (2001);
L. S. Barnby [STAR Collaboration], arXiv:nucl-ex/0404027.

[11] D. Kharzeev and M. Nardi, Phys. Lett. **B 507** (2001) 121.

[12] D. Kharzeev and E. Levin, Phys. Lett. **B 523** (2001) 79.

[13] D. Kharzeev, E. Levin and M. Nardi, *"The onset of classical QCD dynamics in relativistic heavy ion collisions,"* hep-ph/0111315.

[14] D. Kharzeev, E. Levin and L. McLerran, Phys. Lett. B **561** (2003) 93.

[15] D. Kharzeev, Y. V. Kovchegov and K. Tuchin, Phys. Rev. D **68**, 094013 (2003); arXiv:hep-ph/0405045.

[16] K. J. Eskola, H. Niemi, P. V. Ruuskanen and S. S. Rasanen, Nucl. Phys. A **715** (2003) 561 [arXiv:nucl-th/0210005].

[17] T. Hirano and Y. Nara, *"Hydrodynamic afterburner for the color glass condensate and the parton energy loss,"* arXiv:nucl-th/0404039.

[18] Yu.V. Kovchegov, Phys. Rev. **D 54** (1996) 5463; J. Jalilian-Marian, A. Kovner, L. McLerran, H. Weigert, Phys.Rev. **D55** (1997) 5414; E. Iancu and L. McLerran, Phys.Lett. **B510** (2001) 145; A. Krasnitz and R. Venugopalan, Phys. Rev. Lett.**84** (2000) 4309; E. Levin and K. Tuchin, Nucl. Phys. **B573** (2000) 833; **A693** (2001) 787; **A691** (2001) 779; A.H. Mueller, *"Parton saturation: An overview,"* hep-ph/0111244; E. Iancu, A. Leonidov and L. D. McLerran, Nucl. Phys. A692 (2001) 583, hep-ph/0011241; E. Iancu, K. Itakura and L. McLerran, Nucl. Phys. A708 (2002) 327, hep-ph/0203137.

[19] E. Levin and M. Lublinsky, *Nucl. Phys.* **A730** (2004) 191 [arXiv:hep-ph/0308279].

[20] E. Iancu and A. H. Mueller, *Nucl. Phys.* **A730** (2004) 460, 494, [arXiv:hep-ph/0308315],[arXiv:hep-ph/0309276].

[21] M. Kozlov and E. Levin, Nucl. Phys. A **739** (2004) 291 [arXiv:hep-ph/0401118].

[22] A. H. Mueller and A. I. Shoshi, *"Small-x physics beyond the Kovchegov equation,"* arXiv:hep-ph/0402193; *"Small-x physics near the saturation regime,"*. talk at 39th Rencontres de Moriond on QCD and High-Energy Hadronic Interactions, La Thuile, Italy, 28 Mar - 4 Apr 2004 arXiv:hep-ph/0405205.

[23] E. Laenen and E. Levin, Ann. Rev. Nuc. Part. Sci. 44 (1994) 199; Yu. V. Kovchegov and D. Rischke, Phys. Rev. C56 (1997) 1084; M. Gyulassy and L. McLerran, Phys. Rev. C56 (1997) 2219; Yu. V. Kovchegov and A. H. Mueller, Nucl. Phys. B529 (1998) 451 M. A. Braun, Eur. Phys. J. C16 (2000) 337, hep-ph/0010041, hep-ph/0101070; Yu. V. Kovchegov, Phys. Rev. D64 (2000) 114016; Yu. V. Kovchegov and K. Tuchin, Phys. Rev. **D65** (2002) 074026

hep-ph/0111362.

[24] D. N. Triantafyllopoulos, Nucl. Phys. B **648** (2003) 293 [arXiv:hep-ph/0209121].

[25] V. A. Khoze, A. D. Martin, M. G. Ryskin and W. J. Stirling, *"The spread of the gluon k(t)-distribution and the determination of the saturation scale at hadron colliders in resummed NLL BFKL,"* arXiv:hep-ph/0406135.

[26] A. Bialas, M. Bleszynski and W. Czyż, Nucl.Phys. **B111** (1976) 461.

[27] D. Kharzeev, C. Lourenco, M. Nardi and H. Satz, Z. Phys. C **74** (1997) 307, [arXiv:hep-ph/9612217].

[28] E. Gotsman, E. Levin and U. Maor, Phys. Lett. B **452** (1999) 387 [arXiv:hep-ph/9901416].

[29] K. Golec-Biernat and M. Wüsthof, Phys. Rev. **D59** (1999) 014017; Phys. Rev. **D60** (1999) 114023; A. Stasto, K. Golec-Biernat and J. Kwiecinski, Phys. Rev. Lett. **86** (2001) 596.

[30] J. Bartels and E. Levin, *Nucl. Phys.* **B387** (1992) 617.

[31] J. Bartels, G. A. Schuler and J. Blumlein, *Z. Phys.* **C50** (1991) 91; *Nucl. Phys. Proc. Suppl.* **18C** (1991) 147.

[32] S. Bondarenko, M. Kozlov and E. Levin, *Nucl. Phys.* **A727** (2003) 139 [arXiv:hep-ph/0305150].

[33] A. H. Mueller and D. N. Triantafyllopoulos, *Nucl. Phys.* **B640** (2002) 331 [arXiv:hep-ph/0205167];

[34] S. Munier and R. Peschanski, Phys. Rev. Lett. **91**, 232001 (2003) [arXiv:hep-ph/0309177].

[35] E. A. Kuraev, L. N. Lipatov, and F. S. Fadin,it Sov. Phys. JETP **45** (1977) 199 ;
Ya. Ya. Balitsky and L. N. Lipatov, *Sov. J. Nucl. Phys.* **28** (1978) 22 .

[36] E. M. Levin and M. G. Ryskin, Yad. Fiz. **45** (1987) 234 [Sov. J. Nucl. Phys. **45** (1987) 150].

[37] A. H. Mueller, Nucl. Phys. A **724** (2003) 223 [arXiv:hep-ph/0301109].

[38] S. J. Brodsky and G. R. Farrar, Phys. Rev. Lett. **31**, 1153 (1973).

[39] V. A. Matveev, R. M. Muradian and A. N. Tavkhelidze, Lett. Nuovo Cim. **7**, 719 (1973).

[40] A. Szczurek, *"From unintegrated gluon distributions to particle production in hadronic collisions at high energies,"* arXiv:hep-ph/0309146; Acta Phys. Polon. **B34** (2003) 3191 arXiv:hep-ph/0304129, **B35** (2004) 161 arXiv:hep-ph/0311175.

[41] D. Kharzeev, E. Levin and M. Nardi, Nucl. Phys. A **730** (2004) 448 [arXiv:hep-ph/0212316].

[42] S. Eidelman *et al.* [Particle Data Group Collaboration], *"Review of particle physics,"* Phys. Lett. B **592** (2004) 1.

[43] B.B.Back et al (Phobos Collab.), Phys. Rev. Lett. **85** (2000) 3100 ;
Quark Matter 2004, Oakland, Jan. 11-17,2004

[44] B.B.Back et al (Phobos Collab.), nucl-ex/0301017.

[45] N. Armesto and C. Pajares, Int. J. Mod. Phys. A **15** (2000) 2019 [arXiv:hep-ph/0002163].

Cyrille Marquet
Service de Physique Théorique
CEA-Saclay

Testing saturation with forward jets

I derive single inclusive forward-gluon production in the scattering of a dipole off an unspecified target and show how it is related to the dipole-target total cross-section. Using collinear factorization, the result is extented to an incident hadron. Considering then the target to be a virtual photon in order to describe forward-jet production at HERA, the cross-section is expressed in terms of the dipole-dipole scattering. Using a simple GBW-like parametrization for the dipole-dipole cross-section, we perform a fit of the H1 and ZEUS data. Two solutions are obtained, showing either strong or weak saturation effects.

Inclusive gluon production off a dipole

Perturbative calculation with an initial dipole

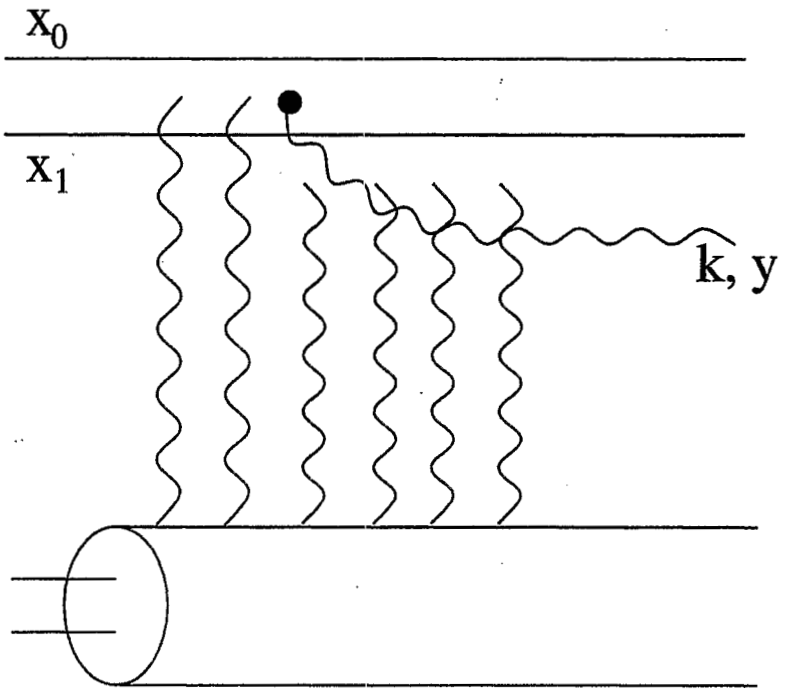

- At lowest order: computing Feynman diagrams
- More generally: with eikonal Wilson lines (work in progress)

Summing the contributions

$$\frac{d\sigma}{d^2k dy}(x_0 - x_1) = \frac{\alpha_s C_F}{\pi^2} \int d^2b \int \frac{d^2z_1}{2\pi} \frac{d^2z_2}{2\pi} \; e^{ik.(z_2 - z_1)}$$
$$\sum_{i,j=0}^{1} (-1)^{i+j} \frac{x_i - z_1}{|x_i - z_1|^2} . \frac{x_j - z_2}{|x_j - z_2|^2} \{\sigma_{dT}(x_i - z_1)$$
$$+\sigma_{dT}(x_j - z_2) - \sigma_{dT}(x_i - x_j) - \sigma_{dT}(z_1 - z_2)\}$$

We recover the result obtained by Kovchegov (2001) for a target nucleus
Generalization including quantum evolution: Kovchegov and Tuchin (2002).

- Integrations over impact parameters can be carried out
- Average over the azimutal angle of $x_0 - x_1$ can be performed

Final result

$$\frac{d\sigma}{d^2k dy}(r_0) = \frac{2\alpha_s C_F}{\pi k^2} \int dz^2 \phi(r_0, z, k) \sigma_{dT}(z)$$

with

$$\phi(r_0, z, k) = J_0(kz)\delta(r_0^2 - z^2) +$$
$$\Theta(r_0 - z)\left(\frac{k}{z} J_1(kz) - \frac{k^2}{2} J_0(kz) \log(r_0/z)\right)$$

$\rightarrow$ A dipole-factorized form for the cross-section

- $r_0 = |x_0 - x_1|$: size of the incident dipole
- The effective distribution ϕ is normalized: $\int dz^2 \ \phi(r_0, z, k) = 1$
- Alternative to write the forward-jet cross-section:

$$\frac{d\sigma}{d^2k dy}(r_0) =$$
$$\frac{2\alpha_s C_F}{\pi k^2} \int_0^{r_0} dz \ J_0(kz) \log \frac{r_0}{z} \frac{\partial}{\partial z}\left(z \frac{\partial}{\partial z} \ \sigma_{dT}(z)\right)$$

From an incident dipole to an incident hadron

Using collinear factorization:

The gluon density inside the dipole r_0 :

$$\begin{aligned} g_d(x_J, k^2) &= \frac{\alpha_S C_F}{x_J \pi^2} \int d^2 r \, \frac{r_0^2}{r^2(\vec{r}_0 - \vec{r})^2} \\ &= \frac{4\alpha_S C_F}{x_J \pi} \log r_0 k \end{aligned}$$

The collinear limit $r_0 k \gg 1$ factorizes g_d as expected:

$$\frac{d\sigma}{d^2 k dx_J}(r_0) \simeq$$
$$\frac{1}{2k^2} \left\{ \frac{4\alpha_s C_F}{\pi x_J} \log r_0 k \right\} \int dz \, J_0(kz) \, \frac{\partial}{\partial z} \left(z \frac{\partial}{\partial z} \, \sigma_{dT}(z) \right)$$

Switching to an incident hadron:

- The hard part of the cross-section is the same
- Only the gluon distribution function carries soft information

The forward-jet cross-section

$$\frac{d\sigma^{h+T\to J+X}}{d^2k dx_J} =$$
$$\frac{1}{2k^2}\, g_h(x_J, k^2) \int dz\, J_0(kz)\, \frac{\partial}{\partial z}\left(z\frac{\partial}{\partial z}\, \sigma_{dT}(z, \Delta\eta)\right)$$

- $\Delta\eta$: rapidity interval between the jet and the target
- Valid for linear BFKL evolution
- Valid beyond? work in progress

Forward-jets at HERA

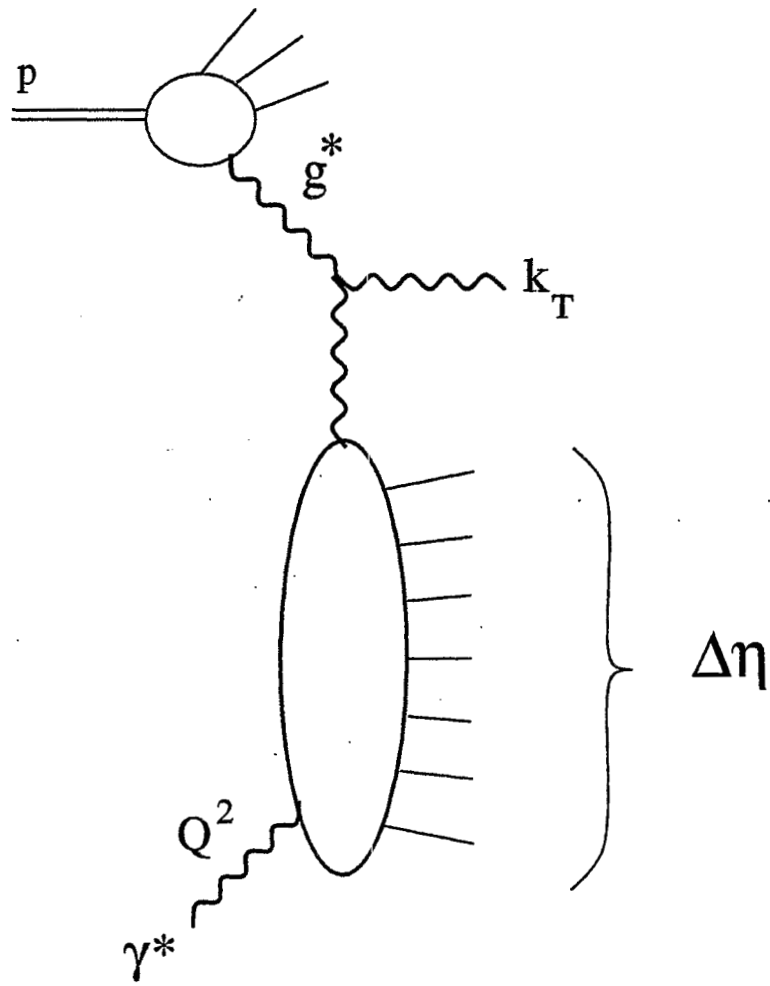

- The target is also a dipole (a virtual photon)
- The dipole-dipole cross-section $\sigma_{dd}(r_1, r_2, \Delta\eta)$ is the relevant quantity
- Its rapidity evolution obeys the JIMWLK equation

The GBW model

The dipole-dipole cross-section is given by

$$\sigma_{dd}(r_1, r_2, \Delta\eta) = \sigma_0 \left\{ 1 - \exp\left(-\frac{r_{eff}^2}{4R_0^2(\Delta\eta)} \right) \right\}$$

- The effective radius is:
  $r_{eff}^2(r_1, r_2) =$
  $\min(r_1^2, r_2^2) \left(1 + \log \frac{\max(r_1, r_2)}{\min(r_1, r_2)} \right)$
- The saturation radius is parametrized by:
  $R_0^2 = \frac{1}{Q_0^2} e^{-\lambda(\Delta\eta - \Delta\eta_0)}, \qquad Q_0 \equiv 1\text{GeV}$

Fitting the data

The cross-section is

$$\frac{d\sigma}{dx dQ^2 dx_J dk_T^2} =$$

$$\frac{\alpha}{2xk_T^2Q^2}\, g_p(x_J, k_T^2) \left\{ \left(\frac{d\sigma_T}{dk_T^2} + \frac{d\sigma_L}{dk_T^2} \right) (1-y) + \frac{d\sigma_T}{dk_T^2} \frac{y^2}{2} \right\}$$

with

$$\frac{d\sigma_{T,L}}{dk_T^2} = \int d^2r_1\, d^2r_2\, |\psi_{T,L}(r_1, Q^2)|^2 \frac{1}{2\pi r_2} J_0(k_T r_2) \times \frac{\partial}{\partial r_2} \left(r_2 \frac{\partial}{\partial r_2}\, \sigma_{dd}(r_1, r_2, \Delta\eta) \right)$$

- x_J, k_T : longitudinal and transverse momenta of the jet
- x, y, and Q^2 : usual kinematic variables of DIS
- We fit the ZEUS and H1 data for $d\sigma/dx$ with three parameters: λ, $\Delta\eta_0$ and a normalization

Results

There are two solutions with a good χ^2 :

fit	λ	$\Delta\eta_0$	$\chi^2(/dof)$
sat.	0.402	-0.82	6.8 (/11)
weak sat.	0.370	8.23	8.3 (/11)

- The first solution corresponds to significant saturation effects
- The second solution corresponds to weak saturation effects
- The intercept λ is in both cases higher than what was found for F_2

Saturation scales

The saturation scale: $Q_s \equiv 1/R_0$

$$\log Q_s^2/Q_0^2 = \lambda(\Delta\eta - \Delta\eta_0)$$

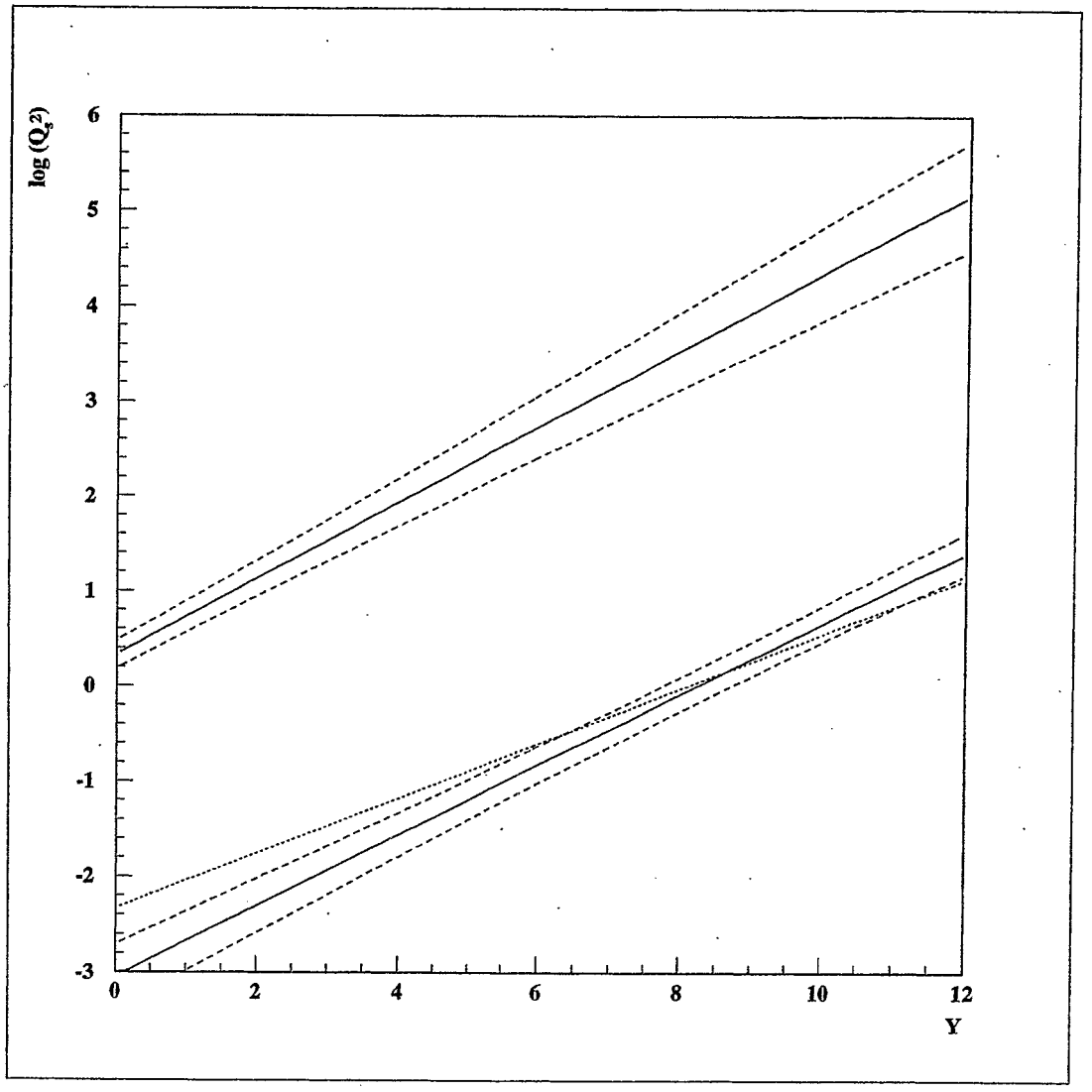

Conclusion

- Derivation of the cross-section dipole+target→forward jet+X:
  A forward-jet emission can be expressed in terms of dipoles
  The extension of the result including quantum evolution is work in progress
- Study of the HERA forward-jet data:
  Using a GBW-like parametrization
  Data consistent with saturation

Heavy Quark Correlators Above Deconfinement

Ágnes Mócsy
Institut für Theoretische Physik, J.W.Goethe University, Frankfurt

in collaboration with
Péter Petreczky (Brookhaven National Laboratory)

Background and Motivation

Current and past experiments at BNL and CERN are and have been colliding heavy ions at relativistic velocities. One of the major goals of these experiments is to produce a deconfined state of matter, known as quark-gluon plasma. In this deconfined phase matter consists of different flavors of quarks and gluons that after a phase transition are not bound inside hadrons anymore. Unlike light quarks, however, bound states of heavy quarks, being smaller in size, could survive inside the plasma to higher temperatures than that of deconfinement. This could be possible due to the color-Coulomb attraction. In the 1980's it was predicted [1] that $c\bar{c}$ bound states would still disappear already at temperatures close to the transition temperature T_c. The idea of Matsui and Satz, based on non-relativistic arguments, was that color screening in the plasma would prevent the strong binding of quarkonia. Thus the dissolution of heavy quark bound states, and therefore the suppression of the J/ψ peak in the dilepton spectra could signal deconfinement.

During the last decades this idea underwent several refinements. It was recognized in the 1970's [2] that what is now known as the Cornell potential (Coulomb plus a linear part) provides a very good description of quarkonia spectra at zero temperature. The essence of potential model calculations in context of deconfinement is to use some finite temperature extension of the zero temperature Cornell potential for understanding the quarkonium spectra. There was quite a substantial effort utilizing such potential models. Later studies, for example, predicted a sequential dissolution pattern [3], which means that higher excitations dissolve earlier. According to [3] the J/ψ peak would still disappear at around $1.1T_c$.

Since the validity of potential models is still dubious, a new way of looking at this problem has been developed. This new way is based on the evaluation on the lattice of the correlators and spectral functions of heavy quark states [4]. But why are correlators of heavy quarks of interest? As we said above, hadronic bound states are expected to dissolve when approaching T_c. So with increasing temperature such resonances become broader and thus unstable, gradually loosing their meaning of resonance. Accordingly, at and/or above T_c they stop being the correct degrees of freedom. Correlation functions of hadronic currents, on the other hand, have an unaltered meaning above and below the transition. These can thus be used in a rather unambiguous manner to extract and follow modifications of properties of quarkonia in a hot medium.

Recently, the numerical analysis of quarkonia correlators and spectral functions was carried out on the lattice for quenched QCD. The produced results were unexpected and interesting [4], and suggest the following: The ground state charmonia, 1S J/ψ and η_c, survive well above T_c, at least up to $1.5T_c$. Not only that these states do not melt at, or close to T_c, as it was expected, but lattice found no change in their properties either, when crossing the transition temperature. For example, the J/ψ mass is $m_{J/\psi}(1.5T_c) \simeq m_{J/\psi}(T=0)$, and the radial wave function at the origin is $|R_{J/\psi}(0)|^2_{1.5T_c} \simeq |R_{J/\psi}(0)|^2_{T=0}$. Furthermore, the same lattice results indicate [4] that properties of the P states, χ_c^0 and χ_c^1, are seriously modified above the transition temparature, and these states are dissolved already at $1.1T_c$. Preliminary lattice results for bottomonium states suggest that $m_\Upsilon(3T_c) \simeq m_\Upsilon(T=0)$ and $|R_\Upsilon(0)|^2_{3T_c} \simeq |R_\Upsilon(0)|^2_{T=0}$. Also, the χ_b survives unaffected up until $T = 2.2T_c$.

These features are in sharp contrast with existing potential model studies and their explanation presents us a puzzle. There have been though some recent attempts to understand these results within present theories. In [5] Zahed and Shuryak estimate the binding energy for the J/ψ, considered as a strongly coupled color-Coulomb bound state, that allows for its survivor until $2.7T_c$. In [6] Wong studied the binding of quarkonia utilizing a potential fitted for the lattice results. He found a spontaneous dissociation temperature of $2T_c$ for the J/ψ.

What we attempt to do here is to accommodate all of the above results within one consistent theory [7]. We provide a unified description for all the features of different charm (J/ψ, η_c, χ_c) and bottom (Υ; Υ', χ_b) quark bound states.

The Model

In this work we investigate the quarkonium correlators and spectral functions in a potential model for different screened Cornell potentials.

The object of our study is the Euclidean correlation function, which can be measured on the lattice. The correlation function is defined for a particular mesonic channel H as

$$G_H(t) = \langle j_H(t) j_H^\dagger(0) \rangle \,. \tag{1}$$

Here $j_H = \bar{q}\Gamma_H q$, and $\Gamma_H = 1, \gamma_\mu, \gamma_5, \gamma_\mu\gamma_5$ corresponds to the scalar, vector,

pseudoscalar and axial vector channels. The spectral decomposition of this meson propagator is

$$G_H(t) = \sum_n |\langle 0|j_H|n\rangle|^2 e^{-E_n t} . \tag{2}$$

On the other hand, the correlator can be expressed in terms of the spectral function

$$G(t,T) = \int d\omega \sigma(\omega,T) K(t,\omega,T) , \tag{3}$$

where K is the integration kernel [4]. Our model spectral function for $T > T_c$ is inspired by its zero temperature version [8] and given by

$$\sigma(\omega,T) = \sum_i F_i \delta\left(\omega^2 - M_i^2(T)\right) + \sigma_c(\omega)\theta\left(\omega - s_0(T)\right) . \tag{4}$$

In the contribution of the continuum (second term) the threshold is equal to twice the pole mass, $s_0 = 2m_p$. It is important here to emphasize, that quarks are propagating with the pole mass given by the constituent mass which received an extra contribution. This contribution is determined by the height of the plateau in the free energy, and was first identified in [9]. Previously, the meaning of the height of the plateau has not been given much attention. Correctly now, we have

$$s_0(T) = 2m_q + \frac{\sigma}{\mu(T)} . \tag{5}$$

From the two expressions of the correlation function, (2) and (3), one can identify

$$F_i = |\langle 0|j_H|i\rangle|^2 . \tag{6}$$

This matrix element is directly related to the radial wave function at the origin. This has been thoroughly discussed in [10] within the framework of non-relativistic QCD, effective field theory relating potentials to quarkonium properties.

The temperature dependence of the quarkonium spectra we determine by solving the Schrödinger equation with the following screened potential [11]

$$V(r,T) = -\frac{\alpha}{r} e^{-\mu(T)r} + \frac{\sigma}{\mu(T)}\left(1 - e^{-\mu(T)r}\right) . \tag{7}$$

In the screened string term and Debye screened Coulomb term the screening mass $\mu(T)$ is properly adjusted to agree with the lattice. The resulting radial wave functions at the origin then can readily be linked to (6) [10].

We repeat the above procedure for another potential, that we have obtained by properly fitting the lattice results of [7].

Results and Discussion

Here we work in pure gauge theory. We expect, however, that the analysis in full QCD can be carried out in a similar manner. We study the lowest states in four channels (scalar, pseudoscalar, vector, axial vector). The complete analysis is presented in [7].

For the sake of illustration we show here our results only for the simple case of the 1P state in the scalar channel, the χ_{c0}. In order to make a direct comparison with lattice results on figure we show the χ_{c0} correlation function normalized to the reconstructed one. $G_{recon}(t,T)$ is constructed using spectral functions at another temperature below the critical one, here at $T=0$:

$$G_{recon}(t,T) = \int d\omega \sigma(\omega, T=0) K(t,\omega,T) \tag{8}$$

Studying the ratio G/G_{recon} can indicate the modifications of the spectral function above T_c. Difference of this ratio from one is an indication of the medium effects.

Figure illustrates that there exists significant system modifications of the χ_{c0} at temperatures already as low as $1.1T_c$. These modifications are present at all distances. Our findings are in agreement with lattice data [4]. The size of the ratio provides us with a rough idea about the magnitude of the medium effects.

For some of the other mesonic correlators we have found rough qualitative but no quantitative agreement with lattice data. In general, the temperature-dependence of the correlators show much reacher structure than the one seen on the lattice. We further found that the results do not depend on the detailed form of the potential and are based on very general physical reasoning. This raises the question whether some physics is missing in the lattice correlators due to lattice artifacts, or the physics of quark gluon plasma is quite subtle in the temperature-region that we studied.

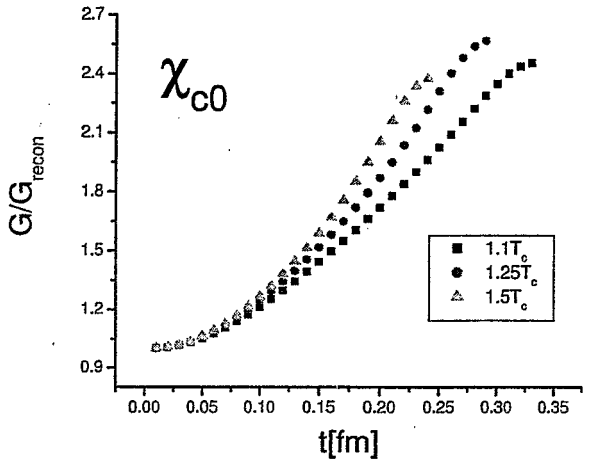

Figure 1: Ratio of correlators of the χ_{c0} for different temperatures.

Bibliography

[1] T. Matsui and H. Satz, Phys. Lett. B **178**, 416 (1986).

[2] E. Eichten, K. Gottfried, T. Kinoshita, K. D. Lane and T. M. Yan, Phys. Rev. D **21**, 203 (1980).

[3] S. Digal, P. Petreczky and H. Satz, Phys. Rev. D **64**, 094015 (2001) [arXiv:hep-ph/0106017].

[4] S. Datta, F. Karsch, P. Petreczky and I. Wetzorke, Phys. Rev. D **69**, 094507 (2004) [arXiv:hep-lat/0312037].

[5] E. V. Shuryak and I. Zahed, arXiv:hep-ph/0307267; arXiv:hep-ph/0403127.

[6] C. Y. Wong, arXiv:hep-ph/0408020.

[7] Á. Mócsy and P. Petreczky, in preparation.

[8] E. V. Shuryak, Rev. Mod. Phys. **65**, 1 (1993).

[9] O. Kaczmarek, F. Karsch, P. Petreczky and F. Zantow, Phys. Lett. B **543**, 41 (2002) [arXiv:hep-lat/0207002].

[10] G. T. Bodwin, E. Braaten and G. P. Lepage, Phys. Rev. D **51**, 1125 (1995) [Erratum-ibid. D **55**, 5853 (1997)] [arXiv:hep-ph/9407339].

[11] F. Karsch, M. T. Mehr and H. Satz, Z. Phys. C **37**, 617 (1988).

New insights in high energy QCD from general tools of statistical physics

Stéphane Munier
CPHT, École Polytechnique, Paris

We show that high energy scattering is a statistical process similar to reaction-diffusion in a system made of a finite number of particles. The Balitsky-JIMWLK equations correspond to the time evolution law for the particle density. The squared strong coupling constant plays the rôle of the minimum particle density. Discreteness is related to the finite number of partons one may observe in a given event and has a sizeable effect on physical observables. Using general tools developed recently in statistical physics, we derive the universal terms in the rapidity dependence of the saturation scale and the scaling form of the amplitude.

Brookhaven, July 16 and July 23, 2004

Goal: understand the energy dependence of hadronic cross sections especially near the unitarity limit

This talk:

Using general results obtained recently in statistical physics, we are able to derive non-trivial properties of the high-energy behavior of QCD scattering amplitudes **from first principles** (parton model):

- rapidity dependence of the saturation scale
- scaling of the scattering amplitude

that are features of the solution to the full Balitsky-JIMWLK equation

Outline

* Rapidity evolution of scattering amplitudes in the parton model
  picture of dipole-dipole scattering and derivation of the evolution equation
* Mean field approximation and its features
  solution to the Kovchegov equation (a review)
* Solution beyond mean field: universal terms
  solution to the Balitsky-JIMWLK equation
* The physical amplitude and its scaling
  effect of fluctuations on the scattering amplitude / breaking of geometric scaling

« Appendix »: example of a model from statistical physics similar to QCD

Amplitudes:

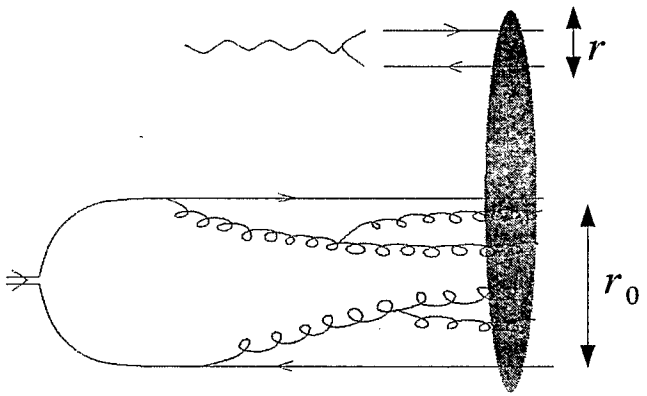

1 « event » = 1 partonic configuration

amplitude $T(r)$

statistical average over events

physical amplitude $A(r,Y)=\langle T(r)\rangle_Y$

Fixed impact parameter dipole amplitude:

$$T(r,r_i)=\alpha_s^2\frac{r^2}{r_i^2} \quad \text{if} \quad r \ll r_i$$

$$=\alpha_s^2\frac{r_i^2}{r^2} \quad \text{if} \quad r \gg r_i$$

up to a number, but not important for the result!

Dipole splitting probability:

$$dP=dY\frac{\overline{\alpha}}{2\pi}d^2r_2\frac{r_1^2}{r_2^2(r_1-r_2)^2}=[\lambda\, dY][\rho(r_2,r_1)d^2r_2]$$

splitting proba — distrib of sizes

$$\overline{\alpha}=\frac{\alpha_s N_c}{\pi}$$

Interaction amplitude for a typical partonic configuration

(deduced from the dipole evolution law)

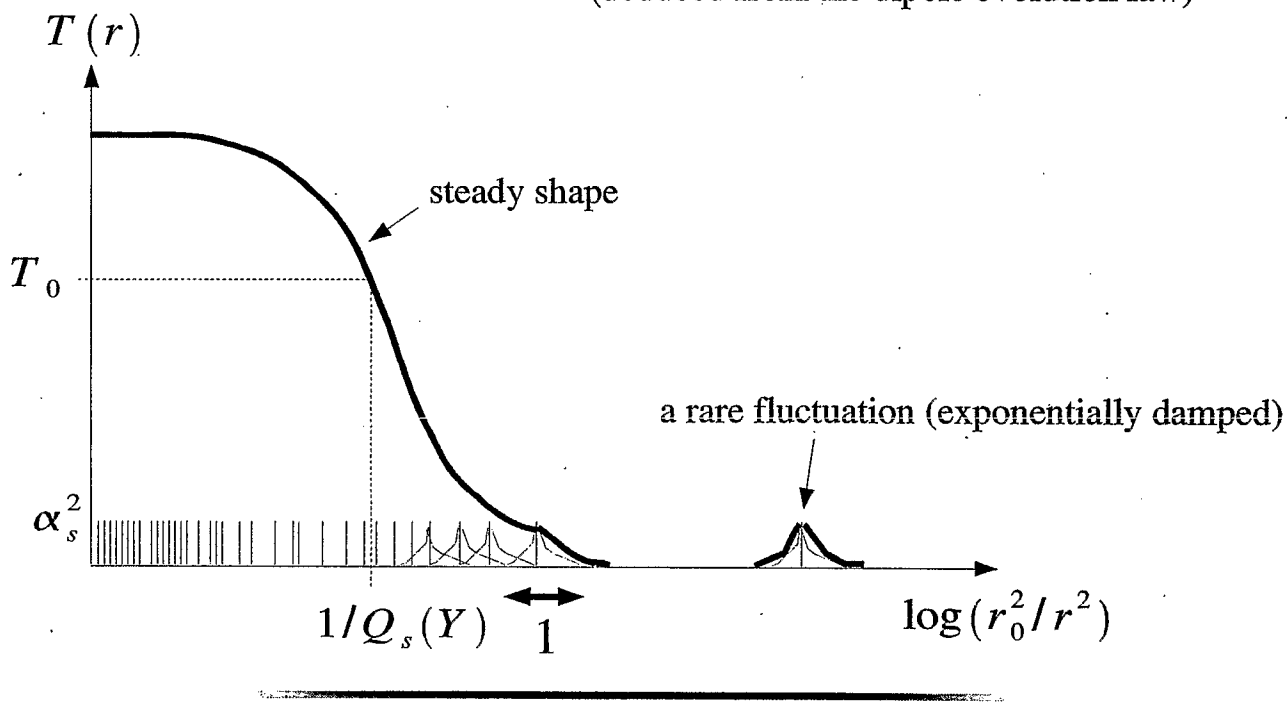

Balitsky hierarchy (first equation):

$$\partial_Y \langle T(r;Y)\rangle = \frac{\bar{\alpha}}{2\pi}\int d^2 z \frac{r^2}{z^2(r-z)^2}\left(\langle T(z,Y)\rangle + \langle T(r-z,Y)\rangle - \langle T(r,Y)\rangle - \langle T(z,Y)T(r-z,Y)\rangle\right)$$

Kovchegov equation (mean field):

$$\partial_Y \langle T(r,Y)\rangle = \frac{\bar{\alpha}}{2\pi}\int d^2 z \frac{r^2}{z^2(r-z)^2}\left(\langle T(z,Y)\rangle + \langle T(r-z,Y)\rangle - \langle T(r,Y)\rangle - \langle T(z,Y)\rangle\langle T(r-z,Y)\rangle\right)$$

$$\phi(k,Y) = \int \frac{d^2 r}{2\pi r^2} e^{ikr}\langle T(r,Y)\rangle \qquad \partial_Y \phi(k,Y) = \bar{\alpha}\chi(-\partial_{\log k^2})\phi(k,Y) - \bar{\alpha}\phi^2(k,Y)$$

Fisher-Kolmogorov equation:

$$\partial_t u(x,t) = \partial_x^2 u(x,t) + u(x,t) - u^2(x,t)$$

Solution:

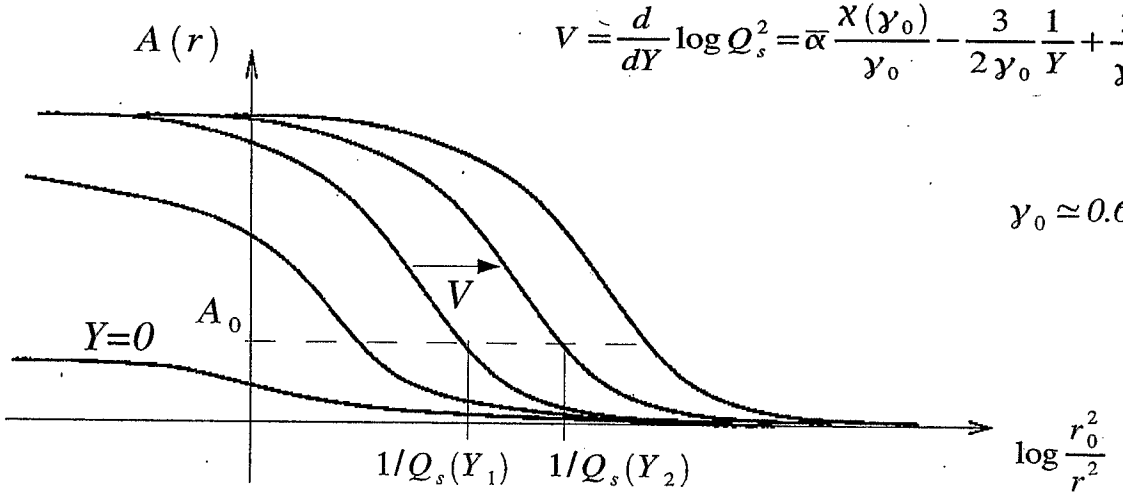

$$V = \frac{d}{dY}\log Q_s^2 = \bar{\alpha}\frac{\chi(\gamma_0)}{\gamma_0} - \frac{3}{2\gamma_0}\frac{1}{Y} + \frac{3}{\gamma_0^2}\sqrt{\frac{\pi}{2\bar{\alpha}\chi''(\gamma_0)}}\frac{1}{Y^{3/2}} + \ldots$$

$\gamma_0 \simeq 0.63$ solves $\dfrac{\chi(\gamma_0)}{\gamma_0} = \chi'(\gamma_0)$

$$V = \frac{d}{dY} \log Q_s^2 = \bar{\alpha} \frac{\chi(\gamma_0)}{\gamma_0} - \frac{3}{2\gamma_0} \frac{1}{Y} + \frac{3}{\gamma_0^2} \sqrt{\frac{\pi}{2\,\bar{\alpha}\chi''(\gamma_0)}} \frac{1}{Y^{3/2}} + \ldots$$

$$\gamma_0 \simeq 0.63 \quad \text{solves} \quad \frac{\chi(\gamma_0)}{\gamma_0} = \chi'(\gamma_0)$$

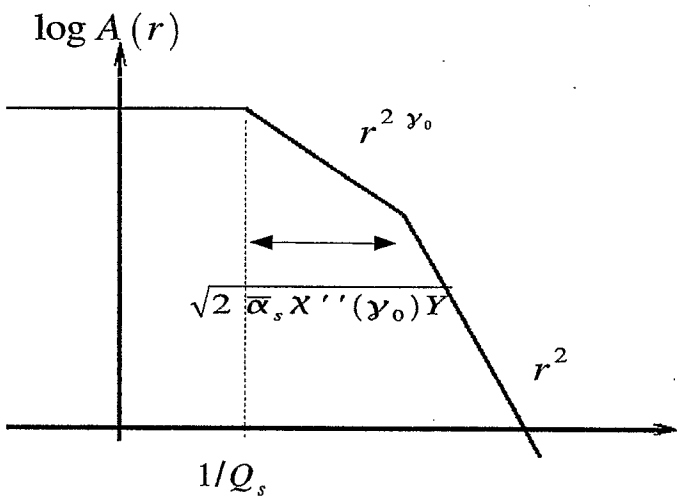

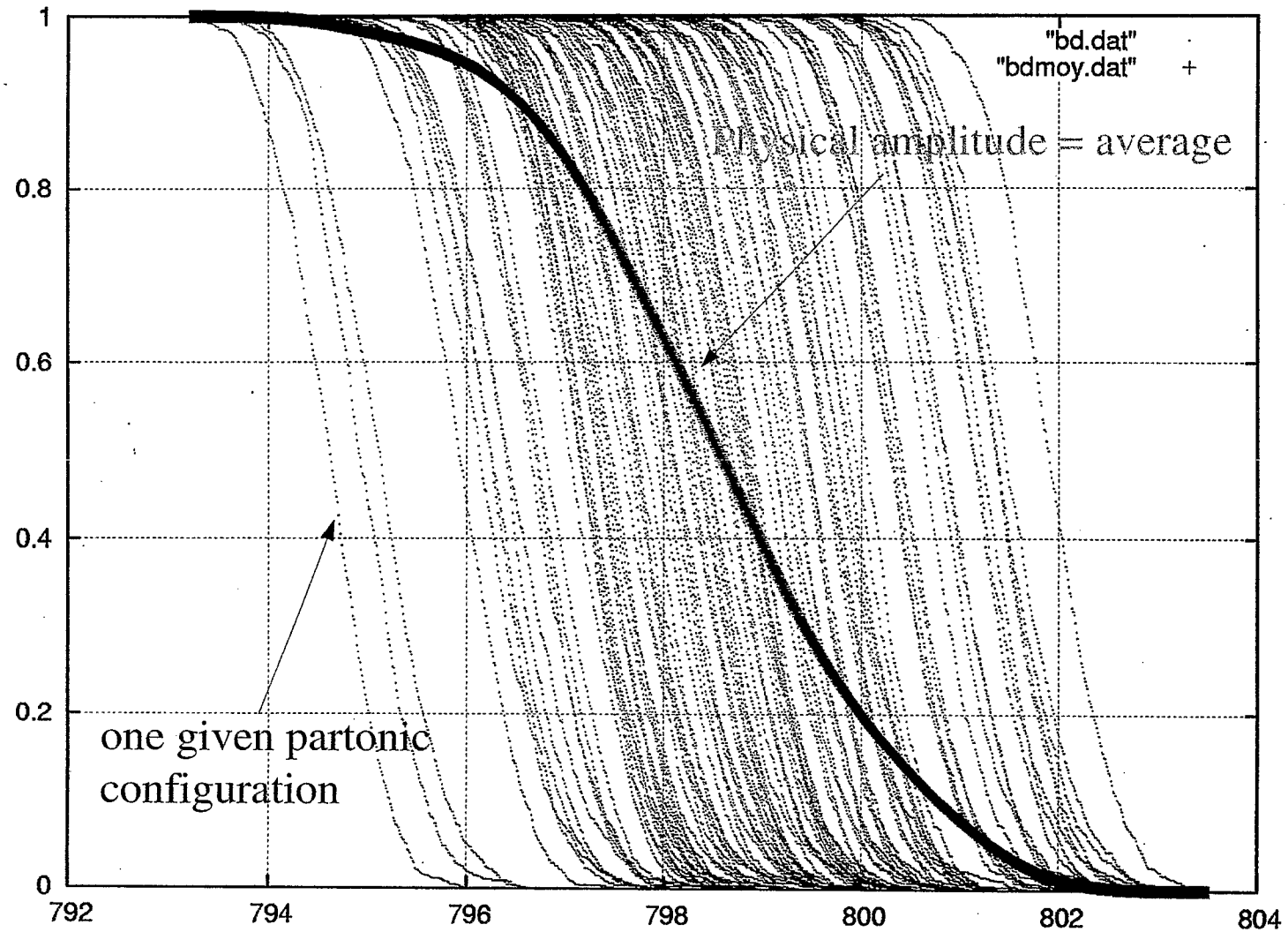
"bd.dat"
"bdmoy.dat"
Physical amplitude = average
one given partonic configuration
1
0.8
0.6
0.4
0.2
0
792
794
796
798
800
802
804

Summary

Using general results obtained recently in statistical physics, we are able to derive non-trivial properties on the high-energy behavior of QCD scattering amplitudes **from first principles** (parton model)

Balitsky-Kovchegov equation is in the universality class of F-KPP equation

$$\partial_t u(x,t) = \partial_x^2 u(x,t) + u(x,t) - u^2(x,t)$$

Balitsky-JIMWLK equation is in the universality class of sF-KPP equation

$$\partial_t u(x,t) = \partial_x^2 u(x,t) + u(x,t) - u^2(x,t) + \sqrt{u(x,t)}\,\eta(x,t)$$

Fluctuations are related to the finite number of partons in a given event

Summary (cont'd)

<u>Main results:</u>

saturation scale: $V = \frac{d}{dY} \log Q_s^2 = \bar{\alpha} \frac{\chi(\gamma_0)}{\gamma_0} - \frac{\pi^2 \gamma_0 \chi''(\gamma_0)}{2 \log^2(\alpha_s^2)} + \ldots$

amplitude: $\langle T(r, Y) \rangle = A \left(\frac{\log r^2 Q_s^2(Y)}{\sqrt{\bar{\alpha} Y / \log^3(1/\alpha_s^2)}} \right)$ NEW

in progress with Mueller, Iancu

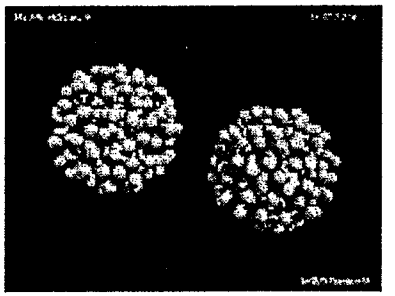

BROOKHAVEN NATIONAL LABORATORY home

RIKEN BNL Research Center

Non-ideal fluid dynamics for relativistic nuclear collisions

Azwinndini Muronga

University of Frankfurt

August 6, 2004

Nuclear Theory/RIKEN Seminar

Outline

- Why non-ideal fluid dynamics
- Basics of non-ideal fluid dynamics
- Standard irreversible thermodynamics
- Extended irreversible thermodynamics
- Relativistic nuclear collisions
  - * 1-dimensional boost invariance fluid dynamics
  - * Transverse expansion + longitudinal boost invariance
- Summary
- Conclusions and outlook

Why non-ideal fluid dynamics?

- Non-equilibrium properties of hot and dense nuclear matter
- Observables:

  Particle Spectra/multiplicities,

  HBT radii, Elliptic flow
- Hydromolecular dynamics
- Fluctuations and transport coefficients

Basics of non-ideal fluid dynamics

Consider a simple fluid (single particle species). This fluid is characterized by:

$N^\mu(x)$ particle 4-current, $T^{\mu\nu}(x)$ energy-momentum tensor and $S^\mu(x)$ entropy 4-current

$N^\mu(x)$ and $T^{\mu\nu}(x)$ conserved: $\partial_\mu N^\mu(x) = \partial_\mu T^{\mu\nu}(x) \equiv 0$

Second law of thermodynamics : $\partial_\mu S^\mu(x) \geq 0$

$$N^\mu = nu^\mu + V^\mu$$

$$T^{\mu\nu} = \varepsilon u^\mu u^\nu - p\Delta^{\mu\nu} + 2W^{(\mu}u^{\nu)} + t^{\mu\nu}$$

$$S^\mu = su^\mu + R^\mu$$

$$t^{\mu\nu} = \pi^{\mu\nu} - \Pi\Delta^{\mu\nu}$$

$$W^\mu = q^\mu + hV^\mu$$

Tensor decomposition

- For an arbitrary u^μ : $u^\mu u_\mu = 1$! $\Delta^{\mu\nu} = g^{\mu\nu} - u^\mu u^\nu, \quad g^{\mu\nu} = \mathrm{diag}(+1,-1,-1,-1)$ $\quad u_\nu \Delta^{\mu\nu} = 0$

$$N^\mu = n u^\mu \qquad + V^\mu$$

$$T^{\mu\nu} = \varepsilon u^\mu u^\nu - p\Delta^{\mu\nu} \qquad + 2W^{(\mu} u^{\nu)} + t^{\mu\nu}$$

$$S^\mu = s u^\mu \qquad + \Phi^\mu$$

$$t^{\mu\nu} = \pi^{\mu\nu} - \Pi\Delta^{\mu\nu}$$

$$W^\mu = q^\mu + h V^\mu$$

$$u_\mu V^\mu = u_\mu W^\mu = u_\mu t^{\nu\nu} = u_\mu \Phi^\mu = \pi^\nu_\nu \equiv 0$$

- Space-time derivative $\partial^\mu = u^\mu \mathrm{D} + \nabla^\mu; \quad \mathrm{D} = u^\mu \partial_\mu, \quad \nabla^\mu = \Delta^{\mu\nu}\partial_\nu$
- Notation $\quad A^{(\mu\nu)} \equiv \frac{1}{2}(A^{\mu\nu} + A^{\nu\mu})$

Physical Meanings

In the local rest frame $u^\mu \equiv (1,\vec{0})$

$n \equiv u_\mu N^\mu$	number density
$V^\mu \equiv \Delta^\mu_\nu N^\nu$	particle flux
$\varepsilon \equiv u_\mu T^{\mu\nu} u_\nu$	energy density
$p + \Pi \equiv -\frac{1}{3}\Delta_{\mu\nu} T^{\mu\nu}$	pressure
$W^\mu \equiv u_\nu T^{\nu\lambda} \Delta^\mu_\lambda$	energy flow
$q^\mu \equiv W^\mu - hV^\mu$	heat flow
$\pi^{\mu\nu} \equiv T^{\langle\mu\nu\rangle}$	stress tensor
$s \equiv u_\mu S^\mu$	entropy density
$\Phi^\mu \equiv \Delta^\mu_\nu S^\nu$	entropy flux

Notation $A^{\langle\mu\nu\rangle} \equiv \left[\frac{1}{2}\left(\Delta^\mu_\alpha \Delta^\nu_\beta + \Delta^\mu_\beta \Delta^\nu_\alpha\right) - \frac{1}{3}\Delta^{\mu\nu}\Delta_{\alpha\beta}\right] A^{\alpha\beta}$

Conservation laws

- Net charge $\partial_\mu N^\mu \equiv 0$:

$$\mathrm{D}n = -n\nabla_\mu u^\mu - \nabla_\mu V^\mu + V_\mu \mathrm{D}u^\mu$$

- Momentum $\Delta^\mu_\nu \partial_\lambda T^{\mu\nu} \equiv 0$:

$$(\varepsilon + p)\mathrm{D}u^\mu = \nabla^\mu p - \nabla_\nu(\pi^{\mu\nu} - \Pi\Delta^{\mu\nu}) + (\pi^{\mu\nu} - \Pi\Delta^{\mu\nu})\mathrm{D}u_\nu - [\Delta^\mu_\nu \mathrm{D}W^\mu + 2W^{(\mu}\nabla_\nu u^{\nu)}]$$

- Energy $u_\nu \partial_\mu T^{\mu\nu} \equiv 0$:

$$\mathrm{D}\varepsilon = -(\varepsilon + p)\nabla_\mu u^\mu + (\pi^{\mu\nu} - \Pi\Delta^{\mu\nu})\nabla_\mu u_\nu - \nabla_\mu W^\mu + 2W^\mu \mathrm{D}u_\mu$$

- 4+1 equations contain 10+4 unknown functions

$\Rightarrow$ 6+3 additional equations required to determine

$\Pi, \pi^{\mu\nu}, V^\mu$ or q^μ

14 Fields Theory

14 unknown functions in 5 equations are:

$n(1)$,$\varepsilon(1)$,$\Pi(1)$,$q^{\mu}(3)$,$V^{\mu}(3)$,$\pi^{\mu\nu}(5)$

u^{μ} is arbitrary.

Eckart or particle frame:

u^{μ} is the particle 4-velocity and $V^{\mu}=0$

14 unknowns are $n,\varepsilon,\Pi,q^{\mu},\pi^{\mu\nu},u^{\mu}$

$$u_N^{\mu} = \frac{N^{\mu}}{\sqrt{N_{\nu}N^{\nu}}}$$

Landau-Lifshitz or energy frame:

u^{μ} is the energy flow 4-velocity and $W^{\mu}=0$

14 unknowns are $n,\varepsilon,\Pi,V^{\mu},\pi^{\mu\nu},u^{\mu}$

$$u_E^{\mu} \equiv \frac{T_{\nu}^{\mu}u_E^{\nu}}{\sqrt{u_E^{\alpha}T_{\alpha}^{\beta}T_{\beta\lambda}u_E^{\lambda}}}$$

Standard non-ideal fluid dynamics

C. Eckart, Phys. Rev. 58 (1940) 919

L. Landau, E.M. Lifshitz "Fluid Mechanics"

Assumption: S^μ is linear (first order) in dissipative quantities

$$\Rightarrow \quad S^\mu = S^\mu_{eq} + \beta q^\mu$$

Then $\partial_\mu S^\mu \geq 0$ with $u_\nu \partial_\mu T^{\mu\nu} = 0$ and $\partial_\mu N^\mu = 0$

$$\Rightarrow T\partial_\mu S^\mu = q^\mu \beta^{-1}(\nabla_\mu \beta + Du_\mu) + \pi^{\mu\nu}\nabla_\mu u_\nu - \Pi \nabla_\mu u^\mu \geq 0$$

$$\Rightarrow \quad \Pi = -\zeta \nabla_\mu u^\mu \qquad \zeta \geq 0 \text{ bulk viscosity}$$

$$q^\mu = \kappa(\nabla^\mu T - T\mathrm{D}u^\mu) \qquad \kappa \geq 0 \text{ thermal conductivity}$$

$$\pi^{\mu\nu} = 2\eta \nabla^{\langle\mu} u^{\nu\rangle} \qquad \eta \geq 0 \text{ shear viscosity}$$

Second law of thermodynamics $\partial_\mu S^\mu = \dfrac{\Pi^2}{\zeta T} - \dfrac{q_\mu q^\mu}{\kappa T^2} + \dfrac{\pi^{\mu\nu}\pi_{\mu\nu}}{2\eta T} \geq 0$

Navier-Stokes-Fourier Laws

Energy conservation + Eckart law

$$\Rightarrow \frac{\partial T}{\partial t} = \chi \nabla^2 T \qquad \text{parabolic, } \Rightarrow \text{infinite speeds}$$

Modified Eckart law : $\tau \dot{\vec{q}} + \vec{q} = -\kappa \vec{\nabla} T$ (Maxwell-Cattaneo)

C. Cattaneo, C.R. Akad. Sci. (Paris) 247 (1958) 431

$$\Rightarrow \tau \frac{\partial^2 T}{\partial t^2} + \frac{\partial T}{\partial t} - \chi \nabla^2 T = 0 \qquad \text{(telegraph equation)}$$

For $T \propto \exp\{i(\vec{k}.\vec{x} - \omega t)\}$

$$\Rightarrow \quad k^2 = \frac{\tau \omega^2}{\chi} + i\omega \qquad \text{(dispersion relation)}$$

Phase velocity: $v_{ph} = \dfrac{\omega}{\mathrm{Re}(k)} = \sqrt{\dfrac{2\chi\omega}{\tau\omega + \sqrt{1+\tau^2\omega^2}}}$

In high frequency limit, ($\omega >> \tau^{-1}$) : $v_{ph} = \sqrt{\dfrac{\chi}{\tau}}$

Causal non-ideal fluid dynamics

Allow entropy 4-current to include terms up to second order in dissipative quantities.

H. Grad, comm. Pure. appl. Math. 2 (1949) 331,; I. Müller, Z. Phys. 198 (1967) 329

W. Israel, J. M. Stewart, Ann. Phys. 118 (1979) 341

$$S^\mu = su^\mu + \frac{q^\mu}{T} - \left(\beta_0 \Pi^2 - \beta_1 q_\nu q^\nu + \beta_2 \pi_{\nu\lambda}\pi^{\nu\lambda}\right)\frac{u^\mu}{2T} - \frac{\alpha_0 \Pi q^\mu}{T} + \frac{\alpha_1 \pi^{\mu\nu} q_\nu}{T}$$

$$\begin{aligned}
\tau_\Pi \dot{\Pi} + \Pi &= -\zeta\Theta && + l_{\Pi q}\nabla_\mu q^\mu \\
\tau_q \Delta^{\mu\nu}\dot{q}_\nu + q^\mu &= \kappa\left(\nabla^\mu T - T\dot{u}^\mu\right) && - l_{q\Pi}\nabla^\mu \Pi - l_{q\pi}\nabla_\nu \pi^{\mu\nu} \\
\tau_\pi \Delta^{\alpha\mu}\Delta^{\beta\nu}\dot{\pi}_{\alpha\beta} + \pi^{\mu\nu} &= 2\eta\sigma^{\mu\nu} && + l_{\pi q}\nabla^{\langle\mu} q^{\nu\rangle}
\end{aligned}$$

$$\tau_\Pi = \zeta\beta_0, \quad \tau_q = \kappa T\beta_1, \quad \tau_\pi = 2\eta\beta_2$$

$$l_{\Pi q} = \zeta\alpha_0, \quad l_{q\Pi} = \kappa T\alpha_0, \quad l_{q\pi} = \kappa T\alpha_1, \quad l_{\pi q} = 2\eta\alpha_1$$

$$\Theta = \nabla_\mu u^\mu = \partial_\mu u^\mu$$

$$\dot{A} = \mathrm{D}A = u^\mu \partial_\mu A$$

$$\sigma^{\mu\nu} = \nabla^{\langle\mu} u^{\nu\rangle}$$

Entropy Production

$$
\begin{aligned}
T\partial_\mu S^\mu = &-\Pi\left[\Theta + \beta_0\dot{\Pi} + \frac{1}{2}\Pi T\partial_\mu\left(\frac{\beta_0}{T}u^\mu\right) - \alpha_0\nabla_\mu q^\mu\right] \\
&- q^\mu\left[\nabla_\mu \ln T - \dot{u}_\mu - \beta_1\dot{q}_\mu - \frac{1}{2}q_\mu T\partial_\nu\left(\frac{\beta_1}{T}u^\nu\right) - \alpha_0\nabla_\nu\pi^\nu_\mu - \alpha_1\nabla_\mu\Pi\right] \\
&+ \pi^{\mu\nu}\left[\sigma_{\mu\nu} - \beta_2\dot{\pi}_{\mu\nu} + \frac{1}{2}\pi_{\mu\nu}T\partial_\lambda\left(\frac{\beta_2}{T}u^\lambda\right) + \alpha_1\nabla_{\langle\mu}q_{\nu\rangle}\right]
\end{aligned}
$$

Causality Check

Relaxation equations are hyperbolic and satisfies causality and equilibria are stable

W. Israel, J.M. Stewart

W. Hiscock, L. Lindblom, Ann. Phys. 151 (1983) 466; Phys. Rev. D 35 (1987) 3723; Phys. Rev. D 31 (1985) 725

A. Muronga, nucl-th/0309055

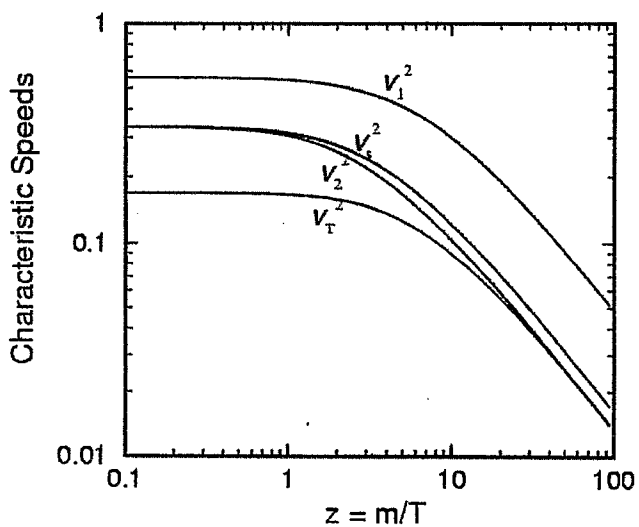

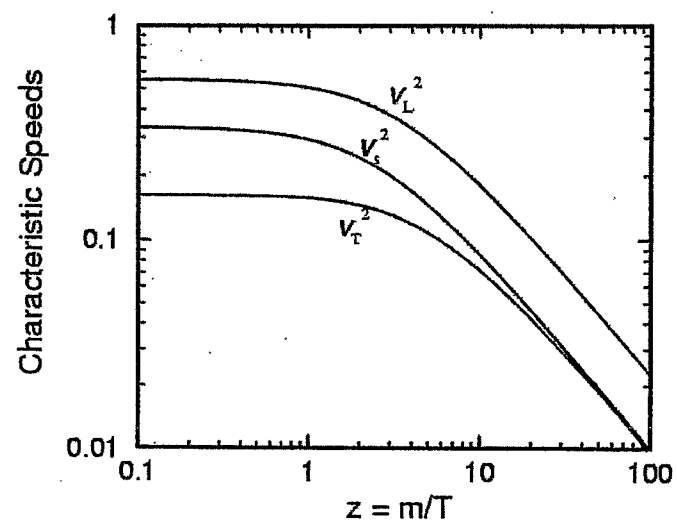

Ultra-Relativistic Nuclear Collisions

J.D. Bjorken
PRD 27 (1983)

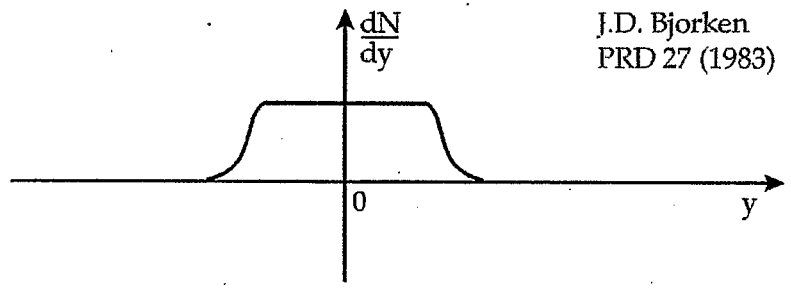

Longitudinal boost invariant

$$v = \frac{z}{t}, \quad t = \tau \cosh y, \quad z = \tau \sinh y$$

$$\tau = \sqrt{t^2 - z^2}, \quad y = \frac{1}{2}\ln\left(\frac{t+z}{t-z}\right)$$

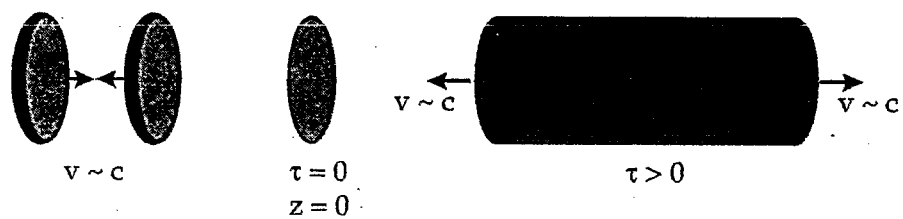

Apply to: $\partial_\mu T^{\mu\nu} = 0, \quad n_B = 0$

$$\Rightarrow \begin{cases} \partial_t T^{tt} + \partial_z T^{tz} = 0 \\ \partial_t T^{zt} + \partial_z T^{zz} = 0 \end{cases}$$

A. Muronga, PRC(03/2004); PRC(04/2004)

A. Muronga, PRL (2002)

Energy-momentum tensor

In LRF

$$T_*^{\mu\nu} = \begin{pmatrix} \varepsilon & 0 & 0 & 0 \\ 0 & p+\Pi-\frac{\pi}{2} & 0 & 0 \\ 0 & 0 & p+\Pi-\frac{\pi}{2} & 0 \\ 0 & 0 & 0 & p+\Pi+\pi \end{pmatrix} \quad T_\nu^\nu = \varepsilon - 3(p+\Pi), \quad \pi_\nu^\nu = \pi^{\mu\nu} u_\nu = 0$$

Boost by $u^\mu = (\cosh y, 0, 0, \sinh y)$

$$T^{\mu\nu} = \begin{pmatrix} w\cosh^2 y - \mathrm{P} & 0 & 0 & w\cosh y \sinh y \\ 0 & \mathrm{P}_\perp & 0 & 0 \\ 0 & 0 & \mathrm{P}_\perp & 0 \\ w\cosh y \sinh y & 0 & 0 & w\sinh^2 y + \mathrm{P} \end{pmatrix}$$

$$w = \varepsilon + \mathrm{P}, \quad \mathrm{P} = p + \Pi + \pi, \quad \mathrm{P}_\perp = p + \Pi - \frac{\pi}{2}$$

Perfect fluid: $\Pi = \pi = 0$

First order: $\Pi = -\zeta \frac{1}{\tau}, \quad \pi = -\frac{4}{3}\eta \frac{1}{\tau}$

Second order: determined from relaxation equations

Perfect Fluid Dynamics

Energy-momentum conservation

$$\frac{\partial \varepsilon}{\partial \tau} + \frac{\varepsilon + p}{\tau} = 0$$

$$\frac{\partial p}{\partial y} = 0$$

$$\Rightarrow \quad \frac{\partial s}{\partial \tau} + \frac{s}{\tau} = 0, \quad \Rightarrow s\tau = s_0 \tau_0 = \text{constant}$$

With EoS : $s = 4aT^3 \quad \Rightarrow \quad p = aT^4 = \frac{1}{3}\varepsilon$

$$\Rightarrow \quad T(\tau) = T_0 \left(\frac{\tau_0}{\tau}\right)^{\frac{1}{3}}$$

$$s(\tau) = s_0 \frac{\tau_0}{\tau}$$

$$\varepsilon(\tau) = \varepsilon_0 \left(\frac{\tau_0}{\tau}\right)^{\frac{4}{3}}$$

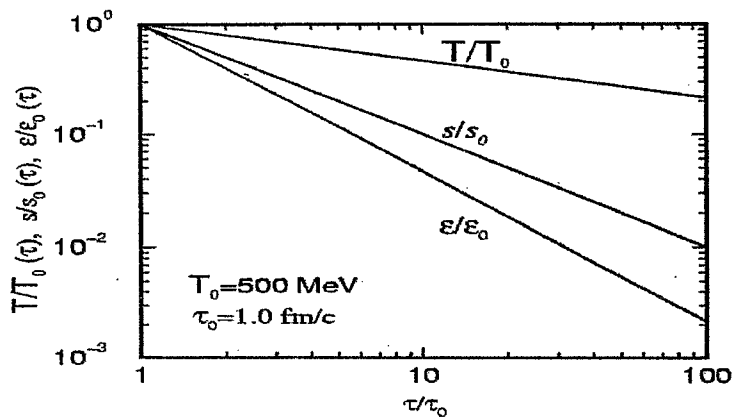

First Order Theories

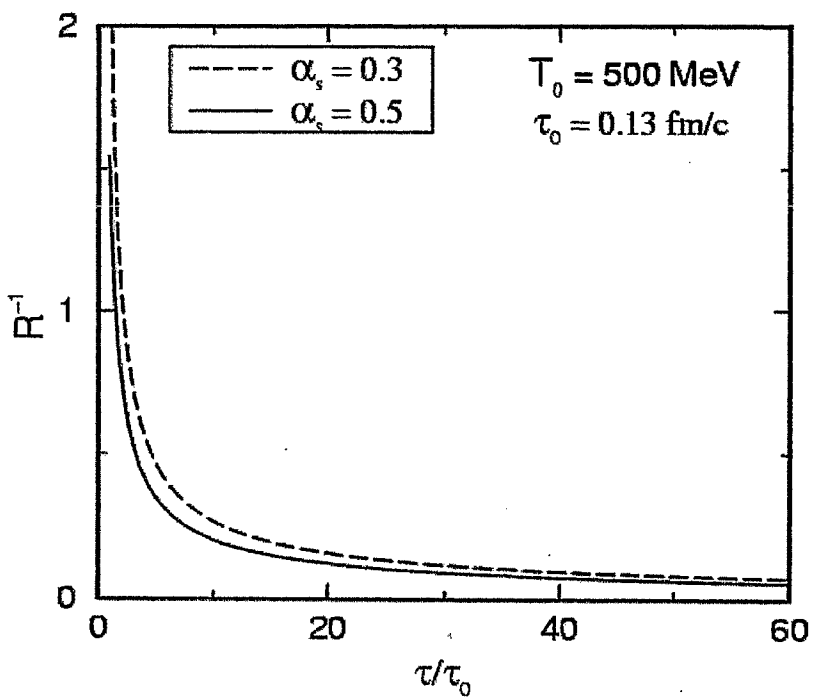

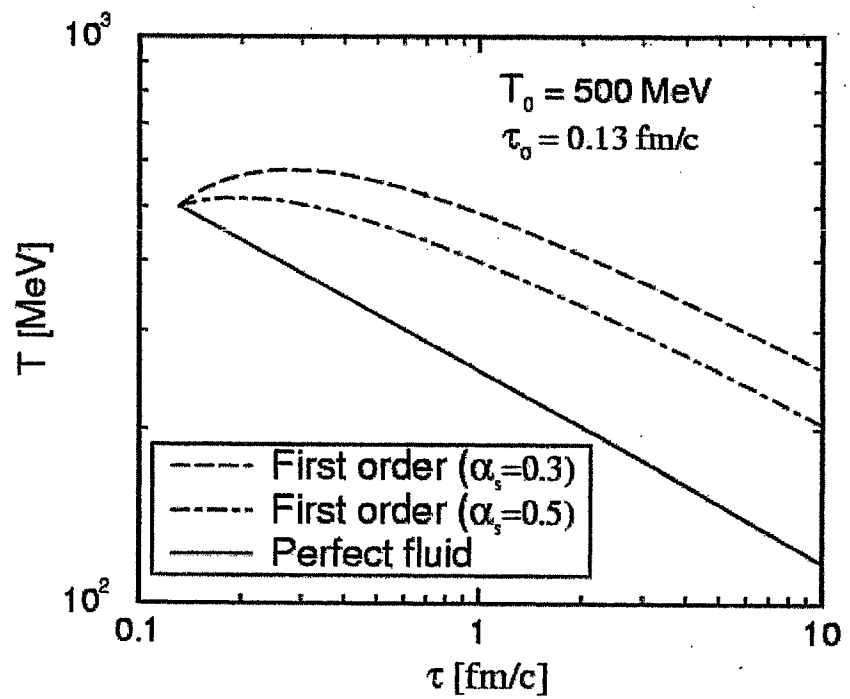

Second Order Theories

Energy equation $$\frac{d\varepsilon}{d\tau}+\frac{\varepsilon+p}{\tau}-\frac{\Phi}{\tau}=0$$

Transport equation $$\frac{d\Phi}{d\tau}=-\frac{\Phi}{\tau_\pi}-\frac{1}{2}\Phi\left(\frac{1}{\tau}+\frac{T}{\beta_2}\frac{d}{d\tau}\left(\frac{\beta_2}{T}\right)\right)+\frac{2}{3}\frac{1}{\beta_2}\frac{1}{\tau}$$

EoS and transport coefficients

$$p=\frac{1}{3}\varepsilon=aT^4,\quad a=\left(16+\frac{21}{2}N_f\right)\frac{\pi^2}{90}$$

$$\eta=bT^3,\ \ b=(1+1.7N_f)\frac{0.342}{\left(1+\frac{N_f}{6}\right)\alpha_s^2\ln\left(\alpha_s^{-1}\right)}T^3,\ \ \beta_2=\frac{3}{4p},$$

Then $$\frac{d}{d\tau}T=-\frac{T}{3\tau}+\frac{T^{-3}\Phi}{12a\tau}$$

$$\frac{d}{d\tau}\Phi=-\frac{2aT\Phi}{3b}-\frac{1}{2}\Phi\left(\frac{1}{\tau}-5\frac{1}{T}\frac{d}{d\tau}T\right)+\frac{8aT^4}{9\tau}$$

Time evolution of thermodynamic quantities

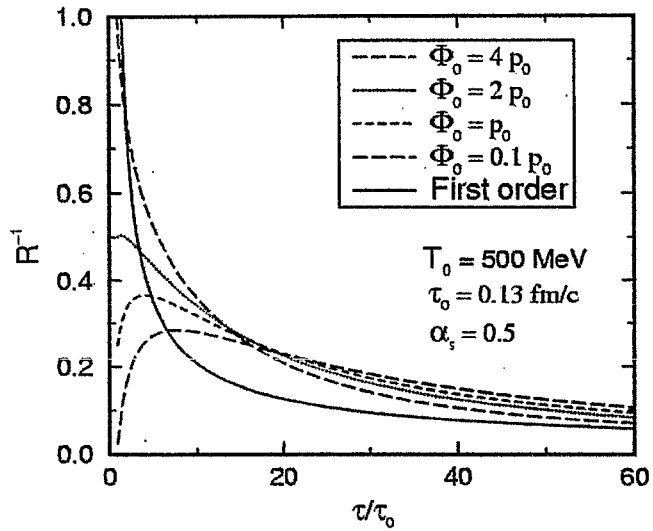

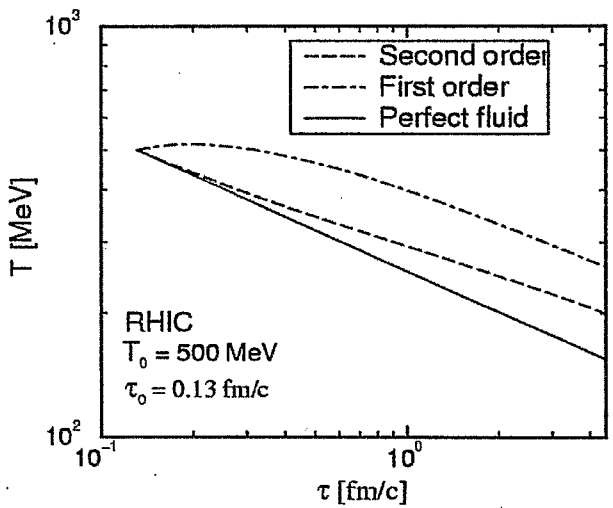

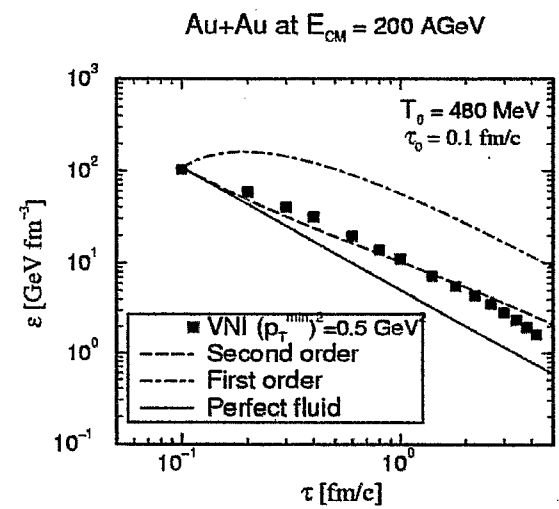

Kinetic theory & transport models

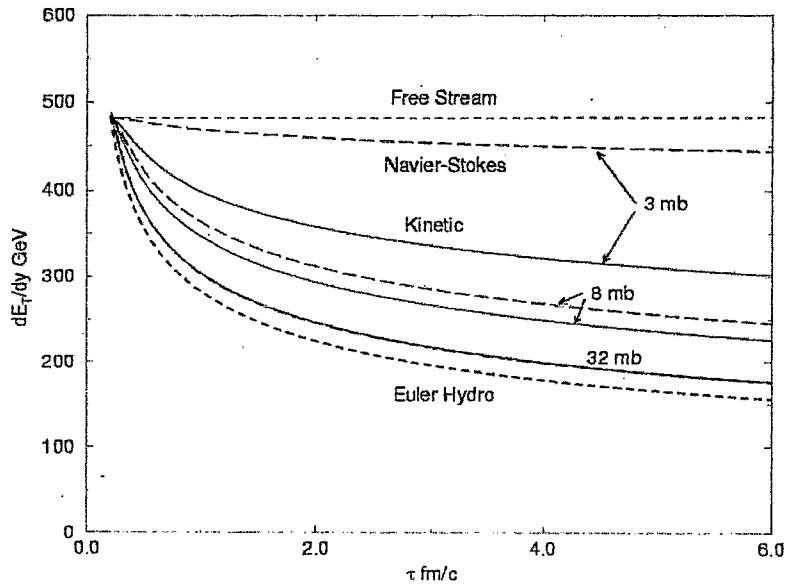

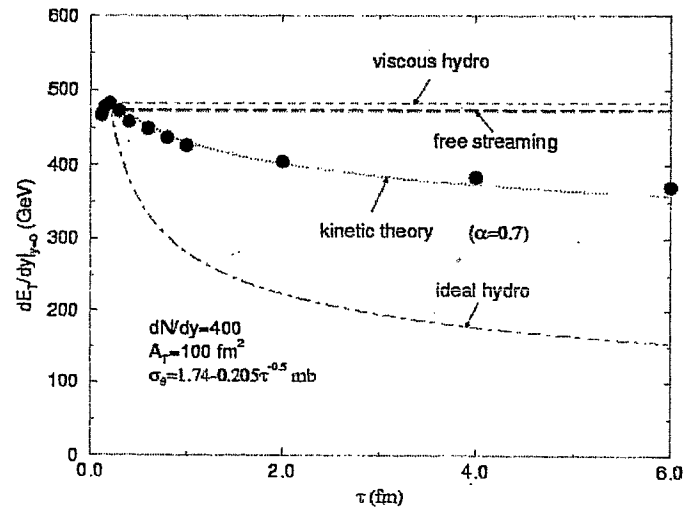

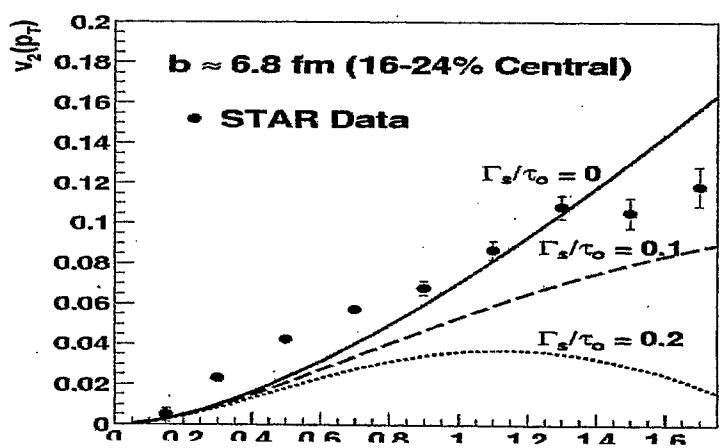

Longitudinal + transverse expansion

A. Muronga and D.H. Rischke nucl-th/0407114

- Boost energy-momentum tensor by

$$u^{\mu} = \gamma_{\perp}(\cosh y, v_{\perp}\cos\phi, v_{\perp}\cos\phi, \sinh y)$$

$$\Rightarrow \quad T^{00} = w\gamma^2 - P_{\perp} + 2q^r v_{\perp}\gamma^2$$

$$T^{0r} = w\gamma^2 v_{\perp} + q^r\left(v_{\perp}^2 + 1\right)\gamma^2$$

$$T^{rr} = w\gamma^2 v_{\perp}^2 + P_{\perp} + 2q^r v_{\perp}\gamma^2$$

$$T^{zz} = P_z$$

$$T^{\phi\phi} = P_{\phi}$$

Equations to solve numerically

- Conservation Equations

$$\partial_\tau T^{00} = -\partial_r\left\{(T^{00}+P_\perp)v_\perp + q^r\right\} - (T^{00}+P_\perp)\left\{\frac{1}{\tau}+\frac{v_\perp}{r}\right\} + (P_\perp - P_z)\frac{1}{\tau} - q^r\frac{1}{r}$$

$$\partial_\tau T^{0r} = -\partial_r\left\{(T^{0r}+q^r)v_\perp + P_\perp\right\} - T^{0r}\left\{\frac{1}{\tau}+\frac{v_\perp}{r}\right\} - (P_\perp - P_\phi)\frac{1}{r} - q^r\frac{v_\perp}{r}$$

$$w = \varepsilon + P_\perp$$

$$P_\perp = p + \Pi + \frac{\pi^{rr}}{\gamma^2}$$

$$P_z = p + \Pi + \pi^{zz}$$

$$P_\phi = p + \Pi + \pi^{\phi\phi}$$

$$v_s = \frac{T^{0r}}{T^{00}}$$

- Velocity and local energy density

$$v_\perp = \frac{T^{0r} - q^r}{T^{00} + P_\perp}$$

$$\varepsilon = T^{00} - \frac{T^{0r^2} - q^{r^2}}{T^{00} + P_\perp} \qquad p = \frac{1}{3}\varepsilon \Rightarrow \varepsilon = -\left(T^{00} + \frac{3}{2}\pi^{rr}\right) + \sqrt{4T^{00^2} - 3\left(T^{0r^2} - q^{r^2}\right) + \frac{9}{2}T^{00}\pi^{rr} + \frac{9}{4}\pi^{rr^2}}$$

Transport equations

- Evolution equations for dissipative fluxes

$$\partial_\tau \Pi = -v_\perp \partial_r \Pi - \Pi \frac{1}{\gamma\tau_\Pi} - \zeta\Theta \frac{1}{\gamma\tau_\Pi} - \frac{1}{2\gamma}\Pi\left(\Theta - \frac{5}{4}\frac{D\varepsilon}{\varepsilon}\right)$$

$$\partial_\tau q^r = -v_\perp \partial_r q^r - q^r \frac{1}{\gamma\tau_q} - \kappa T\left(\frac{1}{4}\frac{\nabla\varepsilon}{\varepsilon} - D\{\gamma v_\perp\}\right)\frac{1}{\gamma\tau_q} - \frac{1}{2\gamma} q^r\left(\Theta - \frac{5}{4}\frac{D\varepsilon}{\varepsilon}\right)$$

$$\partial_\tau \pi^{rr} = -v_\perp \partial_r \pi^{rr} - \pi^{rr}\frac{1}{\gamma\tau_\pi} - 2\eta\sigma^{rr}\frac{1}{\gamma\tau_\pi} - \frac{1}{2\gamma}\pi^{rr}\left(\Theta - \frac{5}{4}\frac{D\varepsilon}{\varepsilon}\right)$$

$$\partial_\tau \pi^{\phi\phi} = -v_\perp \partial_r \pi^{\phi\phi} - \pi^{\phi\phi}\frac{1}{\gamma\tau_\pi} - 2\eta\sigma^{\phi\phi}\frac{1}{\gamma\tau_\pi} - \frac{1}{2\gamma}\pi^{\phi\phi}\left(\Theta - \frac{5}{4}\frac{D\varepsilon}{\varepsilon}\right)$$

$$\partial_\tau \pi^{zz} = -v_\perp \partial_r \pi^{zz} - \pi^{zz}\frac{1}{\gamma\tau_\pi} - 2\eta\sigma^{zz}\frac{1}{\gamma\tau_\pi} - \frac{1}{2\gamma}\pi^{zz}\left(\Theta - \frac{5}{4}\frac{D\varepsilon}{\varepsilon}\right)$$

$$\Theta \equiv \theta + \gamma\left\{\frac{1}{\tau} + \frac{v_\perp}{r}\right\}$$

$$\theta \equiv \partial_\tau \gamma + \partial_r \gamma v_\perp$$

$$D \equiv \left[\gamma\partial_\tau + \gamma v_\perp \partial_r\right]$$

$$\nabla \equiv \left[\gamma v_\perp \partial_\tau + \gamma\partial_r\right]$$

$$\sigma^{rr} \equiv -\theta + \frac{1}{3}\Theta$$

$$\sigma^{\phi\phi} \equiv -\gamma\frac{v_\perp}{r} + \frac{1}{3}\Theta$$

$$\sigma^{zz} \equiv -\gamma\frac{1}{\tau} + \frac{1}{3}\Theta$$

Flux profiles

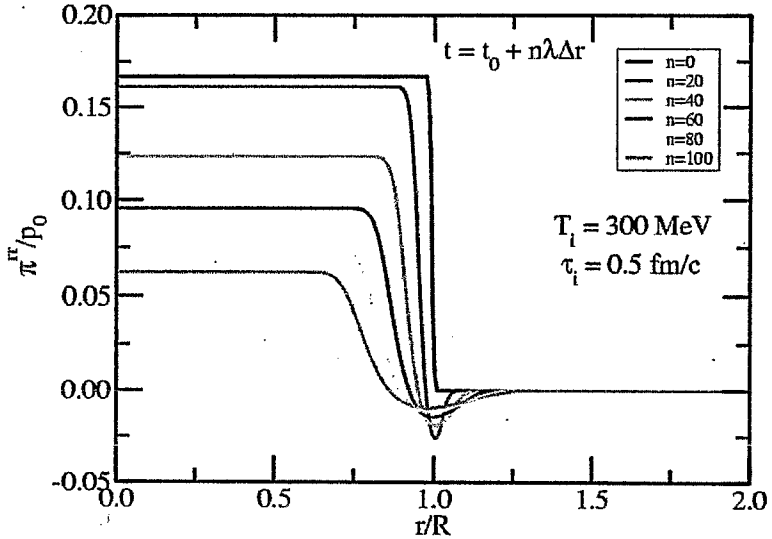

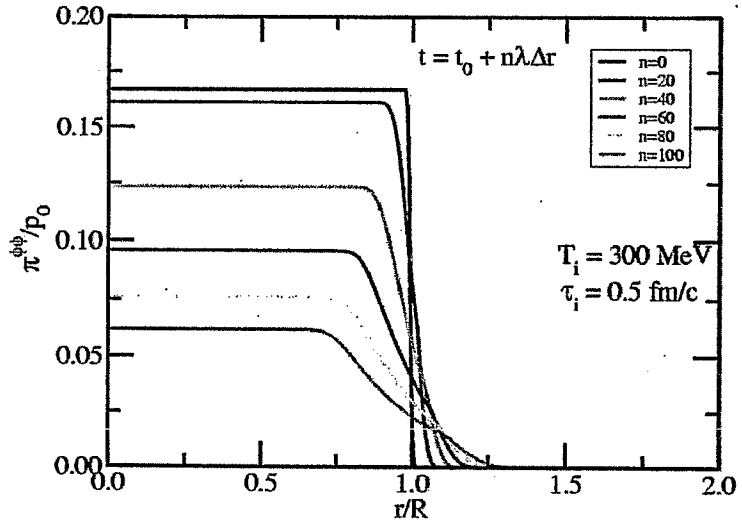

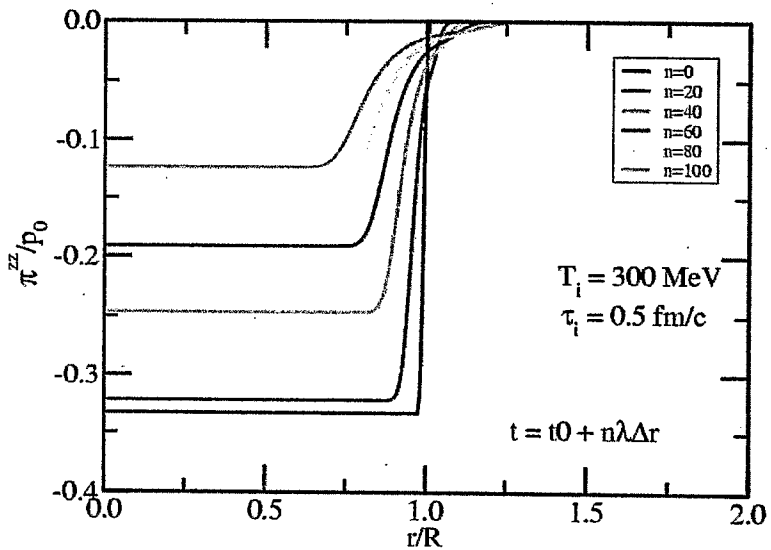

Space-time isotherms

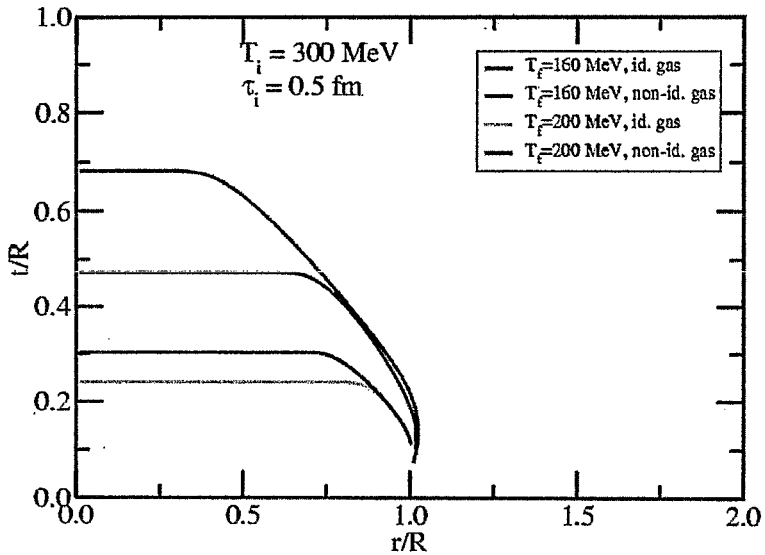

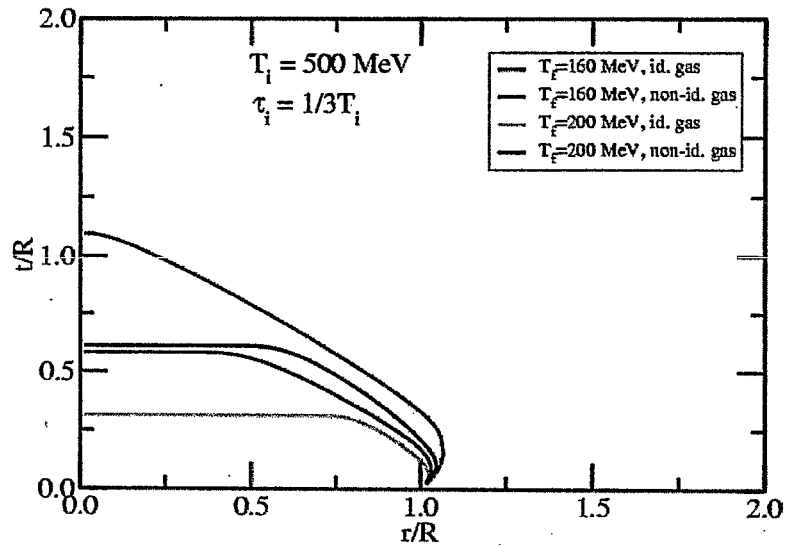

Transverse momentum spectra

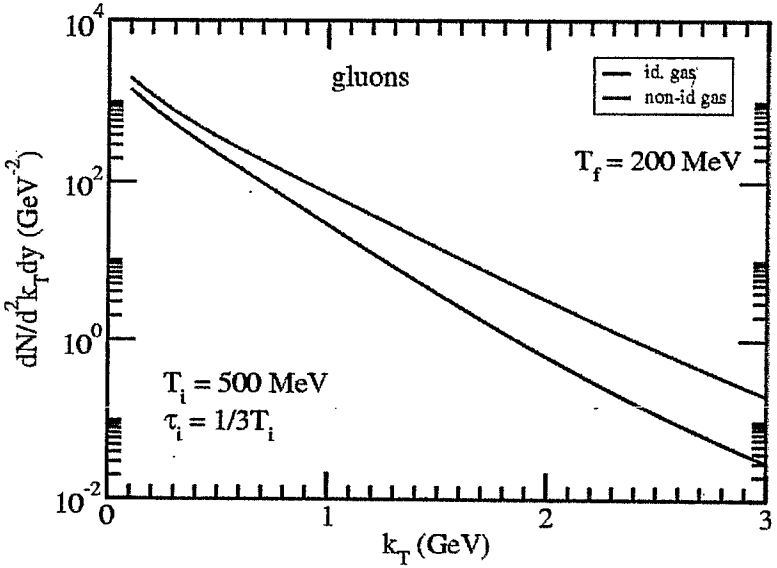

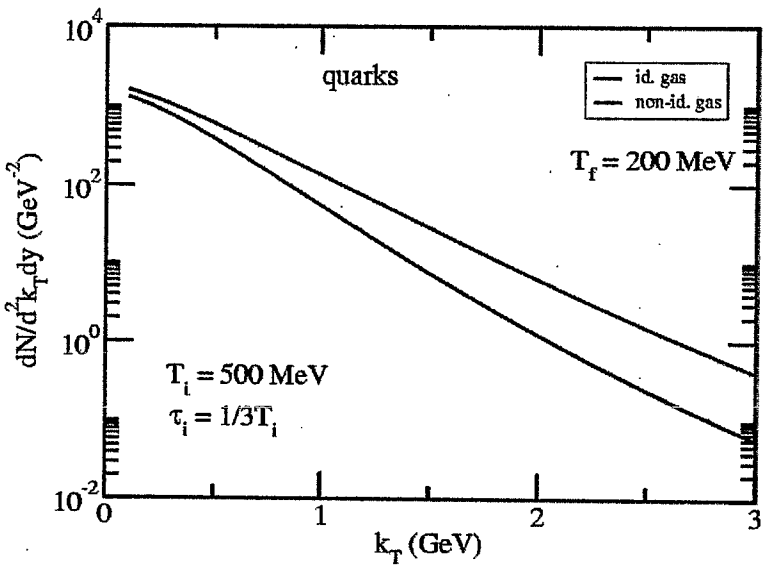

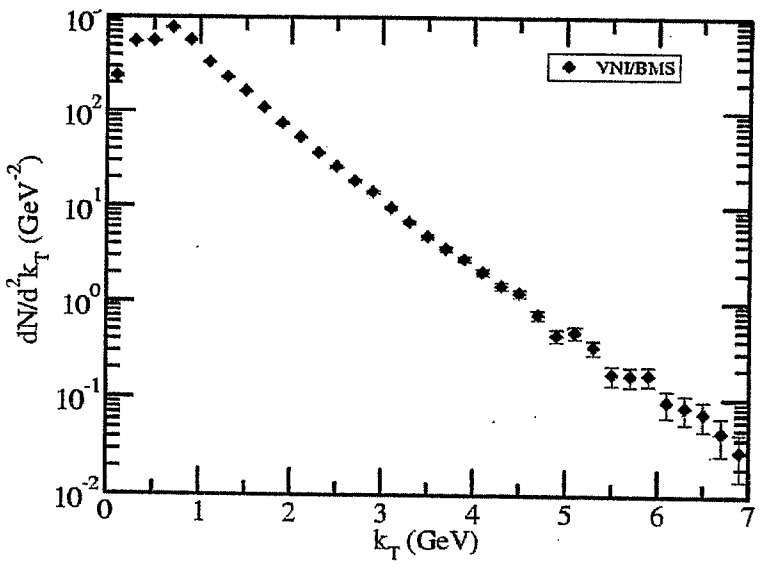

Multiplicity and HBT radii

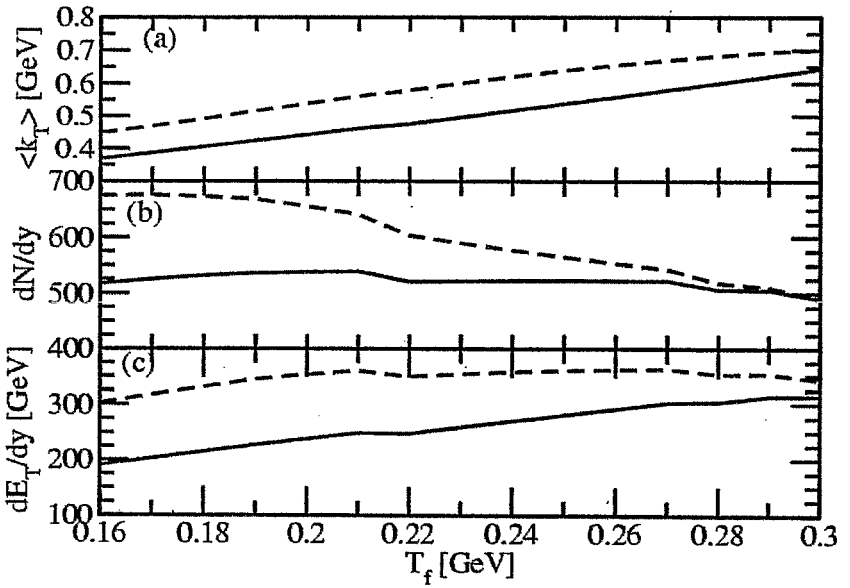

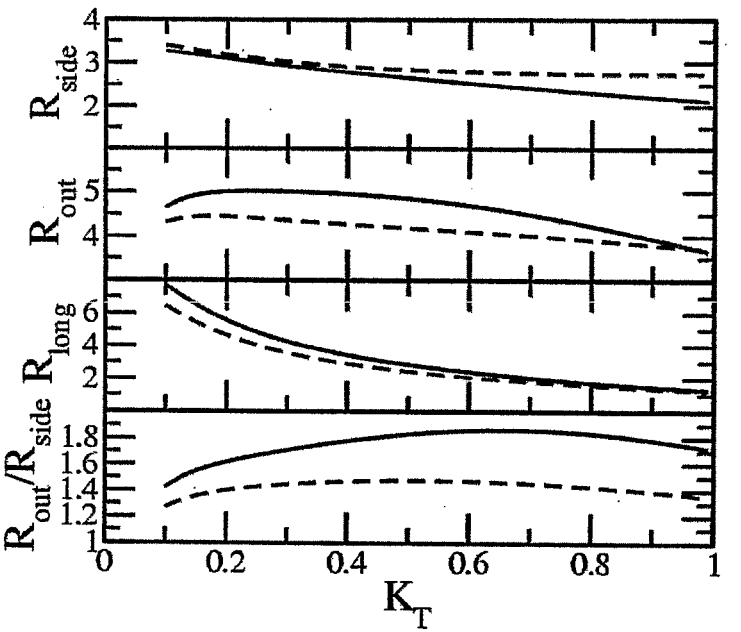

Transport coefficients from microscopic models

A. Muronga, PRC(04/2004)

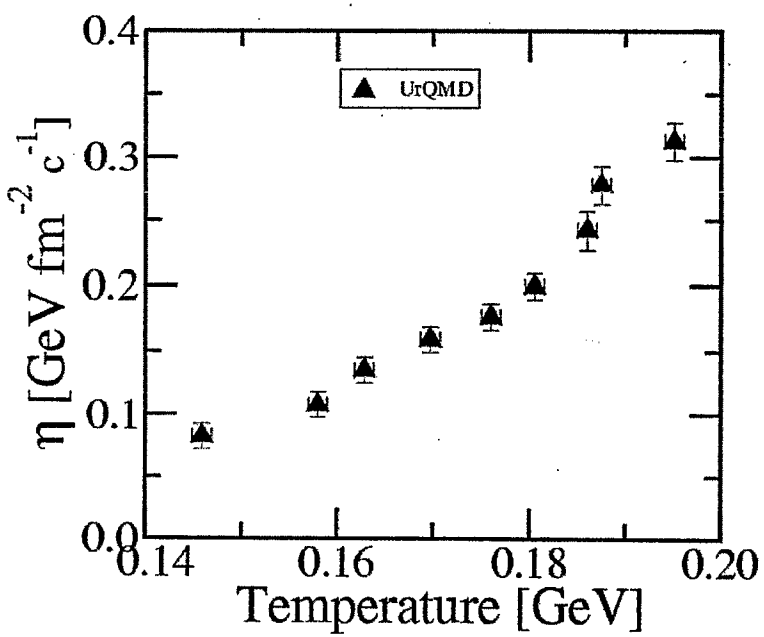

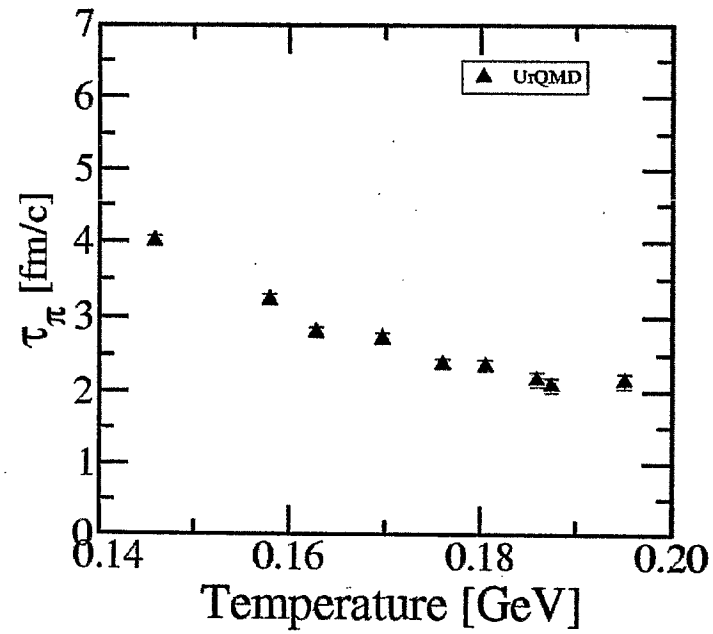

UrQMD simulations

What have we learnt?

In relativistic nuclear reactions,

* longitudinal pressure is reduced
* less longitudinal work is done
* longer freeze-out times
* stronger radial flow created

Yebo Yes! Dissipation is as important as EoS.

Conclusions and outlook

- Causal fluid dynamics should remain valid for important range of times.
- Non-ideal fluid dynamics is the simple way of studying non-equilibrium properties of hot and dense nuclear matter
- 2+1-dimensional calculations/analysis are being done
- EoS with phase transition and transport coefficients for both partons and hadrons
- What happens to the transport coefficients when there is phase transition??????????????????????
- 3+1 non-ideal fluid dynamics simulations: expect the unexpected

Theory Summer Program on RHIC Physics

Brookhaven National Laboratory
Summer 2004

Participants

Name	Affiliation	E-Mail Address
Hisato Eguchi	Niigata University	hisato@nt.sc.niigata-u.ac.jp
Roy Glauber	Harvard University	glauber@physics.harvard.edu
Boris Kopeliovich	Max-Planck-Institut fuer Kernphysik	Boris.Kopeliovich@mpi-hd.mpg.de
Elliot Leader	Imperial College London	e.leader@imperial.ac.uk
Eugene Levin	Tel Aviv University	leving@post.tau.ac.il
Cyrille Marquet	Commissariat A l'Energie Atomique (CEA)	marquet@spht.saclay.cea.fr
Agnes Mocsy	J.W.Goethe University	mocsy@th.physik.uni-frankfurt.de
Stephane Munier	Ecole Polytechnique	munier@cpht.polytechnique.fr
Azwinndini Muronga	University of Frankfurt	muronga@th.physik.uni-frankfurt.de
Marzia Nardi	Universita degli Studi di Torino	nardi@to.infn.it

Additional RIKEN BNL Research Center Proceedings:

Volume 64 – Theory Summer Program on RHIC Physics – BNL-

Volume 63 – RHIC Spin Collaboration Meetings XXIV (May 21, 2004), XXV (May 27, 2004), XXVI (June 1, 2004) – BNL-72397-2004

Volume 62 – New Discoveries at RHIC, May 14-15, 2004 – BNL- 72391-2004

Volume 61 – RIKEN-TODAI Mini Workshop on "Topics in Hadron Physics at RHIC", March 23-24, 2004 – BNL-72336-2004

Volume 60 – Lattice QCD at Finite Temperature and Density – BNL–72083-2004

Volume 59 – RHIC Spin Collaboration Meeting XXI (January 22, 2004), XXII (February 27, 2004), XXIII (March 19, 2004)– BNL-72382-2004

Volume 58 – RHIC Spin Collaboration Meeting XX – BNL-71900-2004

Volume 57 – High pt Physics at RHIC, December 2-6, 2003 – BNL-72069-2004

Volume 56 – RBRC Scientific Review Committee Meeting – BNL-71899-2003

Volume 55 – Collective Flow and QGP Properties – BNL-71898-2003

Volume 54 – RHIC Spin Collaboration Meetings XVII, XVIII, XIX – BNL-71751-2003

Volume 53 – Theory Studies for Polarized *pp* Scattering – BNL-71747-2003

Volume 52 – RIKEN School on QCD "Topics on the Proton" – BNL-71694-2003

Volume 51 – RHIC Spin Collaboration Meetings XV, XVI – BNL-71539-2003

Volume 50 – High Performance Computing with QCDOC and BlueGene – BNL-71147-2003

Volume 49 – RBRC Scientific Review Committee Meeting – BNL-52679

Volume 48 – RHIC Spin Collaboration Meeting XIV – BNL-71300-2003

Volume 47 – RHIC Spin Collaboration Meetings XII, XIII – BNL-71118-2003

Volume 46 – Large-Scale Computations in Nuclear Physics using the QCDOC – BNL-52678

Volume 45 – Summer Program: Current and Future Directions at RHIC – BNL-71035

Volume 44 – RHIC Spin Collaboration Meetings VIII, IX, X, XI – BNL-71117-2003

Volume 43 – RIKEN Winter School – Quark-Gluon Structure of the Nucleon and QCD – BNL-52672

Volume 42 – Baryon Dynamics at RHIC – BNL-52669

Volume 41 – Hadron Structure from Lattice QCD – BNL-52674

Volume 40 – Theory Studies for RHIC-Spin – BNL-52662

Volume 39 – RHIC Spin Collaboration Meeting VII – BNL-52659

Volume 38 – RBRC Scientific Review Committee Meeting – BNL-52649

Volume 37 – RHIC Spin Collaboration Meeting VI (Part 2) – BNL-52660

Volume 36 – RHIC Spin Collaboration Meeting VI – BNL-52642

Volume 35 – RIKEN Winter School – Quarks, Hadrons and Nuclei – QCD Hard Processes and the Nucleon Spin – BNL-52643

Volume 34 – High Energy QCD: Beyond the Pomeron – BNL-52641

Volume 33 – Spin Physics at RHIC in Year-1 and Beyond – BNL-52635

Volume 32 – RHIC Spin Physics V – BNL-52628

Volume 31 – RHIC Spin Physics III & IV Polarized Partons at High Q^2 Region – BNL-52617

Volume 30 – RBRC Scientific Review Committee Meeting – BNL-52603

Additional RIKEN BNL Research Center Proceedings:

Volume 29 – Future Transversity Measurements – BNL-52612
Volume 28 – Equilibrium & Non-Equilibrium Aspects of Hot, Dense QCD – BNL-52613
Volume 27 – Predictions and Uncertainties for RHIC Spin Physics & Event Generator for RHIC Spin Physics III – Towards Precision Spin Physics at RHIC – BNL-52596
Volume 26 – Circum-Pan-Pacific RIKEN Symposium on High Energy Spin Physics – BNL-52588
Volume 25 – RHIC Spin – BNL-52581
Volume 24 – Physics Society of Japan Biannual Meeting Symposium on QCD Physics at RIKEN BNL Research Center – BNL-52578
Volume 23 – Coulomb and Pion-Asymmetry Polarimetry and Hadronic Spin Dependence at RHIC Energies – BNL-52589
Volume 22 – OSCAR II: Predictions for RHIC – BNL-52591
Volume 21 – RBRC Scientific Review Committee Meeting – BNL-52568
Volume 20 – Gauge-Invariant Variables in Gauge Theories – BNL-52590
Volume 19 – Numerical Algorithms at Non-Zero Chemical Potential – BNL-52573
Volume 18 – Event Generator for RHIC Spin Physics – BNL-52571
Volume 17 – Hard Parton Physics in High-Energy Nuclear Collisions – BNL-52574
Volume 16 – RIKEN Winter School - Structure of Hadrons - Introduction to QCD Hard Processes – BNL-52569
Volume 15 – QCD Phase Transitions – BNL-52561
Volume 14 – Quantum Fields In and Out of Equilibrium – BNL-52560
Volume 13 – Physics of the 1 Teraflop RIKEN-BNL-Columbia QCD Project First Anniversary Celebration – BNL-66299
Volume 12 – Quarkonium Production in Relativistic Nuclear Collisions – BNL-52559
Volume 11 – Event Generator for RHIC Spin Physics – BNL-66116
Volume 10 – Physics of Polarimetry at RHIC – BNL-65926
Volume 9 – High Density Matter in AGS, SPS and RHIC Collisions – BNL-65762
Volume 8 – Fermion Frontiers in Vector Lattice Gauge Theories – BNL-65634
Volume 7 – RHIC Spin Physics – BNL-65615
Volume 6 – Quarks and Gluons in the Nucleon – BNL-65234
Volume 5 – Color Superconductivity, Instantons and Parity (Non?)-Conservation at High Baryon Density – BNL-65105
Volume 4 – Inauguration Ceremony, September 22 and Non -Equilibrium Many Body Dynamics –BNL-64912
Volume 3 – Hadron Spin-Flip at RHIC Energies – BNL-64724
Volume 2 – Perturbative QCD as a Probe of Hadron Structure – BNL-64723
Volume 1 – Open Standards for Cascade Models for RHIC – BNL-64722

For information please contact:

Ms. Pamela Esposito
RIKEN BNL Research Center
Building 510A
Brookhaven National Laboratory
Upton, NY 11973-5000 USA

Phone: (631) 344-3097
Fax: (631) 344-4067
E-Mail: pesposit@bnl.gov

Ms. Tammy Heinz
RIKEN BNL Research Center
Building 510A
Brookhaven National Laboratory
Upton, NY 11973-5000 USA

(631) 344-5864
(631) 344-2562
theinz@bnl.gov

Homepage: http://www.bnl.gov/riken

RIKEN BNL RESEARCH CENTER

Theory Summer Program on RHIC Physics

Summer 2004

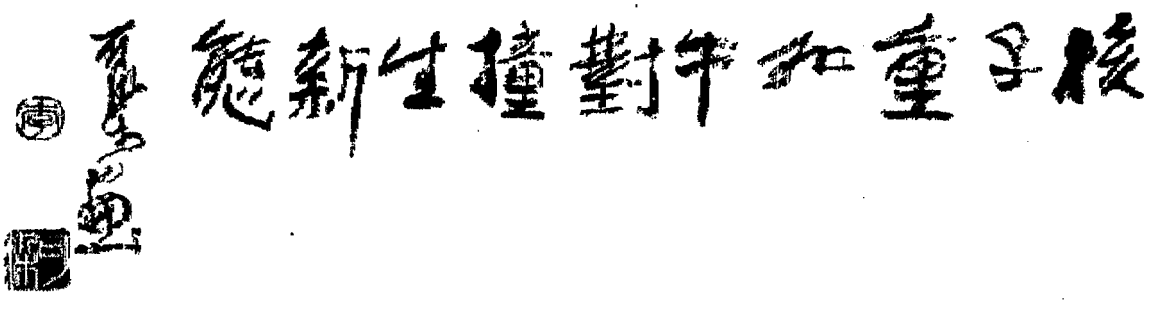

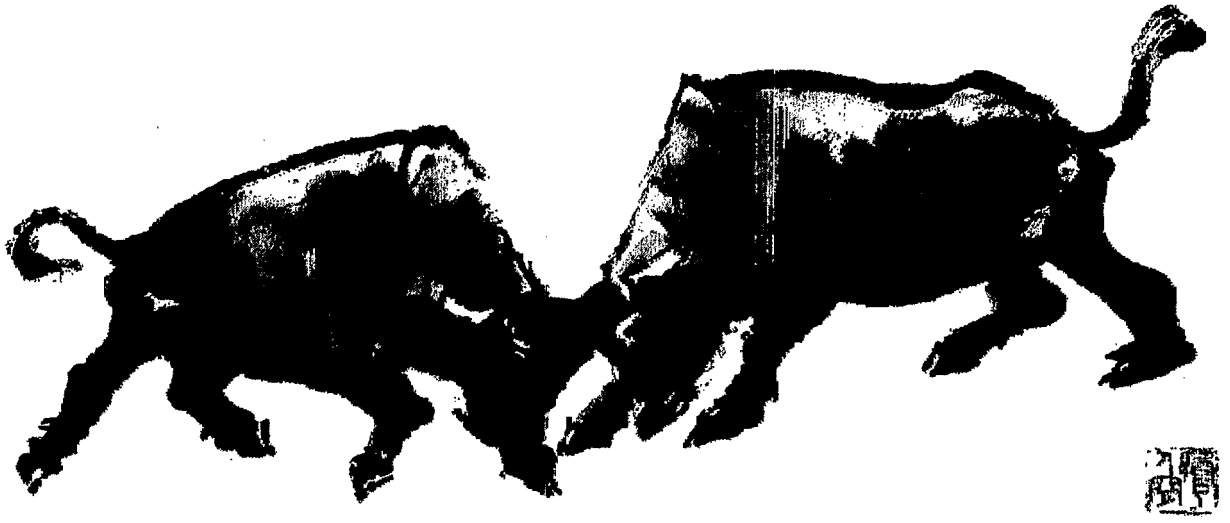

Li Keran

Nuclei as heavy as bulls
Through collision
Generate new states of matter.
T.D. Lee

Copyright©CCASTA

Speakers:

H. Eguchi
E. Leader
A. Mocsy
M. Nardi
R. Glauber
E. Levin
S. Munier
B. Kopeliovich
C. Marquet
A. Muronga

Organizers: D. Kharzeev, S. Kretzer, D. Teaney, K. Tuchin, R. Venugopalan, and W. Vogelsang